1934

Structural beams in torsion, 1934

I. Lyse

B. G. Johnston

~~162~~
161.3

$$\theta = \frac{T}{G \cdot K}$$

FRITZ ENGINEERING LABORATORY
LEHIGH UNIVERSITY
BETHLEHEM, PENNSYLVANIA

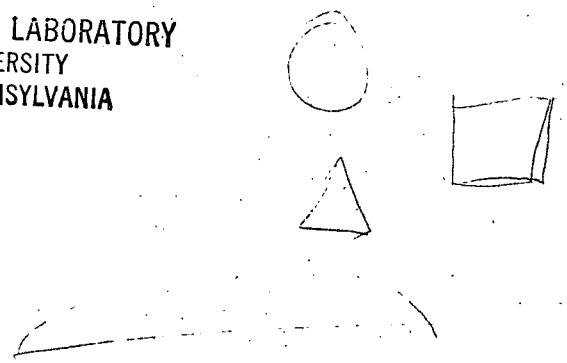

STRUCTURAL BEAMS IN TORSION

by

Inge Lyse and Bruce Johnston
Fritz Engineering Laboratory

1934

TABLE OF CONTENTS

STRUCTURAL BEAMS IN TORSION

by Inge Lyse* and Bruce Johnston**

SYNOPSIS

The following report presents the results of a two-year study of the torsional properties of standard structural steel beams. The purpose of the investigation has been to furnish a reliable basis for the design of structural members subjected to torsional loads.

The report presents an accurate method for the evaluation of the torsion constant, "K", for standard H and I sections, taking full account of all factors involved. This has been made possible by application of the "membrane analogy" to about sixty sections of widely varying flange, web, and fillet proportions.

The investigation includes a study of the effect of end fixity in torsional design, and shows how it may be effectively obtained. Application of the proposed formulas is made to practical design problems, and the formulas checked by torsional tests on structural steel sections ranging in size from a 3-inch I-beam weighing 7.5 lb. per ft. to a 12 by 12-inch beam weighing 190 lb. per ft. The data for these tests are presented.

* Research Associate Professor of Engineering Materials Lehigh University, Bethlehem, Pennsylvania

** Lawrence Calvin Brink Research Fellow in Civil Engineering, Lehigh University, Bethlehem, Pennsylvania in Immediate Charge of Torsion Investigation.

I. HISTORICAL FOREWORD

The problem of pure torsion as applied to non-circular sections was first correctly treated by Saint Venant[1]* in 1855, and his general solution is applicable to any cross section. In 1903 Prandtl[2] showed that if a thin membrane were stretched across a hole having the shape of the cross-section in question and distorted a slight amount the equation of its surface had the same form as the general differential equation involved in the torsion problem.

Prandtl showed that by measuring the volume and slopes of the displaced membrane a direct measurement of the torsional rigidity and stress was obtainable. Prandtl's Analogy, with a thin soap film as a membrane, was used in several torsion investigations, first in England by Griffith and Taylor[3], who studied the torsional strength of aeroplane sections in 1917, and later in this country by Trayer and March[4], who in 1930 made similar studies for a similar purpose.

Important contributions to the torsion problem have been made by Timoshenko[5]. He has shortened the pure torsional theory by slight modifications of Saint Venant's equations and by mathematical application of the principles of the membrane analogy. He was also among the first to consider the effect produced by preventing the warping of a

---

* These numbers refer to references given at the end of the report.

cross-section. This problem has had the attention of numerous investigators in connection with problems of elastic stability and buckling during bending. R. Sonntag[7] has treated the theoretical aspects of this problem in an article published in 1929.

II. INTRODUCTION

(1) Acknowledgment - The torsional investigation was initiated in October 1932, upon the suggestion of the McClintic-Marshall Corporation, subsidiary to the Bethlehem Steel Company, who furnished the steel beams and the material for constructing the test apparatus.

Special acknowledgment is due Jonathan Jones, Chief Engineer; C. H. Mercer, Consulting Engineer, and Sterling Johnston, Engineer - all of the McClintic-Marshall Corporation, and V. E. Ellstrom, Manager of Sales Engineering, Bethlehem Steel Company for their cooperation in the investigation.

The investigation was carried out as a research project at the Fritz Engineering Laboratory. C. C. Keyser, Laboratory Assistant, and all others associated with the laboratory contributed valuable help throughout. Professor J. B. Reynolds, of the Department of Mathematics, gave his assistance to the theoretical studies.

(2) Outline of Investigation - A tentative program for the investigation was outlined early in October 1932. It was at first proposed to test sections three feet in length, welded at the ends to thick plates. A study of the problem, however, showed that such beams would be several times stronger than if they were tested free-ended, and that, unless the exact percentage of end fixity were known, it would not be possible to draw definite conclusions from such tests.

In order to study the effect of end fixity, directly, tests were first made on eight sections of a 3-in., 7.5-lb. per ft. I-beam, varying from 3 in. to 4 ft. 6 in. in length and cut from the same rolled section. The ends of each piece were welded to one-inch thick plates, and the specimens were tested in a standard Olsen 26,000 in-lb. torsion machine.

The results of these tests pointed the way to a revised general program which was mapped out in March 1933, and a torsion testing rig capable of applying torsional load up to 800,000 in-lb. was designed. Provision was made for testing beams either fixed at the ends or free, and of lengths of 1 ft. 6 in., 3 ft., or 6 ft.

Eighteen different tests were proposed, twelve on beams with the ends fixed by welding side and end plates to form a box-section at the ends, and six with ends free. Tensile and shearing properties of the material in each different beam were obtained by standard tensile tests, round bar

torsion tests, and slotted plate shear tests. An additional free-ended test was made during Open House on April 20, 1934.

The torsion testing rig operated by means of cables and specially constructed sheaves. It was completed and the first test was made on May 25, 1933. A progress report on the investigation was submitted to the McClintic-Marshall Corporation on June 7, 1933.

Most of the torsion tests on beams were completed by October 1, 1933, and at this time an auxiliary investigation was initiated to determine accurately the torsion constant, "K", for all structural sections. Soap-film tests on 57 differently proportioned sections were made and these tests were completed by December 28, 1933.

The present report contains the final summary of all phases of the investigation. Use has been freely made of the findings of previous investigators, for which acknolwedgment is made at appropriate points.

(3) Notation

A = Cross-sectional area.

I_x, I_y = Moments of Inertia of a cross-section with respect to the x and the y axes.

J = Polar Moment of Inertia.

q = Intensity of a continuously distributed load.

p = Unit Pressure.

M = Bending Moment.

T = Torsional Moment.

Q = Total Shear over Cross-Section.

f = Normal Stress.

s = Shearing Stress.

ε = Unit Elongation.

E = Modulus of Elasticity in Tension and Compression.

G = Shearing Modulus of Elasticity.

μ = Poisson's Ratio.

ϕ = The Torsion Stress Function.

K = The Torsion Constant.

C = The Equivalent Torsion Constant for a Fixed-Ended Beam.

ψ = Total Angle Change Between Two Cross-Sections.

θ = Angle of Twist in Radians Per Unit Length.

III. THE TORSION THEORY

1. General Problem - The correct solution of the torsional properties of a section of any shape consists primarily in determining the distribution of lateral shearing stresses over the cross-section. The shear components will be of uneven distribution, except in the case of the circular section, and as a result plane sections will be warped during twisting as shown in Fig. 1.

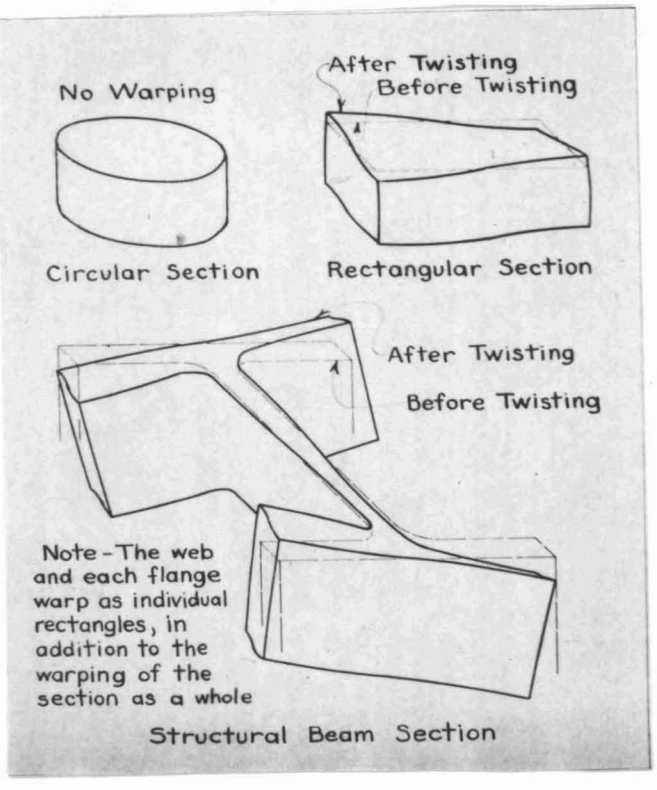

Fig. 1

It is assumed that the lateral displacements are proportional to the angular twist and to the distance from the twisting axis (as is the case in a circular section). The longitudinal displacements cause the warping and the resulting distribution of shearing stress is taken care of by introducing a "stress-function" ϕ of x and y. It is found that this function must satisfy the differential equation:

$$\frac{\partial^2 \phi}{\partial x^2} + \frac{\partial^2 \phi}{\partial y^2} = -2G\theta \qquad (1)$$

It may be shown that the function ϕ must be a constant along the boundary of the section for solid bars, and may therefore be arbitrarily chosen as equal to zero.

If the boundary conditions are such that equation (1) may be solved and ϕ determined, it is then possible to evaluate the torsion constant of the section and find the stress at any point in the cross section. Formulas for the torsion constant and critical shearing stresses have in this manner been derived for such sections as the square, rectangle, ellipse, equilateral triangle, and sector of a circle[1].

In the case of the circular shaft the shearing stress components have a uniform distribution along each radii, and since the longitudinal shear is likewise evenly distributed, there is no longitudinal warping of first order importance. The well known simple theory using the polar moment of inertia is thus applicable to the case of the circular section.

If the warping which takes place in non-circular sections is in some way restrained or prevented, longitudinal fiber stresses will be introduced and the beam stiffened and strengthened. This problem is studied in detail later.

2. The Membrane Analogy - Equation (1) may be solved mechanically for any cross section by means of Prandtl's Membrane Analogy, thereby overcoming the mathematical limitations of the theoretical derivation.

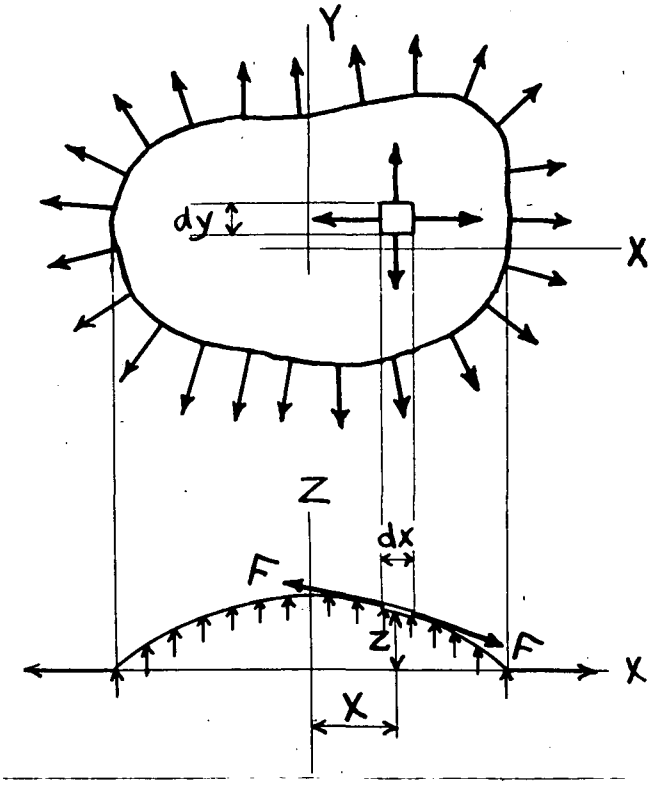

Fig. 2

In the application of this analogy, a soap film is stretched across an opening having the same shape as the structural section under consideration. The bubble is distended slightly by a variation in pressure. We then consider the equilibrium of a small element of area dx dy as indicated in Fig. 2, where:

p = unit pressure acting on the membrane,

F = unit tension in the membrane,

z = displacement of the membrane.

The stresses in the soap film are known to be independent of the shape of the film and have the same intensity in all directions. A section of a film is shown in Fig. 2, with the y axis perpendicular to the plane of the paper. The total stress acting on the element along the edge dy is equal to F dy. The z component of this stress may be considered equal to $-Fdy\frac{\partial F}{\partial z}$. The deflection is considered so small that the tangent and the sine of the angle of inclination are practically equal. We have a similar force F dy acting in nearly an opposite direction, the difference between the two z components being:

$$-Fdy\frac{\partial^2 z}{\partial y^2}dx$$

Positive direction is taken in the direction of the z axis.

Similarly we may write an expression for the force F acting on the dx side of the element.

$$-Fdx\frac{\partial^2 z}{\partial x^2}dy$$

These must be in equilibrium with the pressure p acting on elemental area dx dy; or:

$-Fdy\frac{\partial^2 z}{\partial y^2}dx - Fdx\frac{\partial^2 z}{\partial x^2}dy = pdxdy$ which by dividing by $-Fdxdy$ gives:

$$\frac{\partial^2 z}{\partial x^2} + \frac{\partial^2 z}{\partial y^2} = -\frac{p}{F} \qquad (2)$$

comparing equations (1) and (2) and introducing $\phi = kz$ where k is a dimension constant, we have:

$$2G\theta = k\frac{p}{F} \qquad (3)$$

Hence equation (2) offers a solution to the problem, and Prandtl showed that the following relations obtain --

(1) The torsion constant "K" is proportional to the total volume of the displaced bubble.

(2) The shearing stress at any point is proportional to the maximum slope at that point.

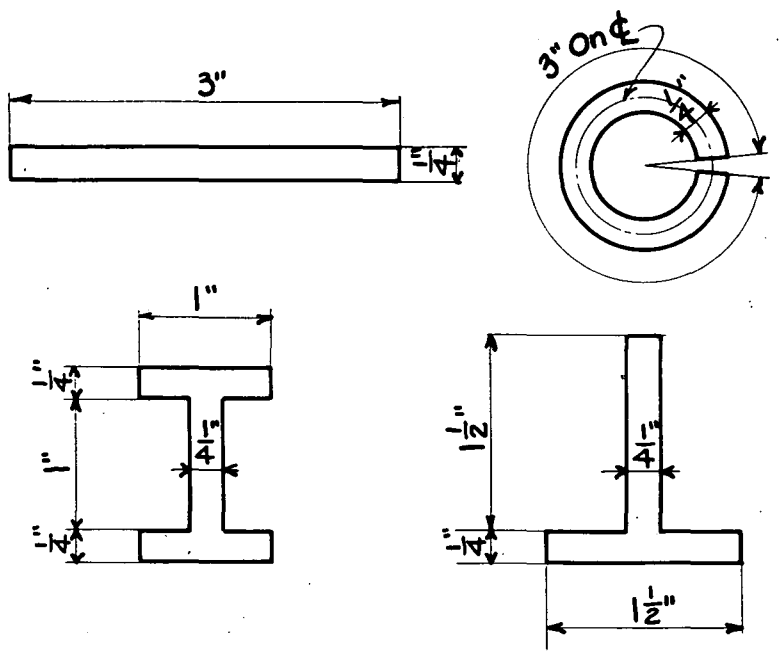

Fig. 3

(3) The contour lines on the bubble give the direction of maximum shearing stress.

The analogy is also useful as an aid in visualizing the rigidity and stress distribution in various sections, and makes evident why the four sections shown in Fig. 3 have approximately equal rigidities in pure torsion; since the volumes of the various soap bubbles are approximately the same in each case. This would not be the case if the ends of the beams were restrained.

IV. EVALUATION OF THE TORSION CONSTANT

(1) Definition - The torsion constant, K, is the measure of the torsional rigidity and twisting deflections. It is also a part of any formula for torsional shearing stresses. K may be determined from test results by observing the ratio of torsional moment to unit twist in radians per inch at any time below the yield point of the beam, and dividing this ratio by the shearing modulus of elasticity.

(2) The Relation Between K and J - When a torsional couple is applied to a circular shaft the maximum shearing stress, at the surface, is given by:

$$s = \frac{Tr}{J} \qquad (4)$$

(r = radius of shaft)

In terms of T we may rearrange equation (4) to read:

$$T = \frac{sJ}{r} \qquad (5)$$

We may also express T in terms of θ, the unit angular twist in radians per inch, and G, the shearing modulus of elasticity.

$$T = JG\theta \qquad (6)$$

For non-circular sections we may again express the torsional resisting moment in terms of θ and G, with the substitution of K, the torsion constant, in place of J.

$$T = KG\theta \qquad (7)$$

The torsion constant K is equal to the polar moment of inertia for circular sections and while for non-circular sections it is always less than the polar moment of inertia, there is no direct relation between the two factors.

(3) The Rectangle - In dealing with structural shapes, two principle types of section require consideration, the rectangle, and the rectangle modified by sloping sides, as in the flange of a standard I-beam. In the case of the rectangle we have an accurate formula derived originally by Saint Venant[1],

$$K = \frac{n^3 b}{3} - 2An^4 \qquad (8)$$

where n = thickness of rectangle

b = width of rectangle

A = a factor depending on the $\frac{b}{n}$ ratio but practically constant for $\frac{b}{n}$ greater than 3.

(See Fig.4 for values of A for $\frac{b}{n}$ from 1 to 3)

For $\frac{b}{n}$ ratios greater than 3, $A = 0.105$, and for $\frac{b}{n}$ greater than 4, $A = 0.10504$.

Equation (8) finds a direct, qualitative interpretation in the soap film analogy. It is evident that for long rectangular sections the bubble will be of constant cross section along the central portion, but at the two ends it will be contracted and brought down to meet the small side. The $-2An^4$, then represents the "end-loss", which for long sections is evidently a function of n only.

It also follows that if the ends were made discontinuous, as if they were portions of infinitely long rectangles, we might say, with no error:

$$K = 1/3\ n^3 b \qquad (9)$$

and for any differential length, dx, along the section:

$$k = 1/3\ n^3 dx \qquad (10)$$

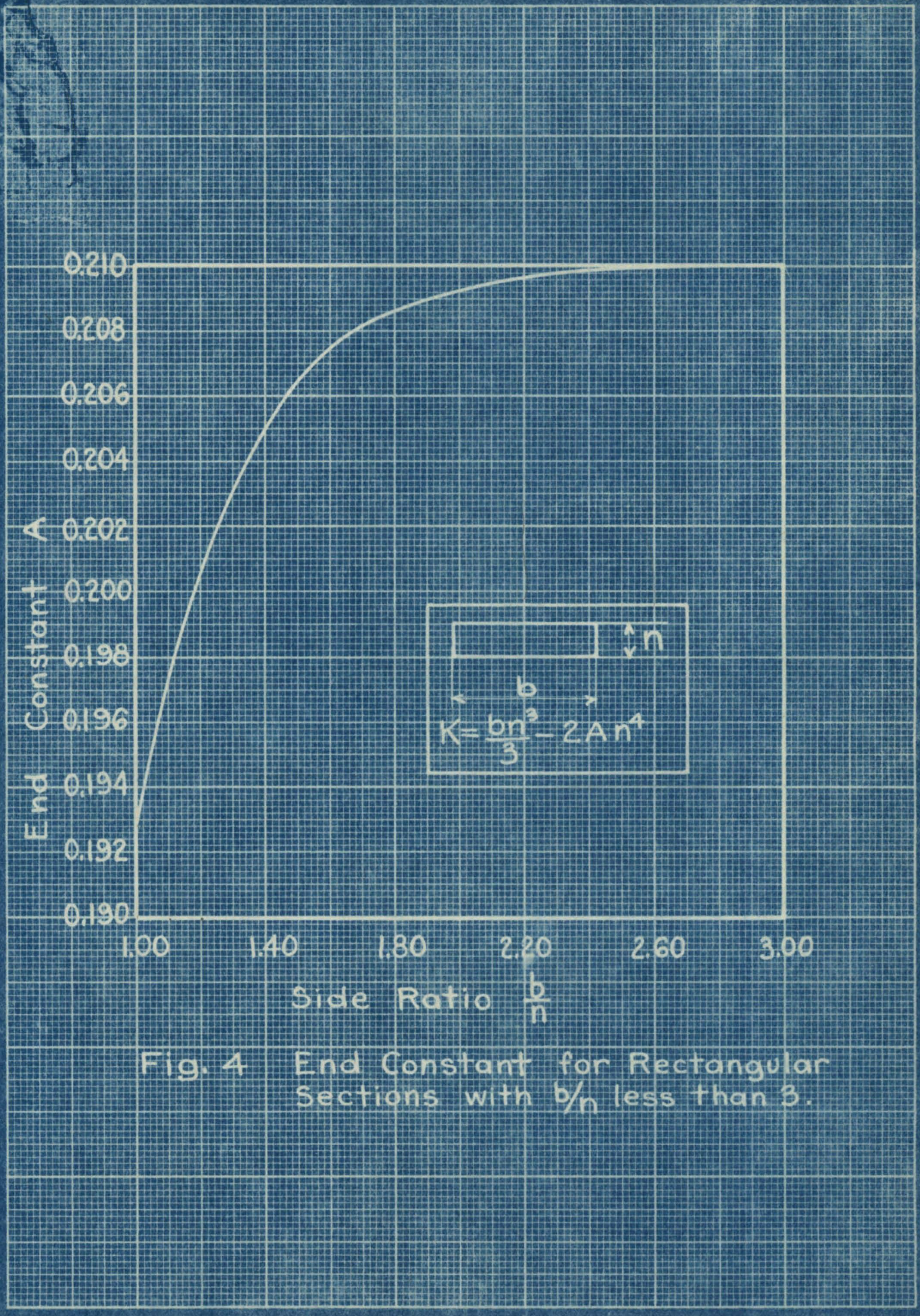

Fig. 4 End Constant for Rectangular Sections with b/n less than 3.

(4) The Sloping Sided Section - Equation (1) provides a basis for evaluating K for the sloping flange section. Considering the section shown in Fig. 5, having dimensions as shown, let the thickness at any point taken as r. Then if the ends are assumed discontinuous, we will have:

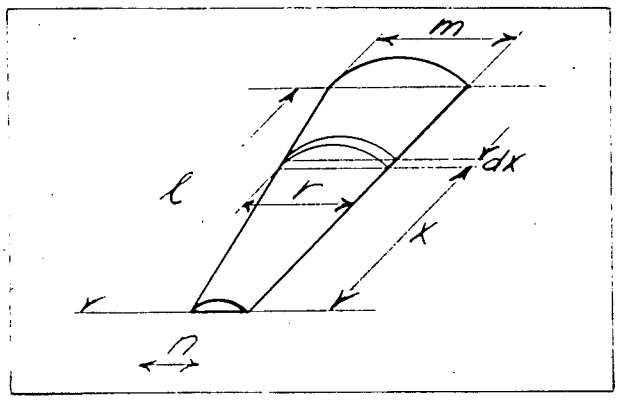

Fig. 5

$$K = 1/3\int_0^b r^3 dx \qquad (11)$$

Evaluating r in terms of m and n, and integrating, we get:

$$K = \frac{b}{12}(m+n)(m^2+n^2) \qquad (12)$$

We must deduct for end effects, as in the case of the simple rectangle and we write:

$$K = \frac{b}{12}(m+n)(m^2+n^2) - A_L m^4 - A_S n^4 \qquad (13)$$

The evaluation of the constants A_L and A_S was the work of Professor J. B. Reynolds, through an analysis of a section having the shape shown in Fig. 6. (See Love, THEORY OF ELASTICITY, 4th ed., p.319).

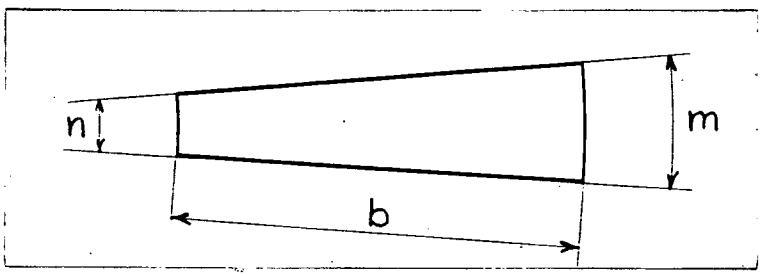

Fig. 6

$$A_L = 0.10504-0.10000S+0.08480S^2-0.06746S^3+0.05153S^4 \qquad (14)$$

$$A_S = 0.10504+0.10000S+0.08480S^2+0.06746S^3+0.05153S^4 \qquad (15)$$

S = Slope of the section. (See Fig.8 for graphs of A_S and A_L)

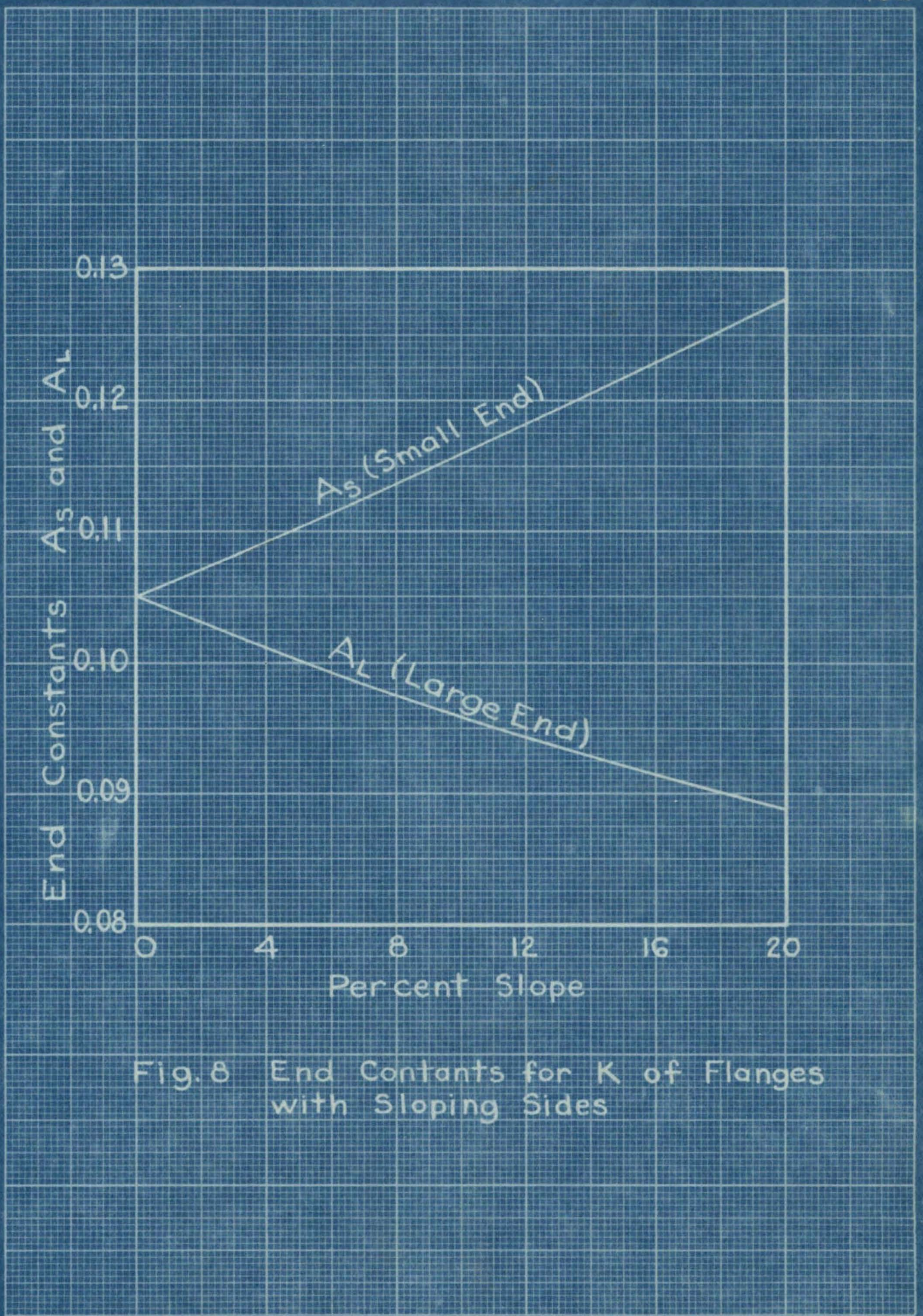

Fig. 8 End Contants for K of Flanges with Sloping Sides

(5) Torsion Constant for H and I Beams - We now have a basis for approaching the K values of the component parts. Taking the section shown in Fig. 7 as a basis for the sloping flange section we will have for the sum of two trapezoids and a small rectangular portion:

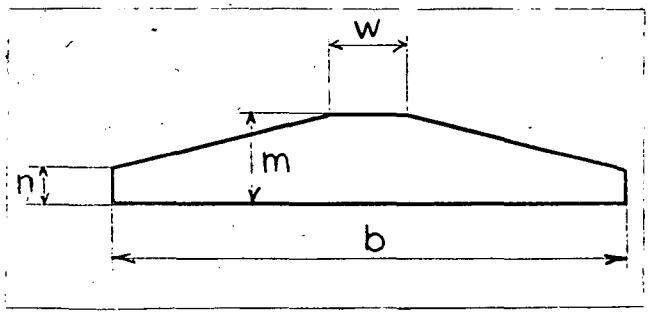

Fig. 7

$$K\ (\text{flange}) = \frac{b-w}{12}(m+n)(m^2+n^2) + \frac{1}{3}wm^3 - 2A_s n^4 \qquad (16)$$

The web is considered as a discontinuous section between the flanges, giving:

$$K\ (\text{web}) = \frac{1}{3}(d - 2m)w^3 \qquad (17)$$

(Refer to Fig. 9 for notation)

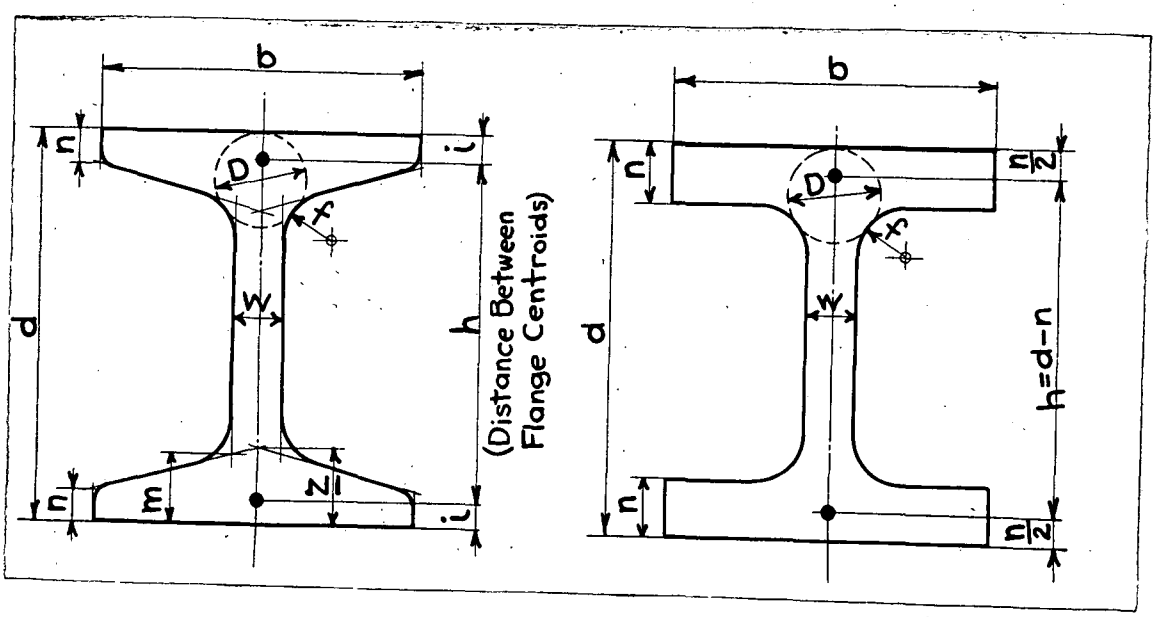

Fig. 9

There still remains the evaluation of the added rigidity due to the connection of the flange and web and also due to the fillet at this point. It is evident that these will cause a considerable "hump" in the soap bubble.

Trayer and March[4] in an investigation of aircraft strut sections assumed this addition to the torsion constant to be proportional to the fourth power of the diameter of the largest circle that can be inscribed at the juncture of the web and flange, giving:

$$K \text{ (additional)} = \alpha D^4 \qquad (18)$$

where D = diameter of inscribed circle

α = a factor, depending on two ratios

$$R_1 = \frac{w}{m} \qquad R_2 = \frac{f}{m}$$

(See Fig. 9 for notation)

Values of α for sections with parallel side flanges, and for sections with 1-6 flange side slope are given in Fig. 10 and 11 respectively. These graphs were experimentally determined as the result of soap film tests which will be described later.

It will be noted in Fig. 10 that for parts of the curves to the right of "a-a", the lines are parallel and uniformly spaced. All standard rolled beams are in this area, in which case:

$$\alpha \text{ (parallel flange sides)} = 0.094 + 0.070\, R_2 \qquad (19)$$

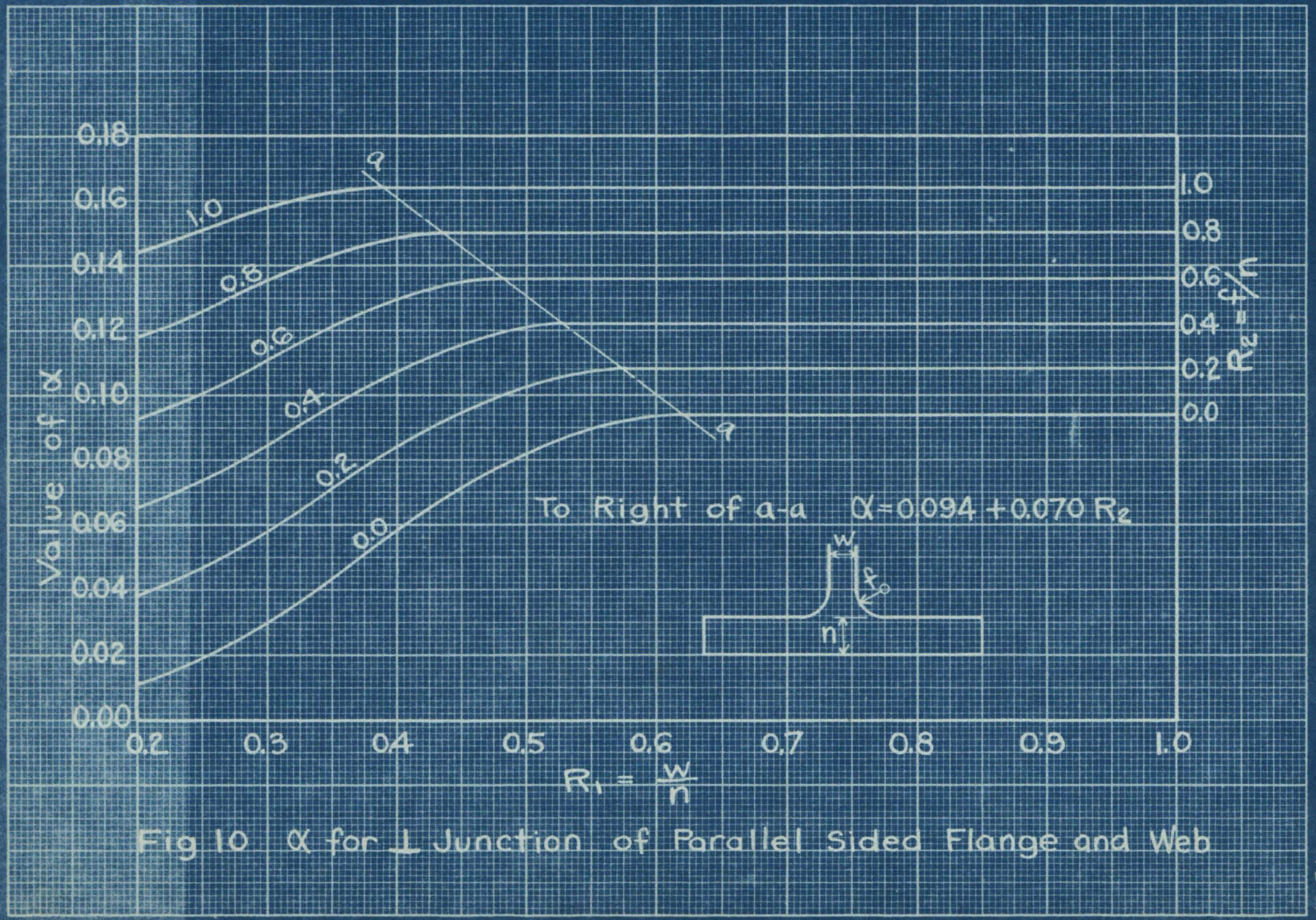

Fig 10 α for ⊥ Junction of Parallel Sided Flange and Web

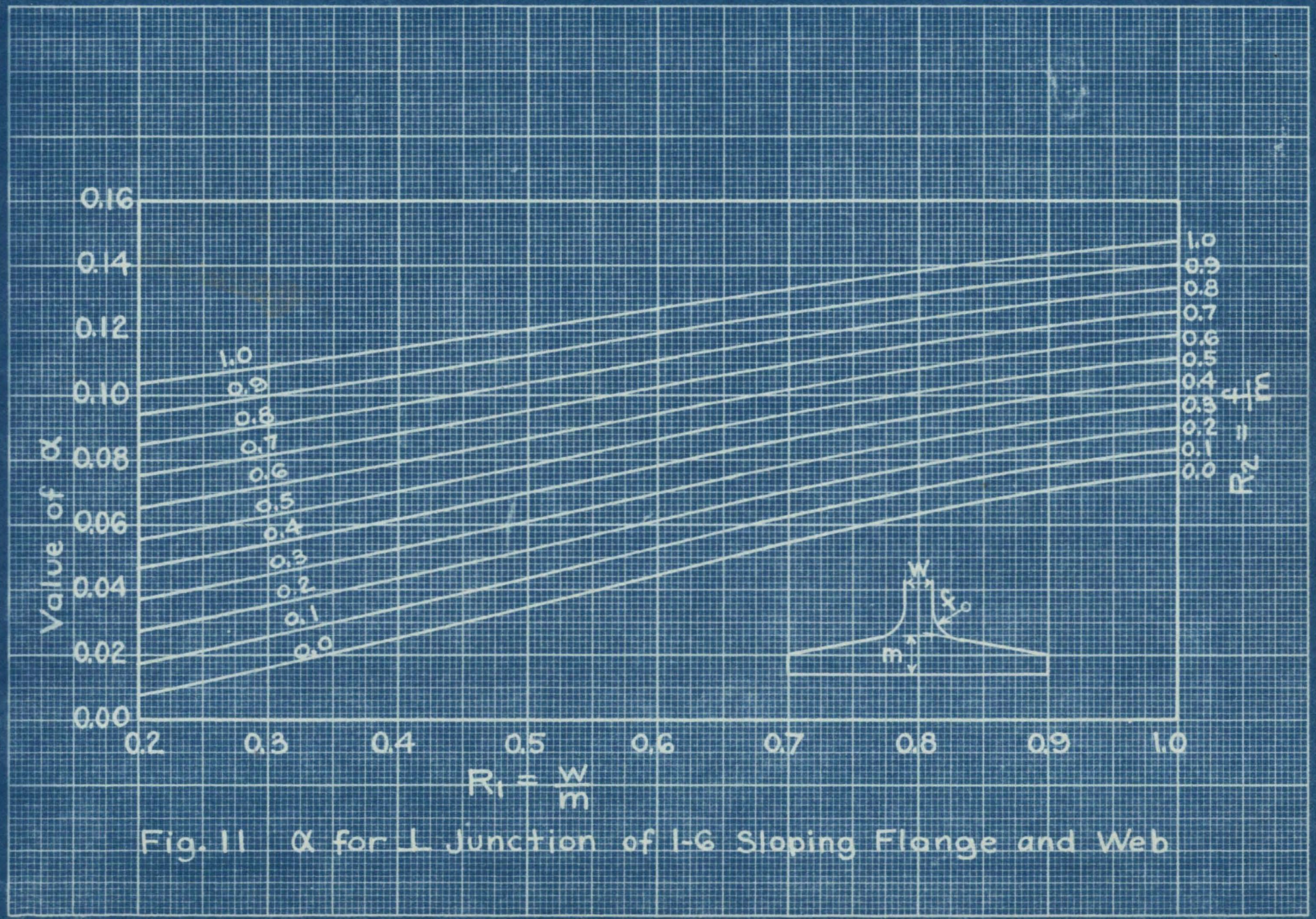

Fig. 11 α for L Junction of I-6 Sloping Flange and Web

And for sections with 1-20 and 1-50 side slope the following formulas represent an interpolation between the curves in Fig. 10 and 11.

$$\alpha(\text{1-20 slope}) = 0.066 + 0.021R_1 + 0.072R_2 \qquad (20)$$

$$\alpha(\text{1-50 slope}) = 0.084 + 0.007R_1 + 0.071R_2 \qquad (21)$$

We can now sum up the various elements entering into the total K values, and write:

$$K(\text{sloping flange sections}) = \frac{b-w}{6}(m+n)(m^2+n^2) + \frac{2}{3}wm^3 + \frac{1}{3}(d-2m)\,w^3 + 2\alpha D^4 - 4A_S n^4 \qquad (22)$$

Values for A_L and A_S for the standard slopes are given in Table I below, and are also shown graphically in Fig. 8.

TABLE I

S	A_L	A_S
1/6	0.09045	0.12441
1/20	0.10026	0.11026
1/50	0.10307	0.10707
1/α	0.10504	0.10504

For sections with parallel sided flanges,

$$K(\text{parallel flange}) = \frac{2}{3}bn^3 + \frac{1}{3}(d-2n)w^3 + 2\alpha D^4 - 0.42016n^4 \qquad (23)$$

D may be determined by a large scale lay-out or by the following formulas.

For parallel sided flange sections

$$D = \frac{(n+f)^2 + w(f+\frac{w}{4})}{2f + n} \qquad (24)$$

For sloping sided flange sections

$$D = \frac{(B+z)^2 + w(f+\frac{w}{4})}{B + f + z} \qquad (25)$$

Where

$$B = fS\left[\sqrt{\frac{1}{S^2} + 1} - 1 - \frac{w}{2f}\right] \qquad (26)$$

Sections Having Equal Areas	Rigidity	Strength
(1) ●	100.0	100.0
(2) ◯	637.0	332.0
(3) ◯ ———	5.5	18.0
(4) ▲	70.0	62.0
(5) ■	88.0	74.0
(6) □	341.0 (Approx.)	280.0 (Approx.)
(7) I	9.9 (Nearly Exact)	22.2 (Disregarding Stress Concentration)
(8) I f=w=⅔n	11.6 (Nearly Exact)	22.8 (Approx.)
(9) I 3in @ Fixed Ends 1'-6"	78.1 (Approx.)	38.3 (Approx.)

Fig. 12

The evaluation* of D and K by the preceding formulas has been made for standard structural H sections and I beams and these properties are listed in Appendix II.

(6) Comparative Efficiencies of Different Sections - Fig. 12 shows the comparative torsional efficiencies of certain different shapes, showing the striking advantages of hollow box or tubular construction.

- - - - - - - - - - - - - - -

* The computations were made by John I. Copp through the courtesy of McClintic-Marshall Corp.

These advantages would not wholly obtain if the section were built up by use of bolts or rivets.

V. TORSIONAL DESIGN

(1) General Statement - Structural members are often called upon to carry torsional loads, generally as a secondary factor combined with bending or direct stress. Problems involving the bending of unsymmetrical sections, and problems of elastic stability, such as the buckling of flanges during bending, also require a knowledge of torsional properties.

In the design of relatively short beams to carry torsional loads considerable advantage may be obtained by fixing the ends, resulting in increased strength and rigidity, with corresponding decrease of angular deflection. External fixity is not needed--it is only necessary to box in the two flanges at each end and thereby prevent as nearly as possible, their relative warping. The two flanges then act as two rectangular fixed ended beams carrying a lateral displacement, mutually opposed in direction.

In designing relatively long beams, the end effect rapidly tapers out toward the center, and the formulas for pure torsion, free-ended, will be adequate and simpler in their application. It would still be of practical advantage and a means of additional safety, however, to box up the ends of the beam.

(2) Free-Ended Torsion - If a beam is to be designed as free-ended, only shearing stresses need by considered. Regardless of what partial restraint does exist as an incidental feature of the details, such a design will be on the safe side.

The critical shearing stresses will occur along the outer surface of the beam where the material is thickest, generally along the outside center-line of the flange and along the inside reentry fillets.

The following formula is proposed for the maximum shearing stress in the flange of an H or I beam in free ended torsion. For parallel sided flange sections,

$$s_F = \frac{T(D+n)}{2K}$$

For sloping flange sections,

$$s_F = \frac{T(D+m)}{2K} \qquad (27)$$

Shear stress in web,

$$s_W = \frac{Tw}{K} \qquad (28)$$

While equation (28) is in accord with torsional theory it gave results which proved low by comparison with actual tests. The following tentative formula was found to give better agreement.

$$s_W = \frac{T(w+0.3f)}{2K} \qquad (29)$$

f = fillet radius. This equation was adopted for use in the present investigation.

(See Fig. 9 for notation)

More accurate stress formulas might be developed by further use of soap film tests, taking slope measurements at critical points, and testing sections with various ratios of web, fillet, and flange as was done in determining the torsion constant. An equation somewhat like equation (29) will give practically the same values for flange stress as (27)

$$s = \frac{T(n+0.3f)}{K} \qquad (30)$$

Equation (27) was used in the present investigation.

(3) Concentration of Shearing Stress at Reentry Fillet - At the reentry fillet of an I-beam torsional shearing stress concentrations occur due to the sharp curvature of the fillet which causes a "piling up" of stress. These stresses are mostly of a local nature and do not greatly influence the yielding of the beam as a whole. While they do not necessarily govern the design of the beam they are important in the study of adequate fillet sizes and in the determination of loads producing strain lines in the fillets. In a beam subjected both to flexural and torsional stresses the total stress concentration at the fillet is the sum of the stresses due to these two causes. Professor Westergaard shows how the shearing stresses due to bending cause a concentration at the fillet of the juncture between web and flange, and several investigations have pointed out the concentration

of torsion stresses at the fillet. In order to get the combined effect it is therefore necessary to add together the concentrated stress due to bending and that due to torsion. Professor Westergaard's analysis of the concentration of shearing stresses at the fillet is given in his paper presented herewith as Appendix I.

The concentration of torsional stress at the fillet between flange and web is illustrated in Fig. 13 for the formulas developed by Foppl[9], Trefftz[8], Timoshenko[5], and Westergaard[Appendix I], and for soap film experiments carried out by Griffith and Taylor[3], and by Cushman[13]. It is noted that all curves indicate a rapid increase in stress concentration with the decrease of the ratio f/b between the radius of the fillet and the thickness of the section next to the fillet, particularly for ratios less than 1.0. Strain lines will therefore appear at relatively small torsional moment for sections having small fillets.

As the fillets become increasingly large another factor is introduced as the increased stress due to the greater thickness of material becomes of more importance. The rigidity of the beam is increased in proportion to the third power of the thickness while the stress varies directly with the thickness. Hence, for any given moment the stress would actually decrease. The curve of soap film tests by Griffith and Taylor indicate this reverse effect but further experiments along this line should be conducted to more definitely establish these relations.

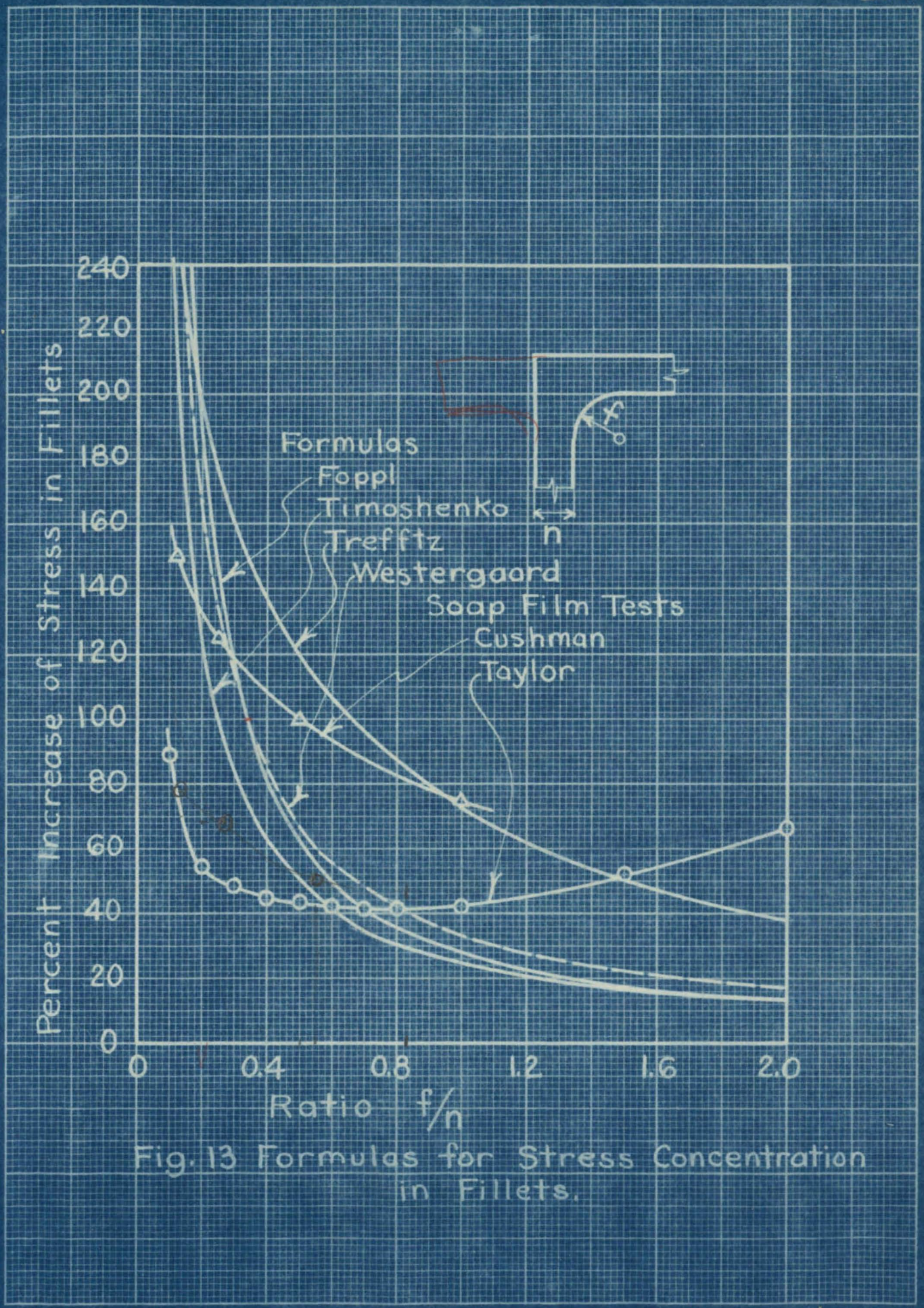

Fig. 13 Formulas for Stress Concentration in Fillets.

(4) Fixed-Ended Torsion

(a) Assumptions and Notation - If the ends of a non-circular section are fixed in some manner so as to prevent free warping of the end section we no longer have pure torsion.

Various investigators have studied this problem; Foppl[7], Timoshenko[5], Sonntag[7], and others. Recently an investigation was made on channel sections at the University of Illinois[10]. These investigators have generally been concerned with the problem of elastic equilibrium involved in the side buckling and twisting of a beam in bending without lateral support. Hence the torsion problem has been a secondary issue.

In the present tests both ends of structural beams have been fixed by welding on heavy end plates and additional side stiffening plates between the flanges at each end of the beam. The major stiffening effect produced is that of fixing the flanges relative to each other. (Refer to Fig. 14)

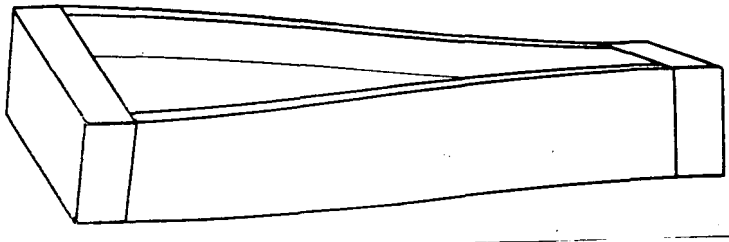

Fig. 14

The prevention of the individual warping of the component rectangular parts would taper out so rapidly that it would be of negligible importance. But by fixing the flanges with respect to each other, the effect of two opposed fixed ended beams is produced, as illustrated in Fig. 14.

The following assumptions have been made:

(1) The flanges remain at right angles to the web.

(2) That the angular deflection is small compared with the length of the beam.

(3) The bending of each flange about its weaker axes is a negligible factor.

(4) That a point on the neutral axis of one flange can be located with sufficient accuracy by coordinates (x,y) measured along and perpendicular to the original position of the axes.

(5) The two ends of the beam are held between mutually parallel planes as twisting takes place.

(6) That the displacement of the flanges due to beam action is due to bending only, i.e., lateral shearing deflection is neglected. (A correction is afterwards made for shearing deflection in very short beams).

(7) $\frac{I_y}{2}$ = Moment of Inertia of one flange about the web axis. This is very close and of great convenience in the case of standard I and H beams for which I_y is given in all handbooks.

The following notation in addition to that given in Fig. 9 will be used:

$$a = \frac{h}{2}\sqrt{\frac{EI_y}{KG}} = 0.806\ h\sqrt{\frac{I_y}{K}} \quad \text{for steel}$$

I_y = Moment of Inertia of the section about the center line of the web.

T = External twisting moment.

T_u = Torque required to twist beam in free-ended condition.

M = Bending moment developed by one flange in the plane of its stronger axis.

Q = Total lateral shearing force developed by one flange.

f_t = longitudinal fiber stress in flange due to bending.

ψ = Total angle of twist which any section turns through.

ℓ = Length of the beam.

h = Distance between flange centroids.

For sloping flange sections:

$$h = d - \frac{2}{3}\left(n + \frac{z^2}{z+n}\right)$$

or approximately $h = d - \frac{m+n}{2}$ (Sufficiently accurate for practical purposes).

(b) Derivation of General Equations - Consider now the equilibrium of any cut section as shown in Fig. 15. The outer torsional moment must be resisted by internal moment of the resisting forces and we have:

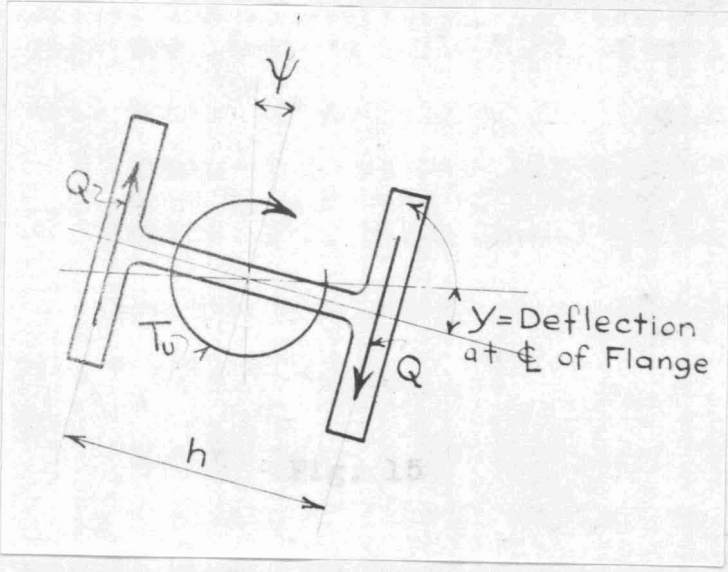

Fig. 15

$$T = T_u + Qh \qquad (31)$$

In terms of the chosen coordinates we have approximately the relation:

$$\frac{h}{2}d\psi = dy$$

and the twist per unit length = $\frac{d\psi}{dx}$

Hence,

$$T_u = KG\frac{d\psi}{dx} = \frac{2KG}{h}\frac{dy}{dx} \tag{32}$$

We may also write, assuming that the larger moment of inertia of one flange is equal to $I_y/2$,

$$\frac{EI_y}{2}\frac{d^3y}{dx^3} = -Q \tag{33}$$

Considering equations (31), (32) and (33), we have:

$$\frac{EI_y}{2}\frac{d^3y}{dx^3} - \frac{2KG}{h^2}\frac{dy}{dx} = \frac{-T}{h} \tag{34}$$

Differentiating with respect to x, and substituting

$a = \frac{h}{2}\sqrt{\frac{EI_y}{KG}}$ we get:

$$a^2\frac{d^4y}{dx^4} - \frac{d^2y}{dx^2} = 0 \tag{35}$$

We get as a general solution of this differential equation:

$$y = A\sinh\frac{x}{a} + B\cosh\frac{x}{a} + C + Dx \tag{36}$$

(c) Torsion with Both Ends Restrained - By proper evaluation of the constants for the conditions obtaining in a beam fixed at both ends, we get--

$$y = \frac{Tha}{2KG}\left(\cosh\frac{x}{a}\tanh\frac{\ell}{2a} - \sinh\frac{x}{a} + \frac{x}{a} - \tanh\frac{\ell}{2a}\right) \tag{37}$$

for $x = \ell$. $y = \frac{Tha}{2KG}\left(\frac{\ell}{a} - 2\tanh\frac{\ell}{2a}\right)$ = total deflection (38)

The moment in each flange

$$M = \frac{EI_y}{2} \frac{d^2y}{dx^2} \quad \frac{Ta}{h} \frac{\sinh u}{\cosh \ell/2a} \tag{39}$$

where $u = \frac{\ell}{2a} - \frac{x}{a}$

and further the shear in each flange:

$$Q = \frac{EIy}{2} \frac{d^3y}{dx^3} = \frac{-T}{h} \frac{\cosh u}{\cosh \ell/2a} \tag{40}$$

The longitudinal stresses along the outer fibres of the flanges will be given by:

$$f = \frac{Mc}{I} = \frac{Mb}{I_y} = \frac{Tab}{hI_y} \frac{\sinh u}{\cosh \ell/2a} \tag{41}$$

Critical stress will be either longitudinal stresses at the end of the beam or the sum of the lateral and torsional shearing stresses at the center of the beam.

At the end of the beam $u = \frac{\ell}{2a}$, so we have,

$$f = \frac{Tab}{hI_y} \tanh \frac{\ell}{2a} \tag{42}$$

And at the center of the beam $u = 0$, giving,

$$Q_c = \frac{T}{h} \operatorname{sech} \frac{\ell}{2a} = \frac{T}{h \cosh \ell/2a} \tag{43}$$

At the center of the beam both the lateral and torsional shearing unit stresses will be maximum in the middle of the flange.

By the simple beam theory, the lateral shearing unit stress will be:

For parallel flange sections,

$$s = \left(\frac{3}{2} \frac{Q}{\text{area one flange}}\right) = \frac{Qb^2}{4I_y} \tag{44}$$

For sloping flange sections we obtain

$$s = \frac{Qb^2(2n + m)}{12mI_y} \tag{45}$$

For torsional shearing stress at the center of the beam, we consider again the approximate formulas proposed in equations (27) and (29). In place of **K**, the torsion constant, we must now use an equivalent constant which is measured by the rate of angular twist at the center of the beam.

To obtain this, we differentiate equation (37) with respect to x, giving the slope of the flange $\frac{dy}{dx}$ at any point. The unit angular twist $\frac{d\psi}{dx} = \frac{2}{h}\frac{dy}{dx}$ and from this relation and the substitution of $x = \ell/2$ we get an expression for $\theta_c = \frac{d\psi}{dx}$ at the center.

$$\theta_c = \frac{T}{KG}\left[\frac{\cosh(\ell/2a)-1}{\cosh(\ell/2a)}\right] \tag{46}$$

This derivation has been based on the assumption[6] that deflection is due to bending only. As we shorten the beam, however, shearing deflection becomes of increasing importance and needs to be considered.

S. Timoshenko[6] has indicated a strain energy method for calculating the deflection due to shear when cross-sections are constrained from warping. By combining his result for the simple cantilever beam we may obtain the following correction for a fixed-ended beam with point of inflexion at the center:

$$1 + 2.95\,\frac{b^2}{\ell^2}$$

$$\theta_c = \frac{T}{KG}\left(\frac{\cosh(\ell/2a)-1}{\cosh(\ell/2a)}\right)\left(1+2.95\frac{b^2}{\ell^2}\right) \qquad (47)$$

and denoting the "equivalent" torsion constant at the center by C_c, we have:

$$C_c = \frac{T}{\theta_c G} = K\left(\frac{\cosh(\ell/2a)}{\cosh(\ell/2a)-1}\right)\left(\frac{1}{1+2.95(b^2/\ell^2)}\right) \qquad (48)$$

Using C_c as the measure of torsional shear developed at the center of the beam in place of K and combining equations (27) with equations (44) and (43) we get the following expressions for combined torsional and lateral shearing stresses.

(d) Total Maximum Shearing Stress at Center of of Beam (Along center line of flange) -

For parallel flange sections:

$$s = T\left(\frac{b^2}{4hI_y\cosh(\ell/2a)} + \frac{(D+n)}{2C_c}\right)$$

For sloping flange sections:

$$s = T\left(\frac{b^2\,(2n+m)}{12hmI_y\cosh\,\ell/2a} + \frac{D+m}{2C_c}\right) \qquad (49)$$

And the stress in the web may be computed by:

$$s_w = \frac{T(w+0.3f)}{C_c} \qquad (50)$$

(e) Total Twisting Deflections of Fixed-Ended Beams - We have in equation (48) an equivalent torsion constant based on the unit angular twist at the center of the beam. We desire to obtain a measure of the total twisting deflection of the beam over the whole length and can do this effectively by evaluating an average equivalent torsion constant which will be denoted as C_A.

The expression for total angular twist is then:

$$\psi = \frac{T\ell}{C_A G} \tag{51}$$

For very short beams most of the deflection is shearing deflection and C_c approaches C_A in value. We have in equation (38) an expression for the total deflection of the flanges due to bending only. From equation (38) C_A may be evaluated insofar as bending deflections are concerned.

The ratio of C_A/C_c reduces to the following expression:

$$C_A/C_c = \frac{\cosh \frac{\ell}{2a} - 1}{\left(\cosh \frac{\ell}{2a}\right) - \left(\frac{2a}{\ell} \sinh \frac{\ell}{2a}\right)} \tag{52}$$

The graph of C_A/C_C is given on Fig. 16, permitting the quick calculation of C_A after C_C is known. As the length approaches zero, C_A should approach C_C in value and the curve on Fig. 17 gives the reduction to be made in C_A for various ℓ/b ratios in terms of a factor to be multiplied by (C_A-C_C)

As an example, let:

$$C_C = 6.00 \text{ by formula} \qquad (48)$$

$$\ell/2a = 2.00$$

$$\ell/b = 5.00$$

From Fig. 16, $C_A/C_C = 1.42$

From Fig. 17, Reduction = $(0.42)(0.105) = .044$

$$C_A = 6.00\ (1.42 - .044) = 8.28$$

(f) Torsion with One End Fixed and One End Unrestrained - It will often occur in cases of combined bending and torsion that one end of the beam will be relatively unrestrained while the other end is fixed. At the free end there will be no lateral shearing stresses in the flanges and the shearing stress formulas (27) for free end torsion will apply. The evaluation of equation (36) for these end conditions gives the following.

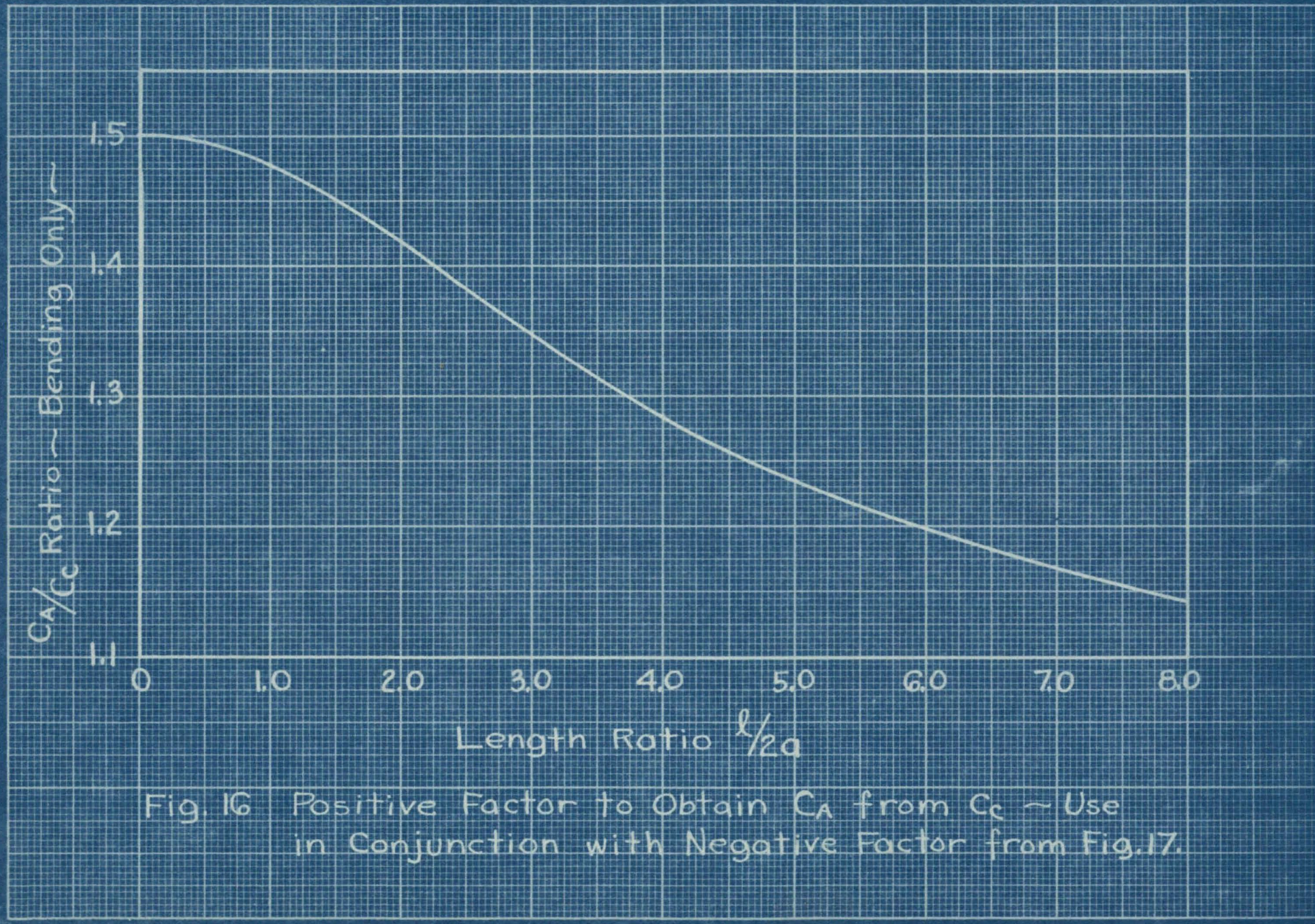

Fig. 16 Positive Factor to Obtain C_A from C_c ~ Use in Conjunction with Negative Factor from Fig. 17.

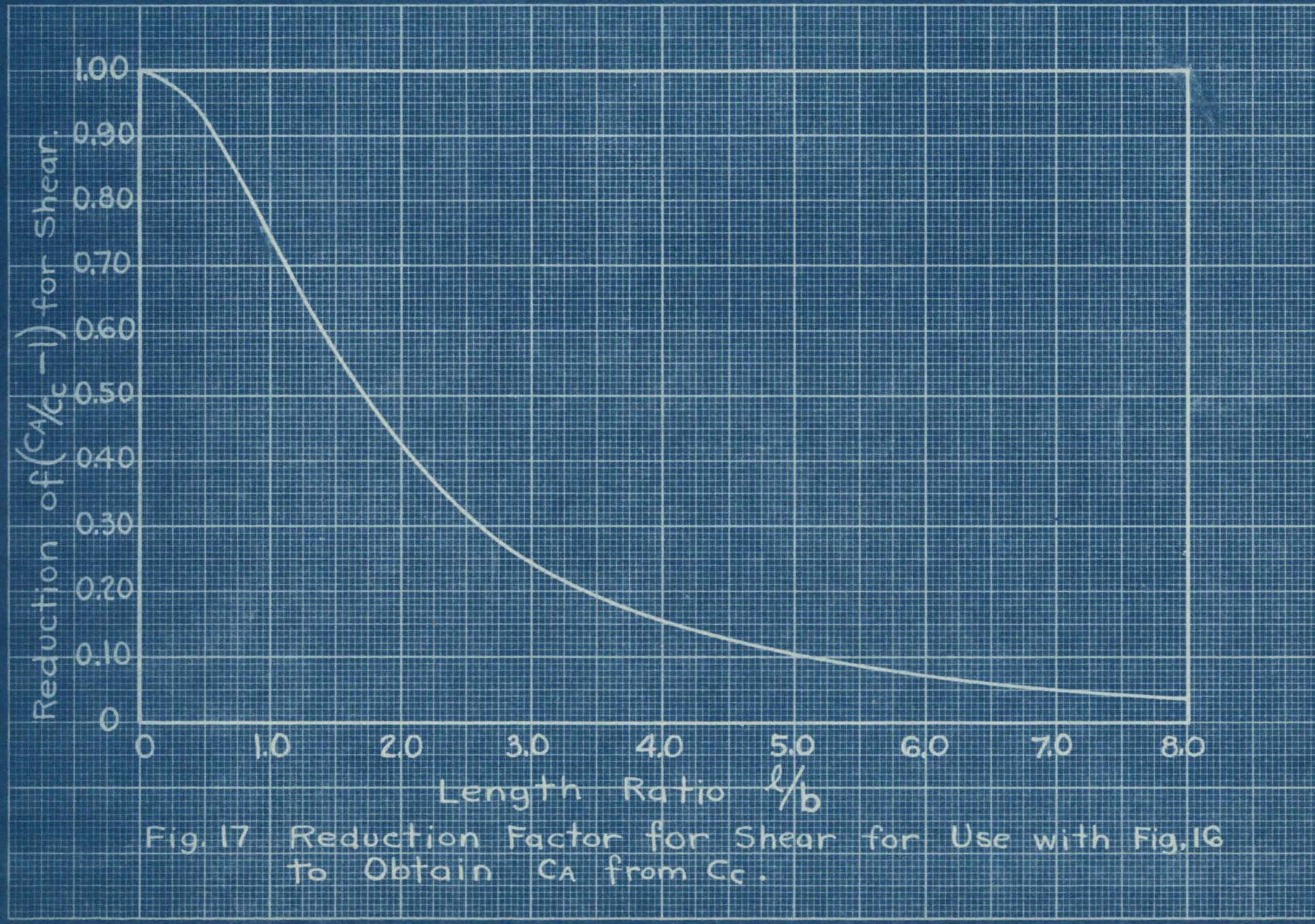

Fig. 17 Reduction Factor for Shear for Use with Fig. 16 to Obtain C_A from C_c.

Maximum bending moment in flange at the restrained end:

$$M_{max} = \frac{Ta}{h} \tanh \frac{\ell}{a} \qquad (53)$$

Maximum direct fibre stress in outer edges of the flanges at the restrained end:

$$f = \frac{Tab}{hI_y} \tanh \frac{\ell}{a} \qquad (54)$$

The total angle of twist is given by:

$$\psi = \frac{Ta}{KG}\left[\frac{\ell}{a} - \tanh \frac{\ell}{a}\right]\left[1+0,74\frac{b^2}{\ell^2}\right] \qquad (55)$$

The preceding equation will be accurate for all except very short beams.

Fig. 18 shows the application of the proposed formulas for maximum longitudinal and shearing stresses to varying lengths of an 8 by 8-in. H-beam fixed at both ends. It is noted that for lengths ranging between about one and nine feet the longitudinal stresses based on an allowable unit stress of 22,000 lb. per sq.in. determine the design. For very short lengths and for long lengths the shearing stresses are critical.

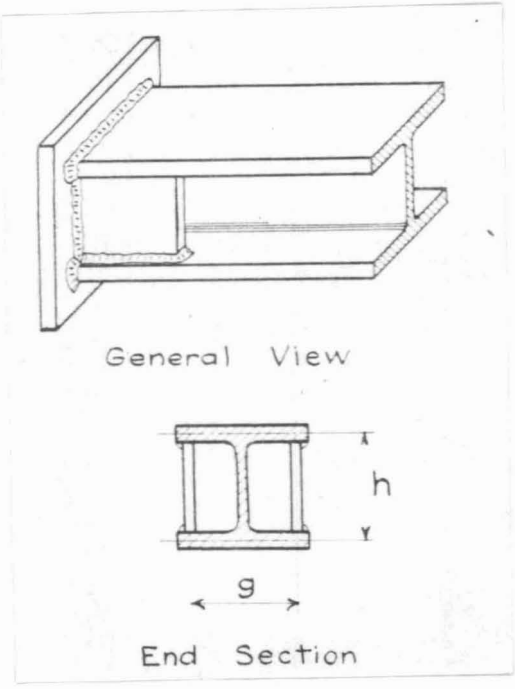

Fig. 19

(g) Design of End Connection - It is suggested that the end connections be built as is illustrated in Fig. 19. Connections of this

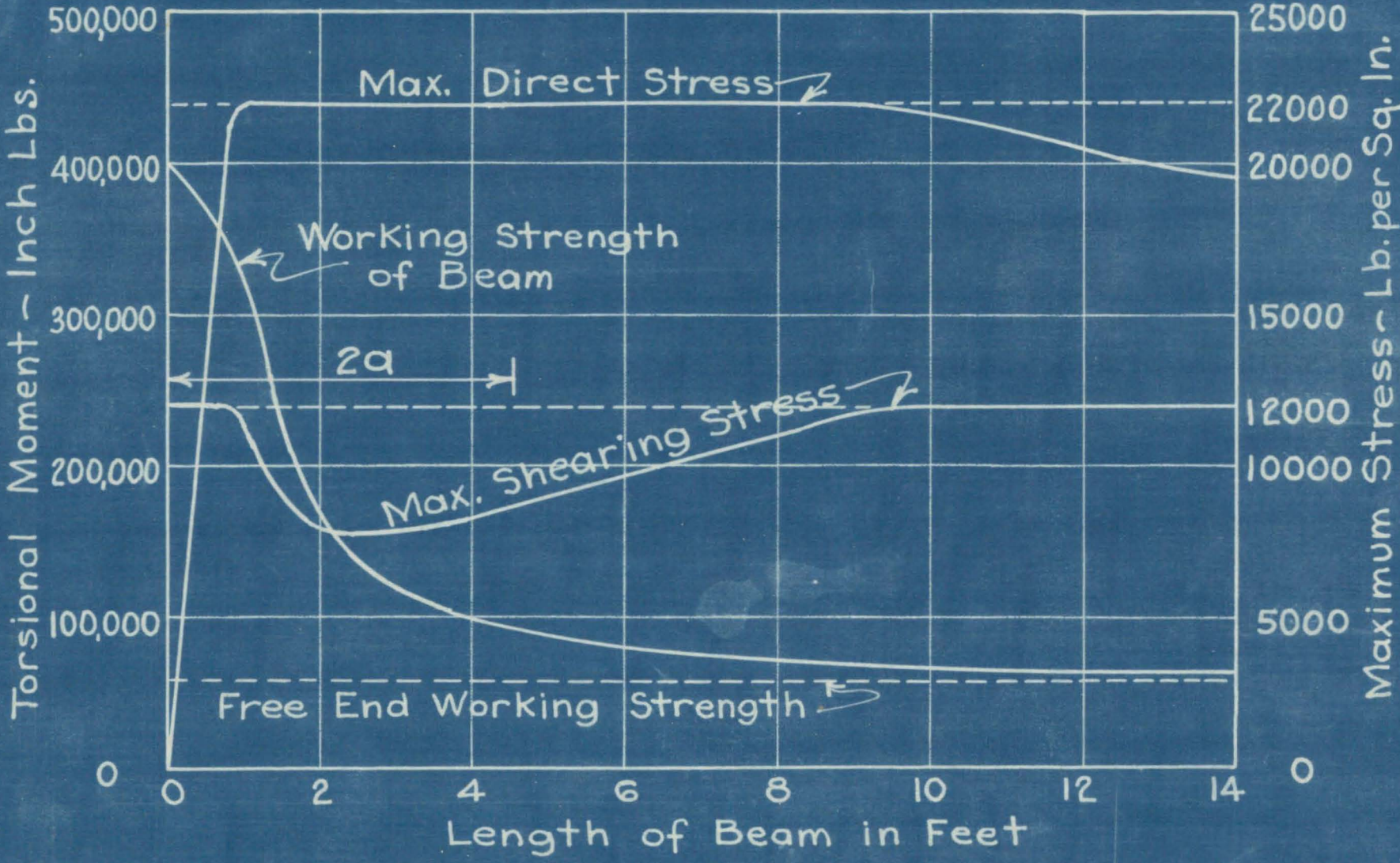

Fig. 18 Working Strength of an 8×8 Beam with Fixed Ends Showing Limiting Stresses for Different Lengths.

type proved very satisfactory in the actual torsion tests and provided comparatively complete end fixity. The purpose of the end plates is to prevent relative warping of the flanges and the following approximate analysis should serve as a guide in the design.

The moment in one flange at the end is obtained from equation (39)

$$M = \frac{Ta}{h} \tanh \frac{\ell}{2a} \tag{56}$$

The length ℓ should be measured as the overall length.

Let: Q = total shear of the beam in stiffening plate

g = distance between stiffening plates.

Then if the stiffening plates alone are assumed to fix the ends of the beam we will have:

$$M = Qg \tag{57}$$

Substituting in (56) we obtain:

$$Q = \frac{Ta}{hg} \tanh \frac{\ell}{2a} \tag{58}$$

The stiffener plate is welded to both flanges and to the end plate as well. The stiffener and the adjoining portion of the end plate act as a short fixed-ended beam holding the flanges in place. No attempt was made to analyze the load distribution and the design of the test beams was largely a matter of judgment.

The following suggestions for end are tentatively made as the result of the tests:

(1) Length of stiffener along the beam should be equal to about 3/4 width of the flange for H sections and equal to the full flange width for I-beams.

(2) The thickness of the stiffener plate material should be greater than that of the web thickness or greater than one-tenth the length of the stiffener plate along the beam.

(3) The stiffeners should be machined to a tight fit between the flanges and welded to flange and end plate continuously on the outer portion.

(4) The end plates should have a thickness equal to twice the maximum thickness of beam material.

(5) The beam should be cut square and welded to the end plate with a continuous fillet weld about the entire beam end.

The stiffener plate and the weld between it and the flange should be designed to resist the shear as computed by equation (54).

(5) Combined Bending and Torsion - The problem of combined bending and torsion occurs when loads producing bending are eceentrically applied with respect to the centroidal axis of the beam. If the loading is symmetrical with respect to the length of the beam, the total torsional moment will be equally divided between the two halves of the beam and each end connection must be designed for half the total torque. It is also to be noted that the torsional

moment will be balanced about the center part of the beam and this section will be restrained from warping regardless of whether or not the extreme ends are restrained.

It will be necessary to combine the stresses due to bending with those due to torsion at critical points. At the center of flange at places of maximum combined torsional and flexural moment, the shearing stresses due to torsion may be combined with the direct stress due to bending to give the maximum principal stress by the following formula:

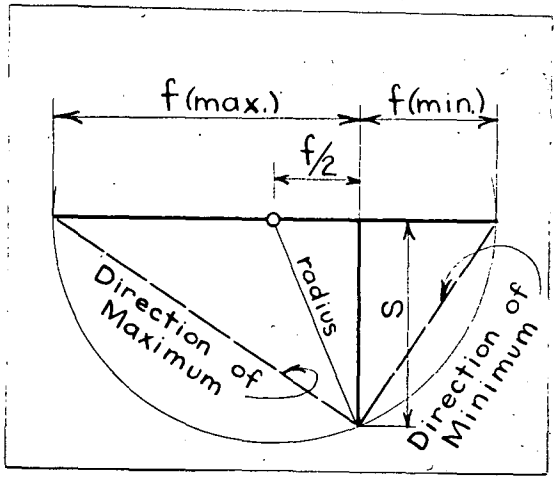

Fig. 20

$$f(\text{max. principal stress}) = -\frac{f}{2} + \sqrt{\frac{f^2}{4} + s^2} \qquad (59)$$

The graphical solution of this equation is shown in Fig. 20.

The longitudinal stresses in the flanges due to torsionally restrained ends are maximum along the outer fibres of the flanges at points of restraint. These stresses are similar in nature to secondary stresses, affecting initially only a small part of the flange and generally not a primary cause of general failure. It is recommended therefore, that they be added directly to the direct stress due to bending and that the allowable stress be raised to that which is used for secondary stress analysis.

The applied torsional moment may vary along the beam and a diagram of its variation will be shaped like the vertical shear diagram for the direct loads producing bending. Exact solutions for special cases may be made by solving equation (34) with the substitution for T of T as a function of X.

(5) Design Examples -

(a) General Remarks - The most economic structural H or I beam for torsional strength is one in which the material is most nearly of constant thickness throughout and is as thick and compact as obtainable. Column sections with parallel sided flanges and of the heaviest rolling in each series most nearly satisfy these requirements.

The torsional design should be made with ends assumed free in the case of riveted or bolted end connections; any percentage of end fixity incidentally present will simply provide an additional factor of safety. Only shearing stresses as computed by equations (27) and (29) need be considered in free end design.

Beams with boxed in and continuously welded end connections will be somewhat stiffer and stronger depending on the length. Both longitudinal stresses and shearing stresses must be considered (see Fig.18). Tests indicate that the shearing stresses generally determine the yield point of the beam as a whole. The local direct stresses at the ends affect initially only a small portion of the beam and are in

the nature of secondary stresses. Shearing yield on the other hand takes place along the entire beam length. The allowable direct fibre stress will be made 22,000 lb.per sq.in. in the present discussion. It is suggested that allowable fibre stresses usual in secondary stress design be applied in general to these stresses.

(b) General Data -

Allowable Working Stresses: (f = 22,000 lb.per sq.in. for secondary stresses due to fixed end torsion; s = 12,000 lb. per sq.in.

E = 29,000,000
G = 11,150,000
Poisson's Ratio = 0.30

1 degree = 0.01745 radians

1 radian = 57.30 degrees

ℓ = overall length of beam including stiffeners along which a uniform torsional moment is assumed to act.

NOTE: Computations in these problems were made with a 10-inch slide rule.

(c) Design Example A - A long beam with torsional deflection limited.

Assumed Conditions - A beam 20 ft. long to resist a total torsional moment of 20,000 in-lb. with maximum total twist under load limited to 1.2 degrees.

Procedure for Design as Free Ended - (1) Determine the unit angle of twist θ in radians per inch.

$$\theta = \frac{1.2 \times 0.01745}{20 \times 12} = 0.0000872 \text{ radians per inch}$$

(2) Calculate required K from equation (7)

$$K = \frac{T}{G\theta} = \frac{20{,}000}{11{,}150{,}000 \times 0.0000872} = 20.6 \text{ in.}^4$$

(3) Refer to tables of K values and pick out the most economical section.

B10b, 10 x 10 at 124 lb. per ft. with K = 20.37 will be satisfactory. We may depend on the end connection to provide a few per cent additional rigidity and allow a small tolerance in picking sections.

(d) Design Example B - Analysis of the torsional strength of a short beam with different end connections.

General Data - B8b, 8 x 8 at 67 lb.per ft.

ℓ = 5'6" overall = 66 in.

K = 5.145 in.^{4}

I_y = 88.6 in.^{4}

n = 0.933 in.

b = 8.287 in.

D = 1.206 in.

h = (9.000)-(0.933)=8.067 in.

$$a = 0.806h\sqrt{\frac{I_y}{K}} = 27.0 \text{ in.}$$

$$\frac{\ell}{2a} = \frac{66}{54} = 1.22 \text{ in.}$$

$$\cosh \frac{\ell}{2a} = 1.8412$$

$$\tanh \frac{\ell}{2a} = 0.8397$$

Free-Ended Working Strength - From equation

(27) $T = \frac{2Ks}{D+n} = \frac{(2)(5.145)(12,000)}{1.206 + 0.933} = 57,700$ in-lb.

Fixed-Ended Working Strength - (a) Based on Shear

Compute the equivalent torsion constant C_c for the center of the beam by equation (48).

$$C = 5.145\left(\frac{1.8412}{1.8412-1}\right)\left(\frac{1}{1+2.95\left(\frac{8.29}{66}\right)^2}\right) = 10.77 \text{ in.}^4$$

Then from equation (49)

$$T = \frac{12,000}{\left[\frac{8.29^2}{(4)(8.067)(88.6)(1.841)} + \frac{1.206+0.933}{(2)(10.86)}\right]} = 108,000 \text{ in-lb.}$$

(b) Based on longitudinal fiber stresses at ends (tension or compression). From equation (42)

$$T = \frac{22,000}{\left[\frac{(27.0)(8.287)}{(8.067)(88.6)}\right](0.8397)} = 84,000 \text{ in-lb.}$$

The longitudinal stresses therefore determine the design of the beam and the allowable torsional moment is 84,000 in-lb.

(c) Design of end connection (see page 31)

The shear to be resisted by the end plate is computed by equation (54).

$g = 6.5$ in. (assumed)

$$Q = \frac{(84,000)(27.0)}{(8.067)(6.5)}(0.8397) = 36,300 \text{ lb.}$$

A 5/8-in. plate fitted into the 7.13 in. space between the flanges and 6 in. in length along the beam will satisfy the requirements suggested on page 33. Assume a 5/8-in. fillet weldbetween stiffener and flange.

$$g = 8.827 - (3)(5/8) = 6.41$$

$$Q = \frac{6.5}{6.41} \times 36,300 = 36,800 \text{ lb.}$$

The stress in the plate is:

$$s = \frac{36,800}{(5/8)(6)} = 9800 \text{ lb. per sq.in.}$$

and in the weld:

$$s = \frac{36,800}{(5/8)(0.707)(6)} = 13,900 \text{ lb. per sq.in.}$$

(too high)

Make the plate 7-1/2 in. long rather than 6 in.

Stress in weld:

$$s = \frac{6}{7.5} \times 139,000 = 11,100 \text{ lb. per sq.in.}$$

which is below the 11,300 lb. per sq.in. limit specified by the A.B.W.S. recommendations.

VI. TEST RESULTS

(1) Soap Bubble Tests

(a) Purpose and program - The purpose of the present series of tests was that of accurately evaluating the torsion constant of structural H and I sections. Specifically this problem narrowed down to determining the added torsional rigidity introduced by the juncture of two rectangles, with fillets at the reentry corners,

over and above the torsional rigidity of these rectangles treated as separate members. The problem was therefore that of determining α in equation (18). In order to establish the value of α for any shaped section it was necessary to consider two variables, R_1, the ratio of web to flange thickness, and R_2, the ratio of fillet radius to flange thickness. It was further essential to study sections with sloping flanges as well as those with parallel sides.

A program of tests was outlined to cover a wide range of the two variables, R_1 and R_2. While it would have been desirable to measure the slopes of the bubbles and thereby study the stresses, particularly in the fillets, such a study would have greatly reduced the total number of tests possible. It was thought better to definitely establish the torsion constant in which case it was only necessary to measure the volume of the displaced bubble. In each series a basic web and flange thickness was adopted and after testing the section with zero fillet radius, the variously sized fillets were cut away in sequence as pictured in Fig. 21.

(b) Apparatus - Fig. 22 shows a general view of the apparatus set up for operation. The equipment consisted of two essential parts; (1) the volume displacement apparatus and (2) the box holding and measuring the soap films.

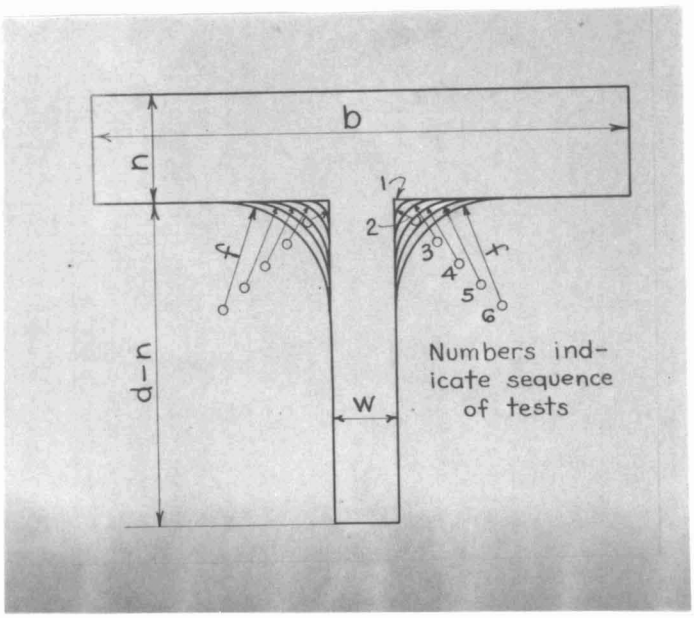

Fig. 21

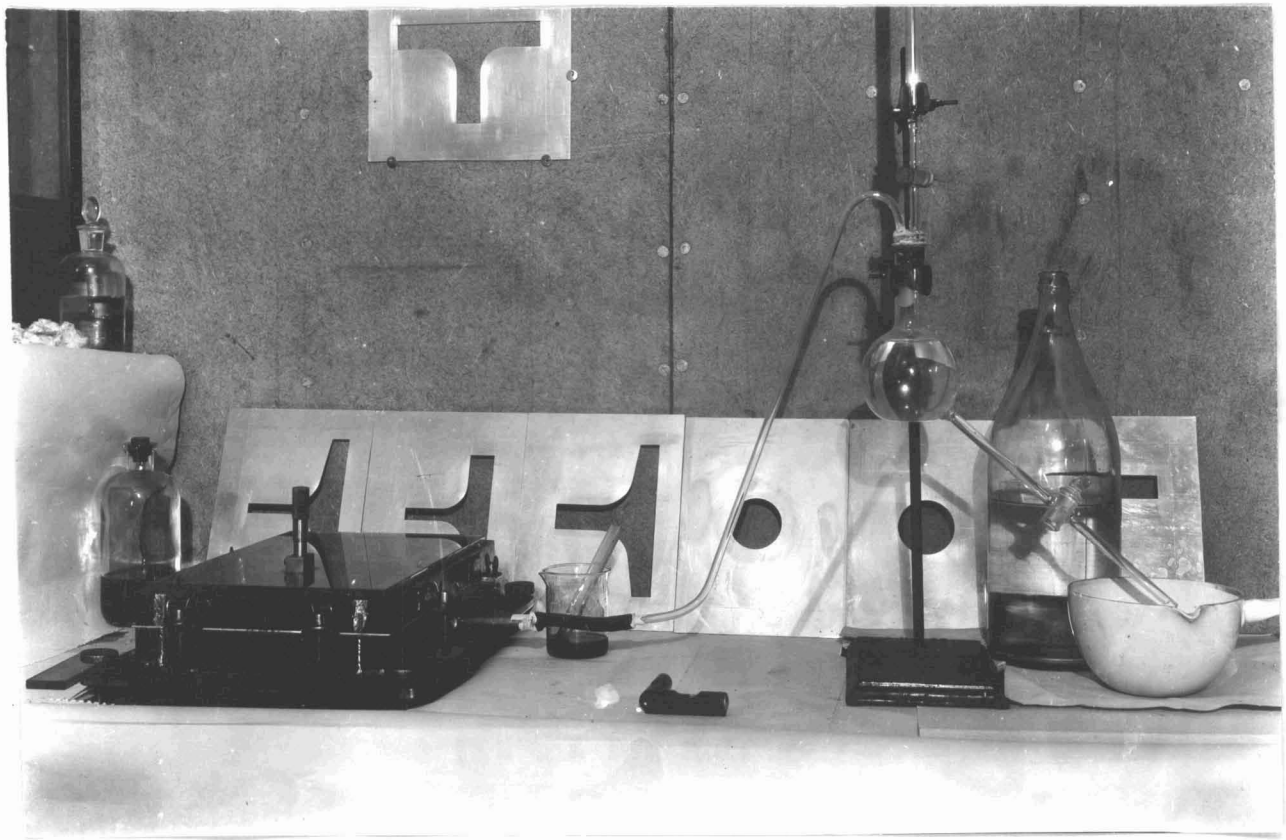

Fig. 22

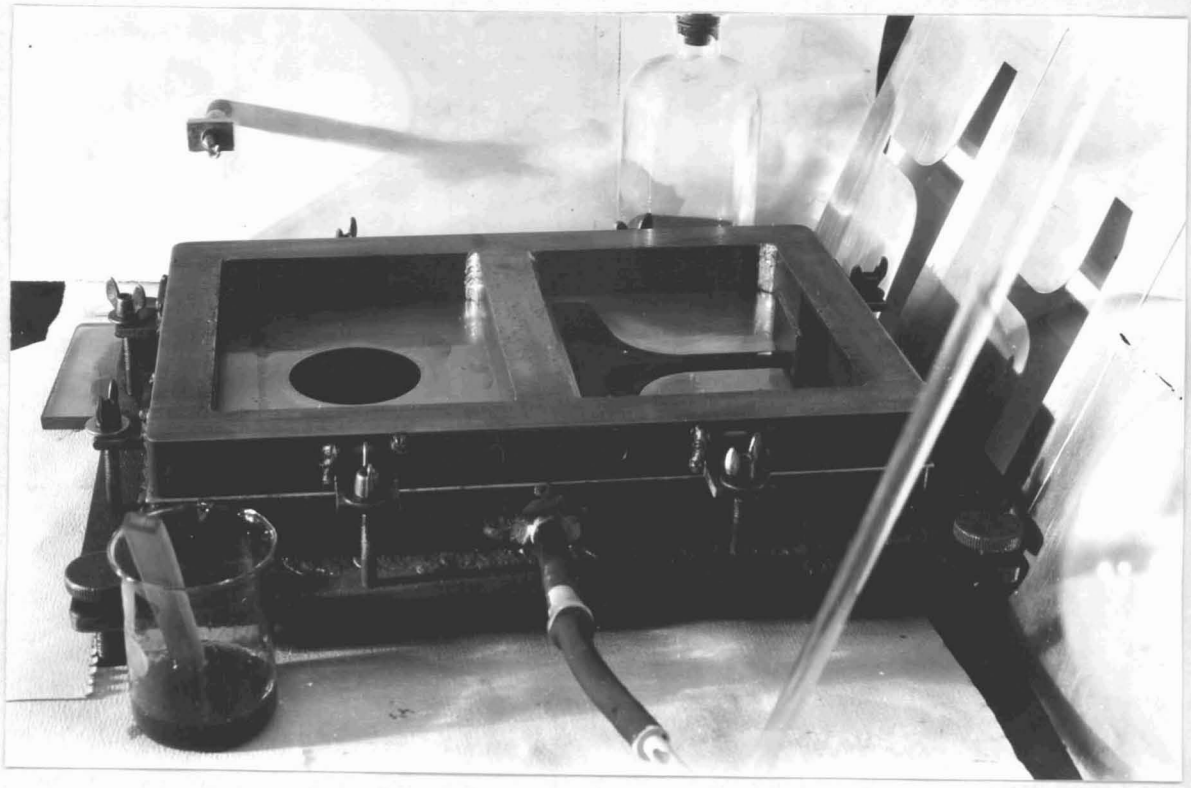

Fig. 23

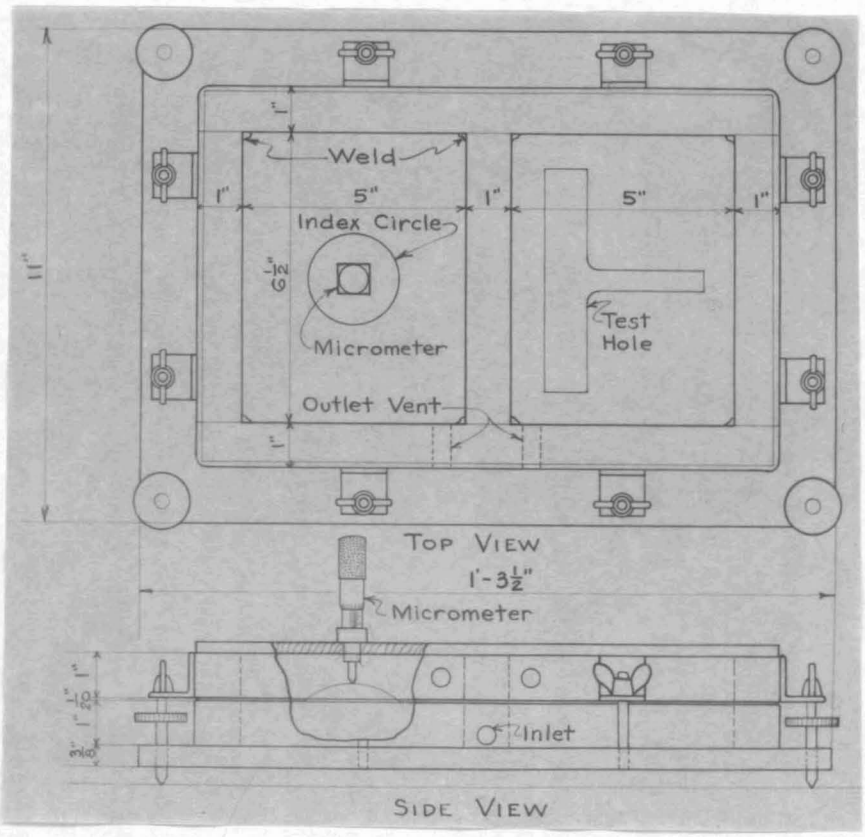
Weld
1"
5"
1"
5"
1"
Index Circle
Micrometer
Test Hole
Outlet Vent
11"
TOP VIEW
1'-3½"
Micrometer
Inlet
SIDE VIEW

Fig. 24

The volume displacement chamber was made with a 250 cc flask to the bottom of which was welded a drainage tube with a stop-cock. A two-hole rubber cork in the top of the flask received a 50 cc burette, graduated to 0.1 cc, and a glass tube for transmitting air to the box. All joints were treated with white lead paint and were air tight.

The receptacle for holding the soap films is shown in Fig. 23 and is detailed in Fig. 24. The lower part consisted of a flat plate to which was soldered the double box frame made of one inch square bars welded together. Thumb screws in each of the four corners provided a means of supporting and leveling the apparatus. Eight stud bolts were fitted in the plate to receive and tighten down the upper box with wing nuts and washers. The entry tube for air from the volume displacer was of brass, screw threaded at the end to enter a tapped hole in the lower frame. The air had free access to both lower chambers by means of a recess in the end of the lower frame center piece. The top of the lower frame was machined to receive the two aluminum test pieces. The detachable upper frame was made in the same shape as the lower part and machined on both faces. The small clip angles welded on the upper frame had holes in their outstanding legs to receive the eight bolts from the lower frame. Two holes from each of the upper chambers permitted escape of displaced air. All joints in the apparatus were sealed. Over the

upper chamber rested a removable section of 1/4-in. plate glass fitted with a pointed micrometer for measuring the height of the circular bubble.

(c) Test Plates - The test plates were made from stock aluminum sheets 0.05-in. thick. The holes were laid out with a scribe and roughed in with a power jig-saw. Small steel files were used to cut close to the line and the final shaping was made with fine emery cloth. The under side of the cut was beveled as shown in Fig. 25.

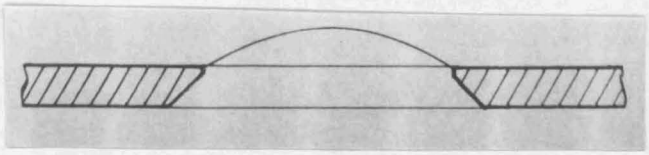

Fig. 25

At the end of the web it was desired to provide discontinuity to the bubble, and a small section of steel angle with machined surfaces was provided for this purpose. Fig. 26 shows the entire series after the tests had been made.

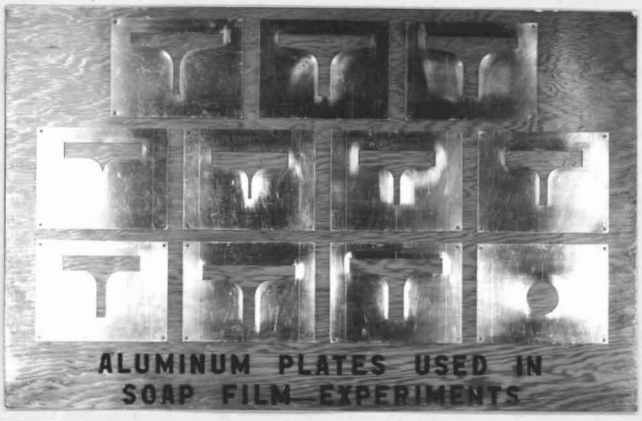

Fig. 26

The method of volume measurement used in the present investigation was that of measuring directly the total displacement of the two bubbles, and subtracting from the total increase in volume the calculated volume of the circular bubble. Water from a burette is introduced into an air tight compartment which serves as a displacement chamber. The displaced air is transmitted into the soap film apparatus to displace the soap bubbles. The total volume of the water introduced will not be exactly equal to the total volume of the bubbles because of the slight increase of pressure in the compartment. An experimentally determined correction curve must therefore be made preliminary to the actual tests. This correction is based upon tests between sections of known torsional properties. The preceding method of volume measurement proved to be rapid, convenient, and accurate.

(d) Test Results - As stated above, it was necessary to establish a correction factor which when multiplied by the volume of water drained from the burette would give the actual net volume of the displaced soap bubbles. To insure that the pressure change during each test be a constant, the same initial and final height of the circular bubble was used during each trial. Four circular index holes were made in all, these having diameters of 2.000, 2.100, 2.250, and 2.400 inches. In addition a square calibration section was made 2.001 by 2.001 inches in size and

a 1.000 by 5.000-inch rectangle was also cut. These sections and circles of known torsional properties were tested against each other so as to give the proper correction factor to use for various proportions of volume. The two variables best adapted to serve as a base for the correction factor were: first, the total volume of water (V_w) introduced from the burette, and second, the known volume of the circular bubble (V_c) calculated from the measured height. The correction factors were evaluated in terms of the ratio $\frac{V_w}{V_c}$. The results are shown graphically in Fig. 27. Most of the points are within a range of 0.5 per cent and the error in the tests should therefore be less than 0.5 per cent.

The test results are shown graphically in Fig. 28 and 29. It will be noted that most of the scattered points occur along the lines of 0.0 and 0.2 fillet radius. These variations may be due to the difficulty in machining the plates with the small fillets, a very slight inaccuracy causing considerable variation in the diameter of the inscribed circle D. A further difficulty is encountered in the plates of zero fillet radius due to the tendency of the soap film to jump across these sharp corners. Most of the structural beams actually rolled have ratios of R_1 and R_2 both greater than 0.5 and in this area it will be seen that the data are quite consistent.

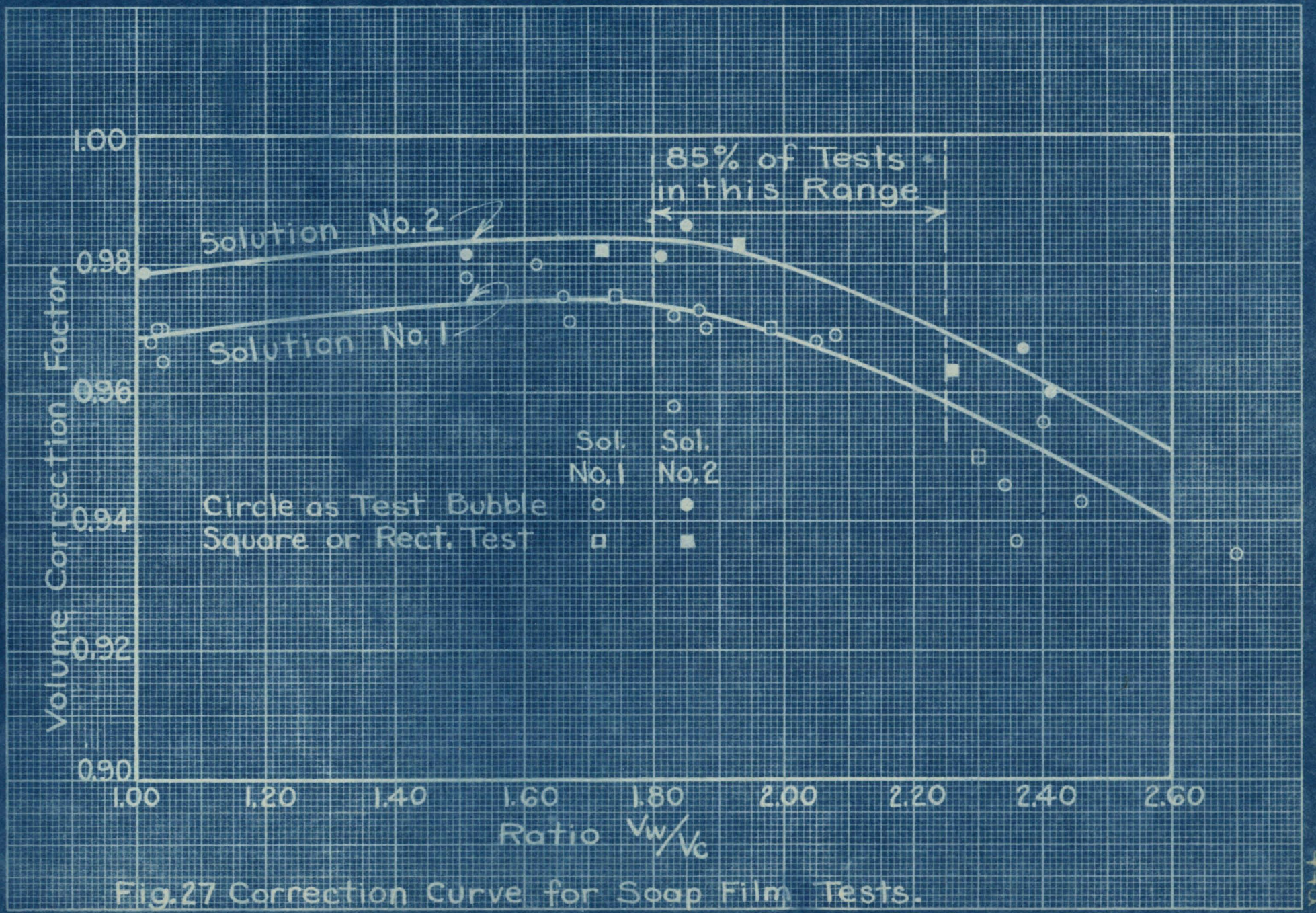

Fig. 27 Correction Curve for Soap Film Tests.

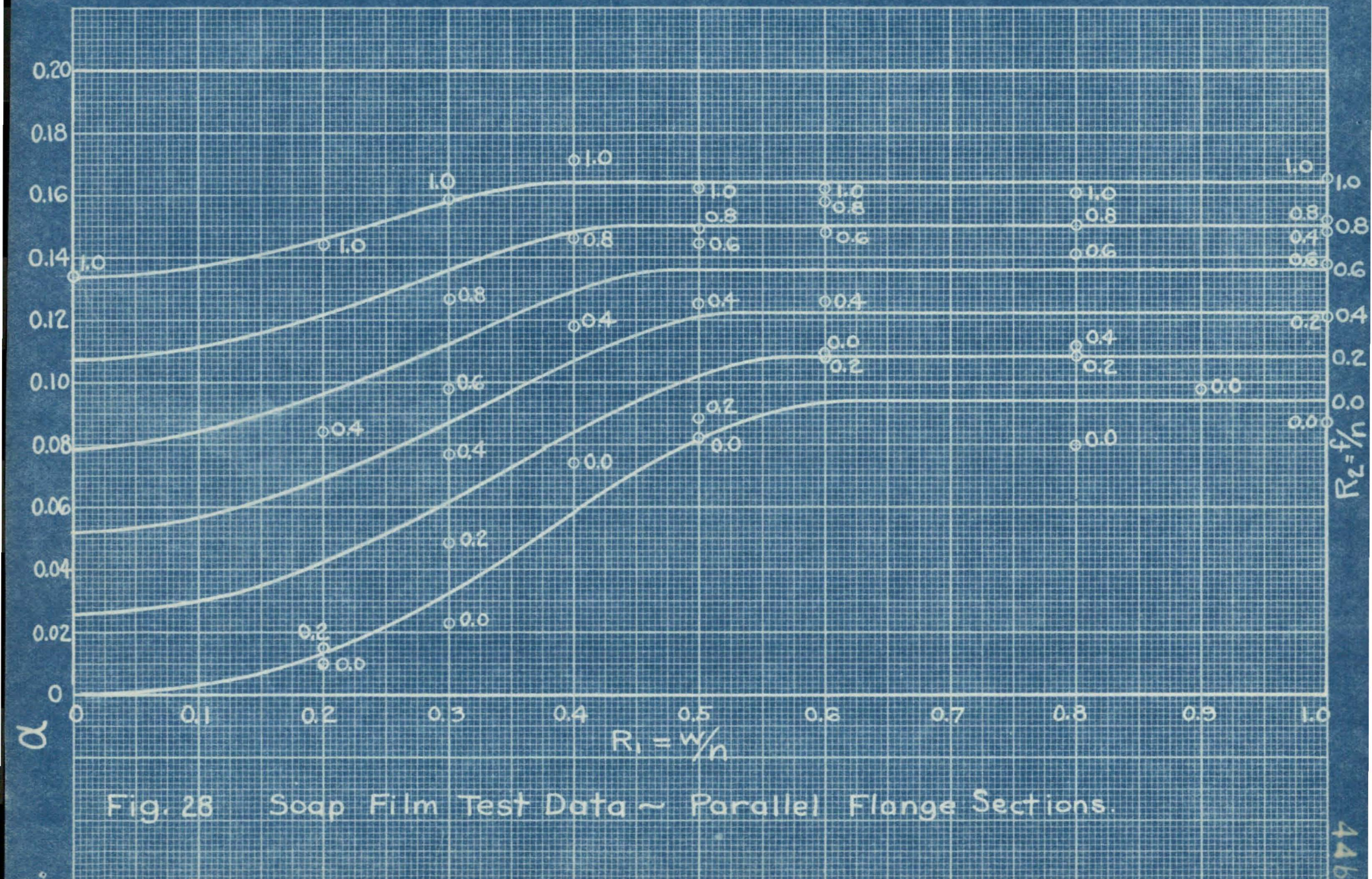

Fig. 28 Soap Film Test Data ~ Parallel Flange Sections.

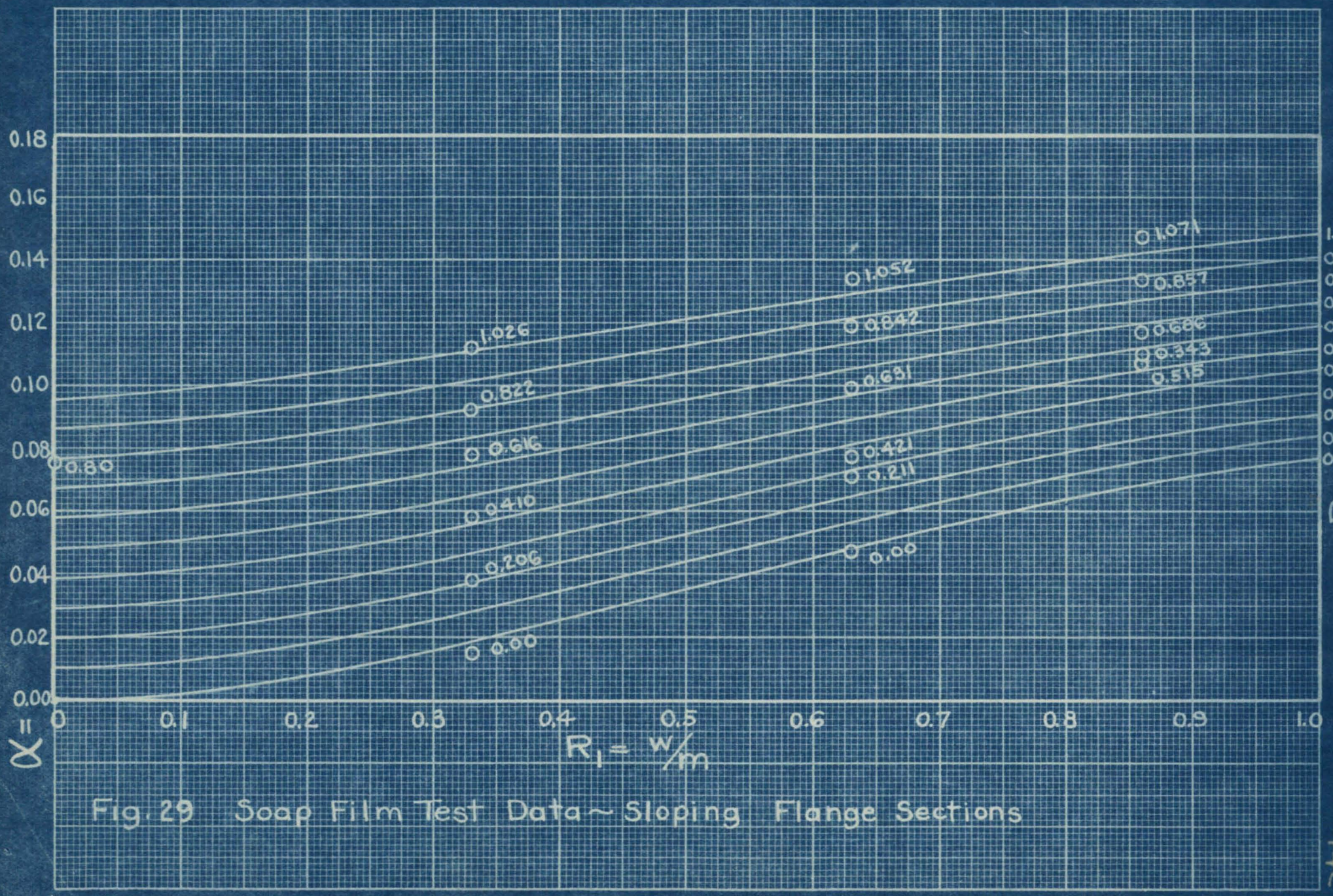

Fig. 29 Soap Film Test Data ~ Sloping Flange Sections

(2) Tests of Steel Beams

(a) Purpose - The torsion tests made on steel beams were made with several objects in view. The sections themselves were chosen so as to give as great as possible a range in shape and size, and tests of certain unusual shaped sections which are not at present standard were nevertheless valuable in the present investigation.

Free ended tests were made on a number of beams in order to check the results of the soap film experiments and corresponding method of calculating the torsion constant. In these tests the distribution of shearing stress was studied, and a check obtained on the proposed approximate formulas for stress.

Fixed ended tests were made on different shaped beams and the effect of variations in the length was studied. A type of end connection design was developed to give a considerable degree of fixity.

(b) Apparatus - The first torsion machine was built to test beams three feet long welded at the ends to one-inch plates. It had a capacity of 200,000-inch-pounds and was used in connection with a standard four-screw Olsen testing machine of 300,000 lb. capacity. The torsional moment was transmitted by two cross beams which acted in compression through rollers to apply a twisting moment to two I-beams fixed to the end plate of the test specimen. The machine

functioned properly but only one test was made with it. A simpler and more flexible machine was designed as an outgrowth of the first; the new machine operating on the same general principle but applying the twist by means of cables and sheaves instead of rollers in compression.

A standard Olsen Torsion machine of 26,000 in-lb. capacity was used to test 3-in. I beams fixed ended, of various lengths. It was also used for torsion tests of round bar samples of all material to determine the shearing modulus of elasticity.

The cable torsion rig, illustrated in Fig. 30 and 31 had an ultimate capacity of 800,000 in-lb. and was applicable to either free ended or fixed ended tests. Most of the large beams were tested in lengths of six feet but two tests each were made on beams one foot six inches and three feet long, by means of the same sheaves and cables adapted for use with shorter top and bottom beams. During the tests of light beams 5/8-in. diameter cables were used because of their flexibility and ease of handling, but in the tests of the heavier and shorter sections the cable was changed to 1 in. diameter in order to develop the full capacity of the machine.

The sheaves were made of 2-in. thick material and were machined to a 17-in. minimum diameter. A hole bored through one of the diameters allowed continuous action and

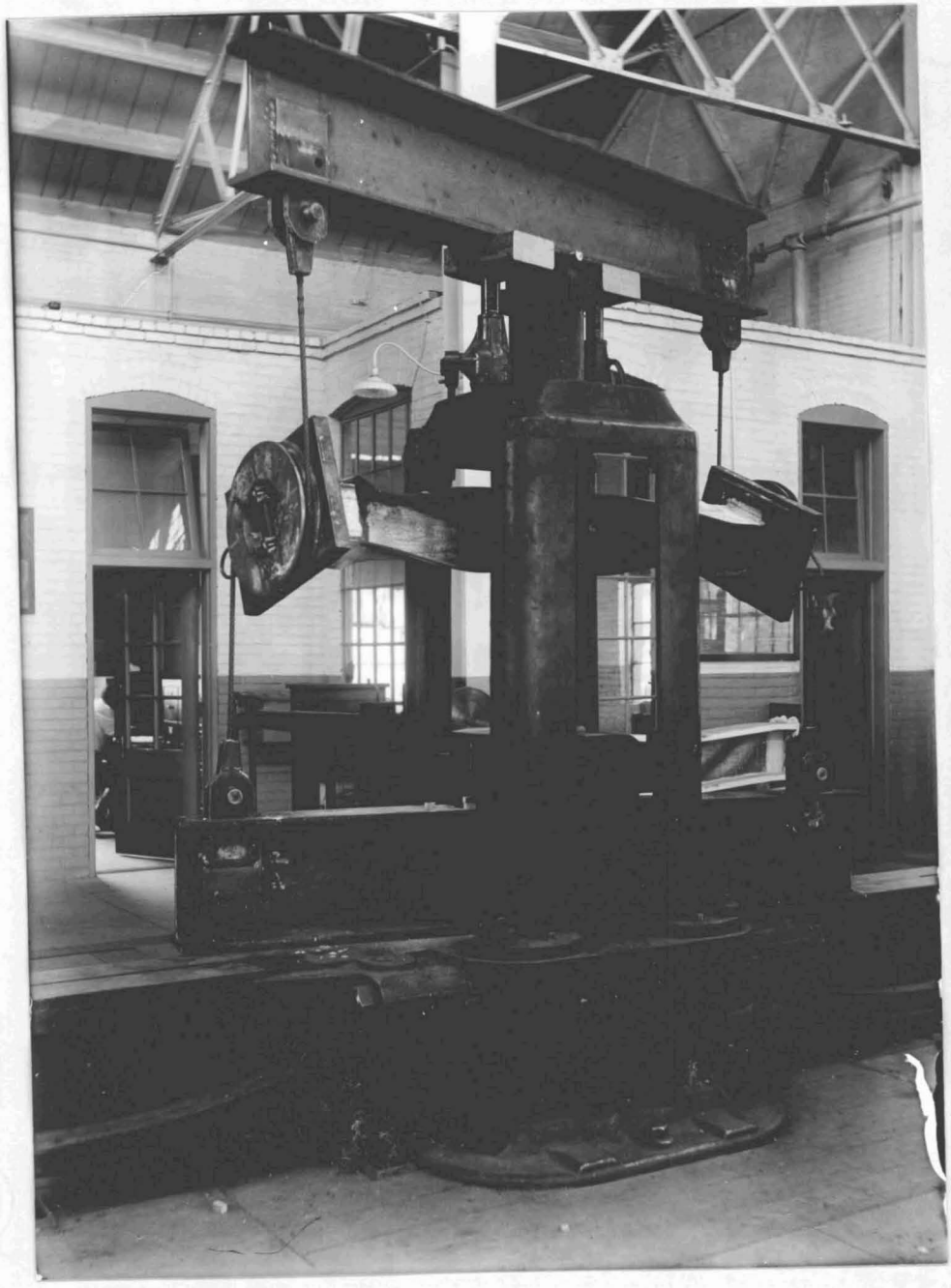

Fig. 30

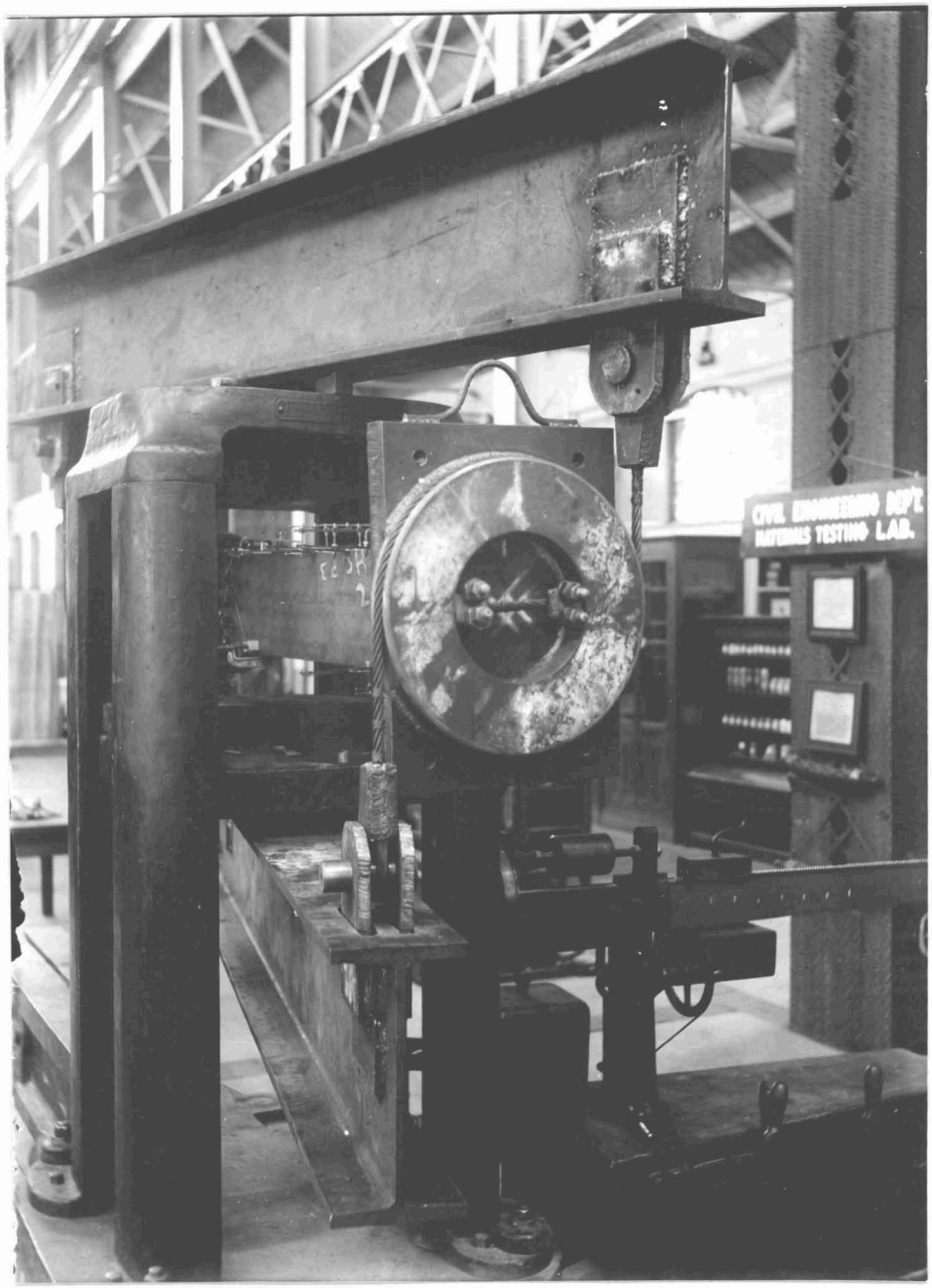

Fig. 31

reversing of the cable without fouling or introducing of bending moment. The sheaves were welded to two-inch thick rectangular end plates which were tapped to receive the bolts passing through the end plates. The pulling beams (B15a at 72) were eight feet in length and the flanges were slotted at each end to allow passage of the connecting plates which received the cable socket pin and transmitted the load directly to the web by means of welds.

This machine gave perfect satisfaction in every respect and was easily dismantled and set up. During tests the apparatus was in such a state of balance that the heavy pulling beams could be easily tilted either way by hand while maintaining a heavy torsional load on the test specimen.

Measuring Devices - The Level Bar illustrated in Fig. 32 was built to measure the change in relative altitude of two points three inches apart. It was used to measure relative angle changes in all of the beam tests. The micrometer was verniered to give readings to 1/10,000 of an inch and the level bubble was sensitive to micrometer changes of about 3/10,000 of an inch. The total range of the instrument was about 9° 30' plus or minus from original level position.

The Torsion Meter - This instrument was used in the torsion tests of round bars in the 26,000-in.lb. capacity Olsen torsion machine to measure the angular twist over a

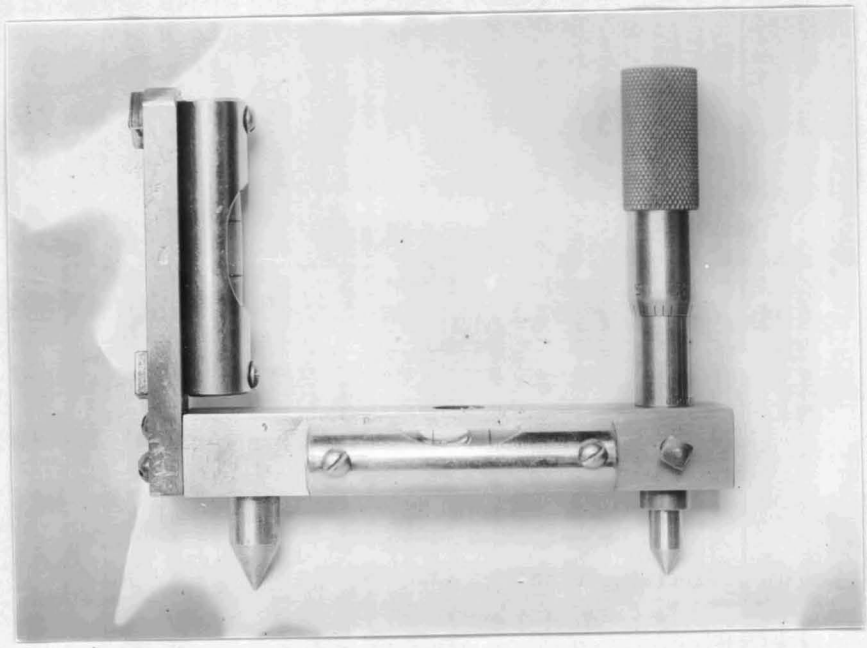

Fig. 32

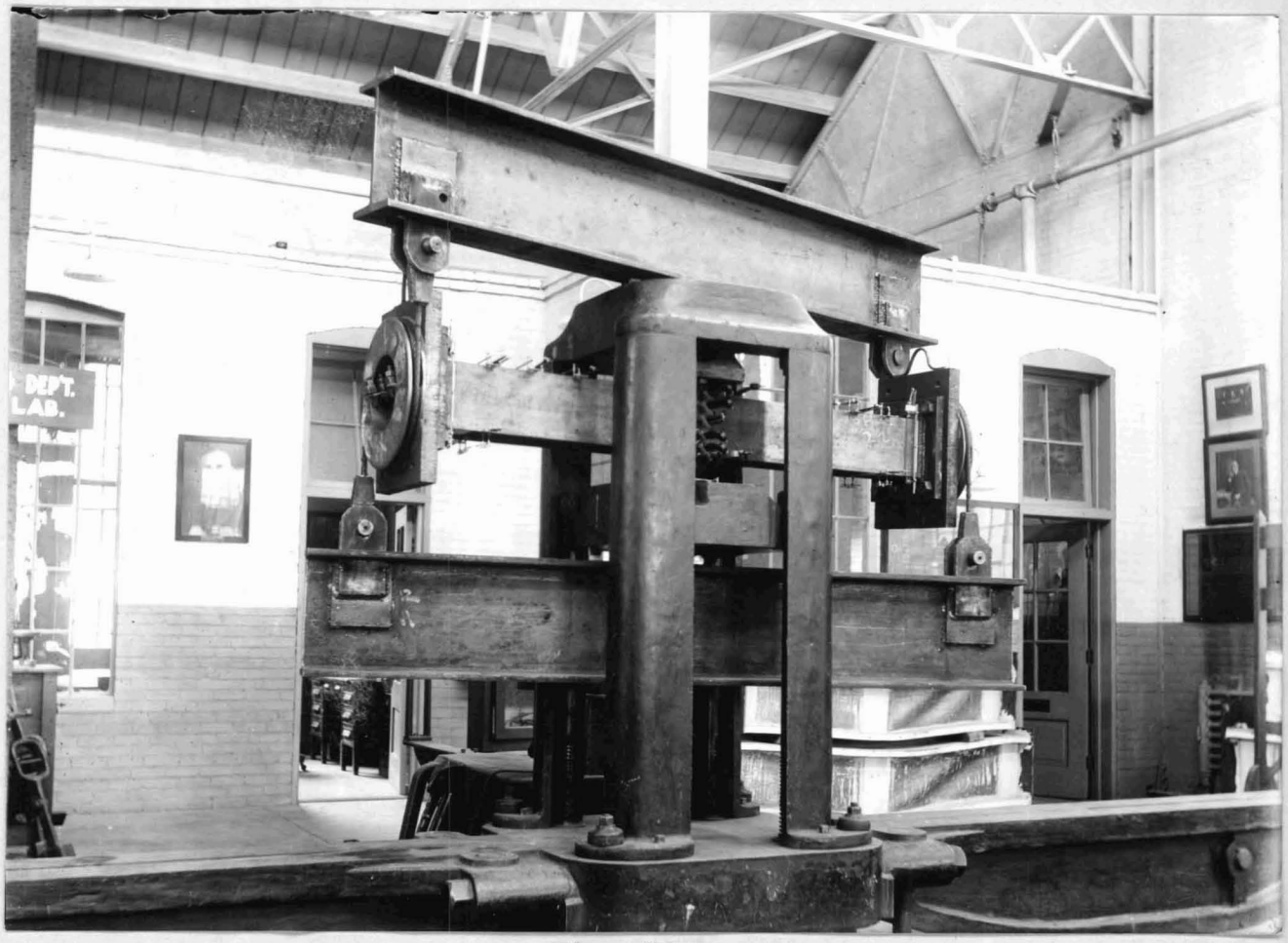

Fig. 33

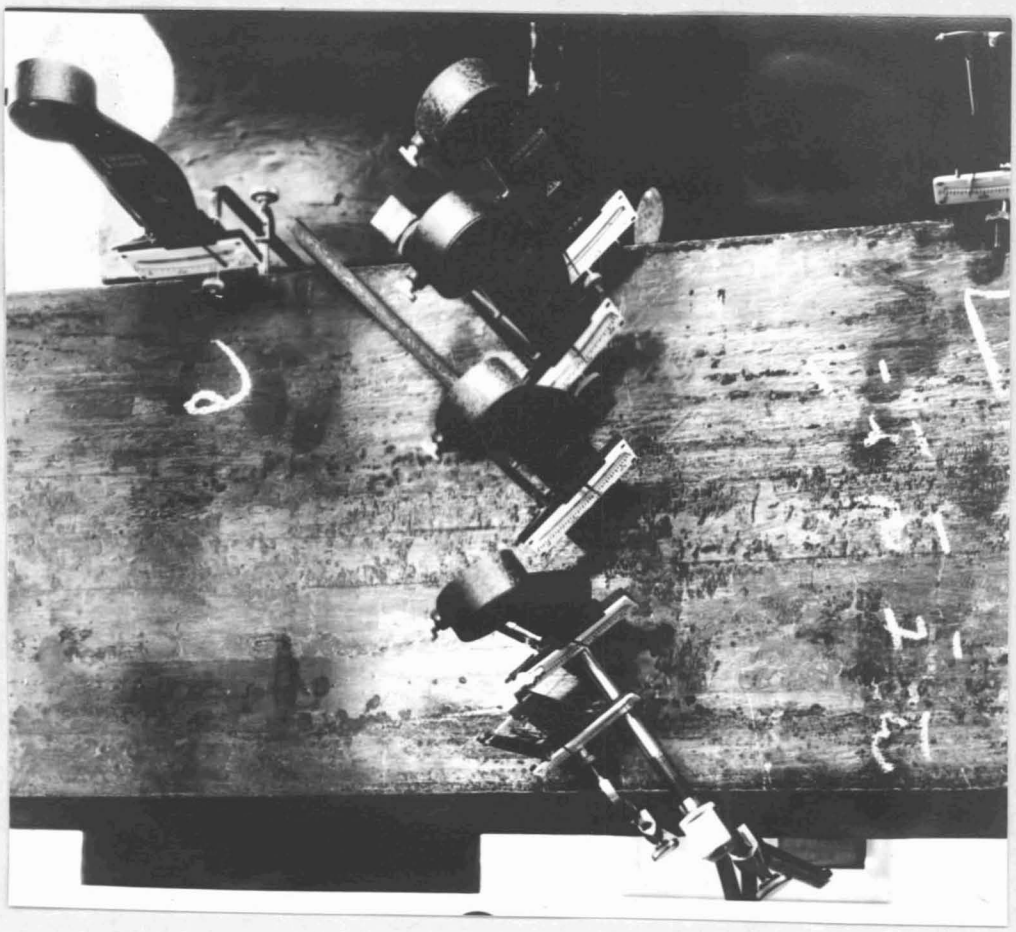

Fig. 34

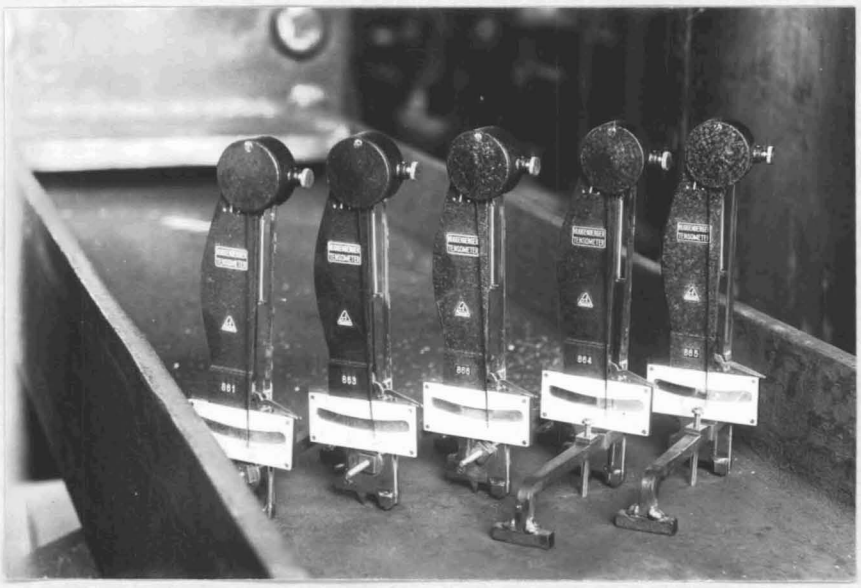

Fig. 35

three-inch portion of the bar. This device, consisted of two steel collars attached by pointed thumb screws to the bar and provided with two 1/1000 Ames dials for measuring the tangential displacements. The instrument was the same as that used and described in a previous investigation at the Fritz Laboratory*.

Huggenberger Tensometers - Through the courtesy of the Baldwin-Southwark Corporation of Philadelphia, 16 tensometers were loaned to the university during these tests, making 20 available in all. These were used to obtain the strains at all critical points during tests and their use is well-illustrated in Fig. 33, 34, and 35.

Fig. 33 shows the entire set up for torsion test T-21. Tensometers for measuring longitudinal fiber stresses due to secondary bending in the flanges are in position along the top of the beam and those for measuring the combined lateral and torsional shear at the center are inclined at an angle of 45°.

Fig. 34 shows a closeup of the shear tensometers on the outer surface of the flange and Fig. 35 shows those measuring the shear distribution in the web of a 12-in. I beam in test T-29.

- -

* SHEARING PROPERTIES AND POISSON'S RATIO OF STRUCTURAL AND ALLOY STEELS by Inge Lyse and H. J. Godfrey, A.S.T.M. Proceedings, 1933.

(c) Test Procedure and Method - In each torsion test, whether fixed or free-ended, there were three principal objectives; first, to learn as much as possible about the strain and stress distribution; second to measure the torsional stiffness, or ratio of torsional load to angular twist; and third, to learn the useful torsional load carrying limit of the beam as a whole.

The strain and stress distribution was studied in two ways; first, by use of Huggenberger tensometers, which are sensitive to changes in strain corresponding to from 150-300 lb. per sq.in. in stress, depending on the model type; secondly, the beams were whitewashed with a mixture of water and hydrated lime which showed the distribution and location of the first surface strain-slip lines.

In figuring the stresses from the observed strains the following values of physical constants were used.

$E = 29{,}000{,}000$ lb. per sq.in.

$G = 11{,}150{,}000$ lb. per sq.in.

$\mu = 0.30$

The torsional stiffness was gauged by measuring the relative angle changes between two points along the beam by use of the level bar. In the free-ended tests the angle changes were measured over a 36-inch length along the center portion of the beam. In the fixed-ended beam the unit angle change varied along the length and a measure of the average stiffness was obtained by measuring the relative rotation of the end plates and of points a short distance from each end where the reinforcing ended.

The yield point of the beam as a whole was obtained by a study of the torque-twist diagrams together with a knowledge of the load when first strain-slip lines appeared. In a few cases a definite drop of the beam was noted and this was in such case taken as the yield point. In most of the tests the yield point was taken as the torsional moment corresponding to the point on the torque-twist diagram where the cotangent of the slope was 1-1/2 times the value of the cotangent of the slope of the straight portion.

(d) Test Results

General Data - Table II gives a general summary of all the tests made including dimensions of beams and computed K values based on actual dimensions. The dimensions were obtained by means of micrometers and calipers. Readings were taken at a number of different places on the beam and averages from them were used to calculate the weight of the beam per foot of length. The beams were also actually weighed and any discrepancy between computed and actual weight was taken care of by adjusting the average measured dimension to give the actual weight.

Table III presents the physical properties based on tests of samples taken from the test beams. The tensile values are based on the average of two tests of A.S.T.M. standard two-inch gage length tension test specimens. The

TABLE II

Test No.	Nominal Size	Nominal Weight Lbs. per Ft.	Actual Weight Lbs. per Ft.	End Connection	Length in Inches	Measured Dimensions Adjusted to Actual Weight						D	K
						d	b	w	m	n	f	Measured	Computed
T-4	3" I	7.5	7.4	Fix.	3.2	2.98	2.51	0.342	0.342	0.162	0.27	0.532	0.0865
T-5	"	"	"	"	6.0	"	"	"	"	"	"	"	"
T-6	"	"	"	"	9.0	"	"	"	"	"	"	"	"
T-7	"	"	"	"	12.1	"	"	"	"	"	"	"	"
T-8	"	"	"	"	18.1	"	"	"	"	"	"	"	"
T-9	"	"	"	"	23.9	"	"	"	"	"	"	"	"
T-10	"	"	"	"	39.0	"	"	"	"	"	"	"	"
T-11	"	"	"	"	53.9	"	"	"	"	"	"	"	"
T-12	"	"	"	"	5.5	"	"	"	"	"	"	"	"
T-13	"	"	"	"	8.8	"	"	"	"	"	"	"	"
T-14	6x6	20	19.6	Free	72	6.06	6.01	0.257	—	0.362	0.28	0.566	0.243
T-15	"	"	"	Fix.	72	"	"	"	—	"	"	"	"
T-16	"	"	20.9	"	72	6.08	6.06	0.303	—	0.372	0.24	0.581	0.281
T-17	"	40.5	39.0	"	72	6.73	6.25	0.501	—	0.699	0.35	0.928	1.738
T-18	6x10	40	38.1	"	72	6.20	9.91	0.431	—	0.447	0.35	0.735	0.802
T-19	8x8	31	29.4	"	18	8.05	8.04	0.290	—	0.401	0.41	0.676	0.463
T-20	"	"	"	"	36	"	"	"	—	"	"	"	"
T-21	"	"	"	"	72	"	"	"	—	"	"	"	"
T-22	"	"	"	Free	72	"	"	"	—	"	"	"	"
T-23	"	67	66.1	Fix.	72	9.05	8.29	0.606	—	0.907	0.42	1.208	4.912
T-24	10x12	62	60.9	"	72	10.05	11.92	0.390	0.659	0.546	0.45	0.919	2.101
T-25	"	"	"	Free	72	"	"	"	"	"	"	"	"
T-26	12" I	31.8	31.3	"	72	12.06	4.97	0.350	0.705	0.345	0.42	0.882	0.833
T-27	"	55	53.6	Fix.	18	12.07	5.74	0.730	0.900	0.449	0.54	1.244	3.318
T-28	"	"	"	"	36	"	"	"	"	"	"	"	"
T-29	"	"	"	"	72	"	"	"	"	"	"	"	"
T-30	"	"	"	Free	72	"	"	"	"	"	"	"	"
T-31	12x12	190	186.7	"	72	14.39	12.56	1.069	—	1.714	0.62	2.186	48.437
T-32	8x8	67	66.8	"	72	9.02	8.23	0.641	—	0.906	0.38	1.199	4.928
T-33	12x12	65	65.6	"	72	12.14	12.03	0.409	—	0.604	0.58	0.953	2.227

Table III

Physical Tests of Material in Test Beams

Samples	Tensile Properties						Shearing Properties				
							Slotted Plates		Round Bar Torsion Tests		
Taken from Test Beam No.	Upper Yield Point Stress	Lower Yield Point Stress	Stress at Ultimate	-E- Modulus of Elasticity	% Elong. in 2 in.	% Reduc. in Area	Shearing Yield Point	Shearing Ultimate	Shearing Yield Point	Apparent Shearing Ultimate	G Shearing Modulus
T-4-T-13	38,900	—	63,550	29,100,000	32.0	62.1	21,800	52,850	—	—	—
T-14-T-15	41,000	37,860	60,450	29,200,000	35.8	66.4	25,600	48,500	26,400	80,600	12,080,000
T-16	39,710	35,790	58,130	29,150,000	35.5	66.7	22,000	45,100	22,000	50,700	11,280,000
T-17	43,020	37,000	60,220	28,500,000	37.0	67.3	23,700	49,900	24,000	64,100	12,020,000
T-18	34,180	31,570	56,570	28,250,000	40.0	65.4	22,600	47,900	22,200	65,600	11,500,000
T-19-T-22	42,880	38,290	61,280	29,450,000	36.0	66.1	25,500	51,000	22,300	64,700	10,780,000
T-23	34,890	31,580	61,180	28,600,000	38.8	66.1	21,200	50,700	20,200	65,700	11,780,000
T-24-T-25	40,860	35,530	59,600	29,150,000	36.3	64.9	23,700	49,800	24,400	64,100	12,350,000
T-26	38,310	33,900	56,330	29,400,000	38.0	69.3	24,600	52,800	21,400	71,000	11,920,000
T-27-T-30	32,380	30,990	59,850	29,400,000	34.5	65.9	18,200	47,700	20,900 18,700	66,200 64,500	11,770,000 10,780,000
T-31	32,910	28,620	60,000	29,200,000	38.0	63.7	21,200	51,600	20,300	64,600	11,260,000
Average	38,090	34,110	59,740	29,040,000	36.5	65.8	22,740	49,800	22,070	65,620	11,590,000

torsion tests and slotted-plate shear tests were made in the same manner as described in a previous investigation at the Fritz Engineering Laboratory (p.48). The tensile test specimens and round bar torsion specimens were cut in most cases from the material where the flange and web join, as it is at this point that critical torsional stresses develop. The material for the slotted plate test specimens was cut from the webs of the beams.

Free-Ended Tests - Free-ended tests were made on eight beams*. The purpose of these tests has been previously discussed. The beams were held in the torsion rig by means of two bolts at each end which passed with a loose fit through the web and through the two angles, the angles being welded to end plates which were in turn bolted to the sheave plates of the testing rig. Torsional moment was applied by means of lugs welded to the end plates which engaged the flanges of the test specimens. The flanges were thus free to warp and the beams were almost entirely unrestrained at the ends. Fig. 36 shows the details at one end of the largest beam tested and is typical of all the free end tests which were made. Fig. 38 shows the entire setup during the same test. Fig. 38 and 39 show typical torque-twist diagrams of two of the tests (T-26 and T-31). Fig.40 and 41 show the stress distribution based on tensometer

---

* At the date of writing test T-32 has yet to be made. Data will be furnished on this test when available.

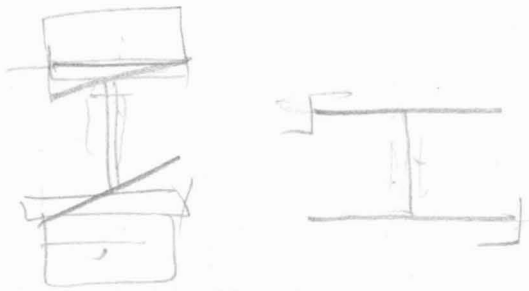

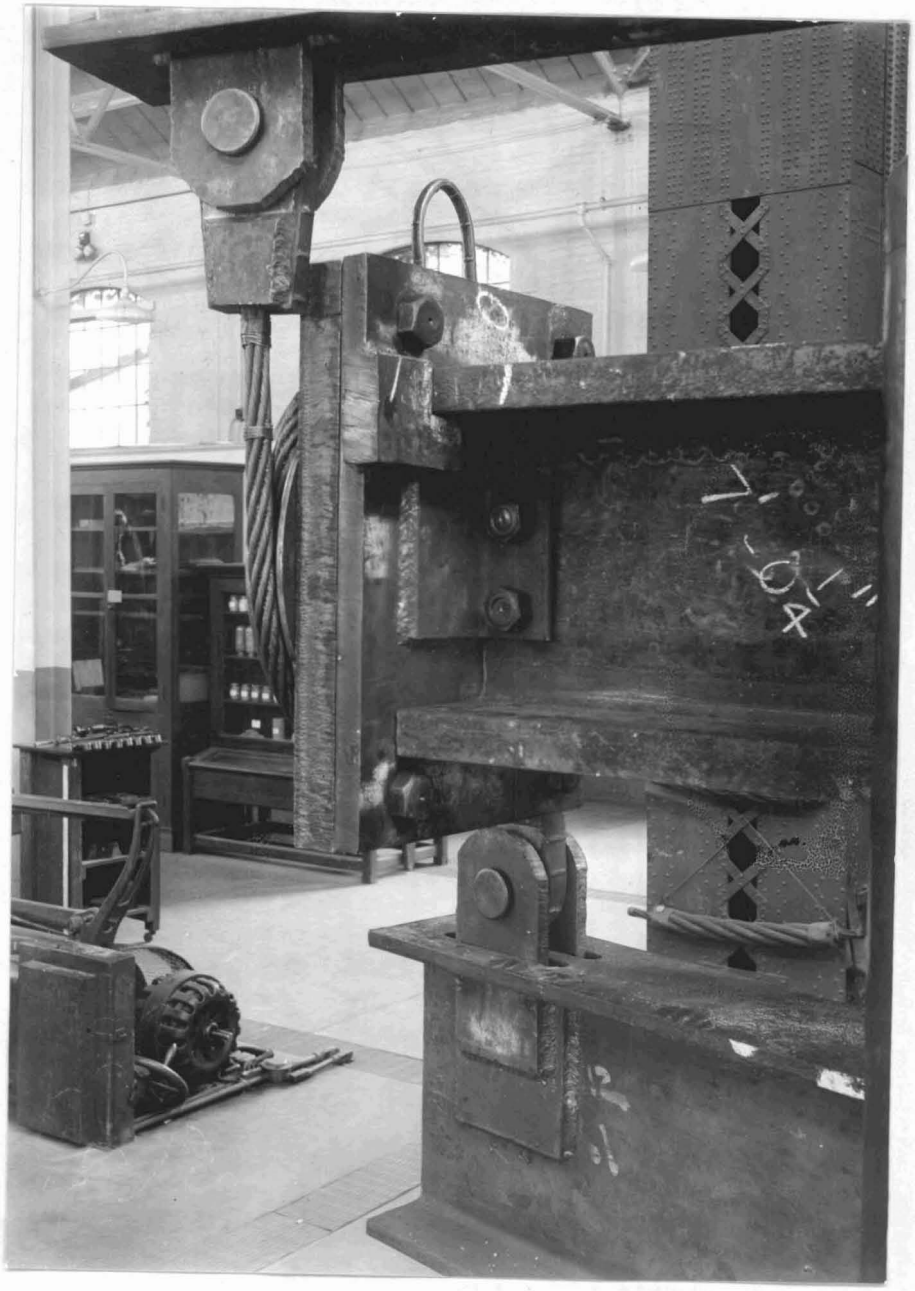

Fig. 36

Fig. 37

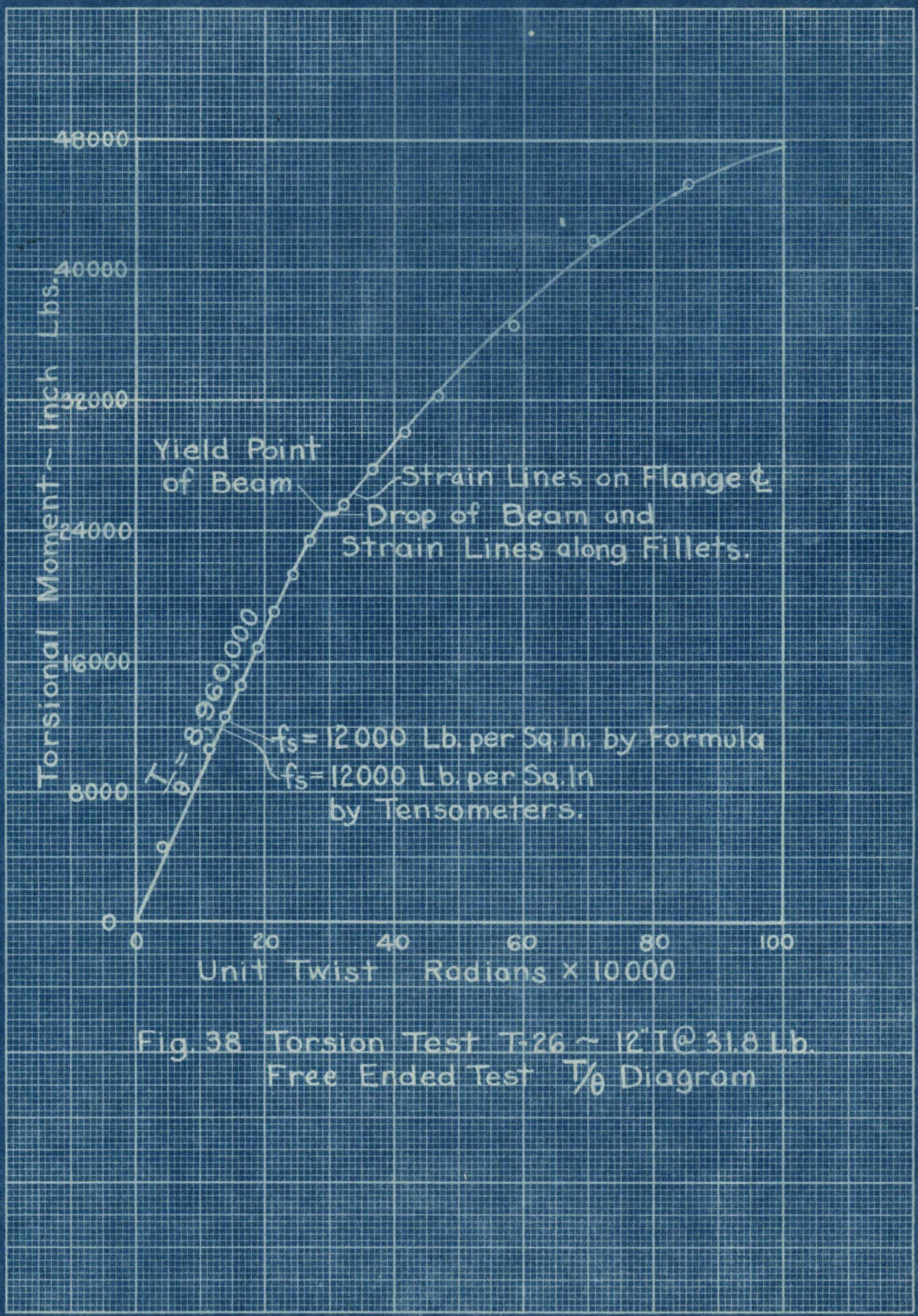

Fig. 38 Torsion Test T-26 ~ 12"I @ 31.8 Lb.
Free Ended Test T/θ Diagram

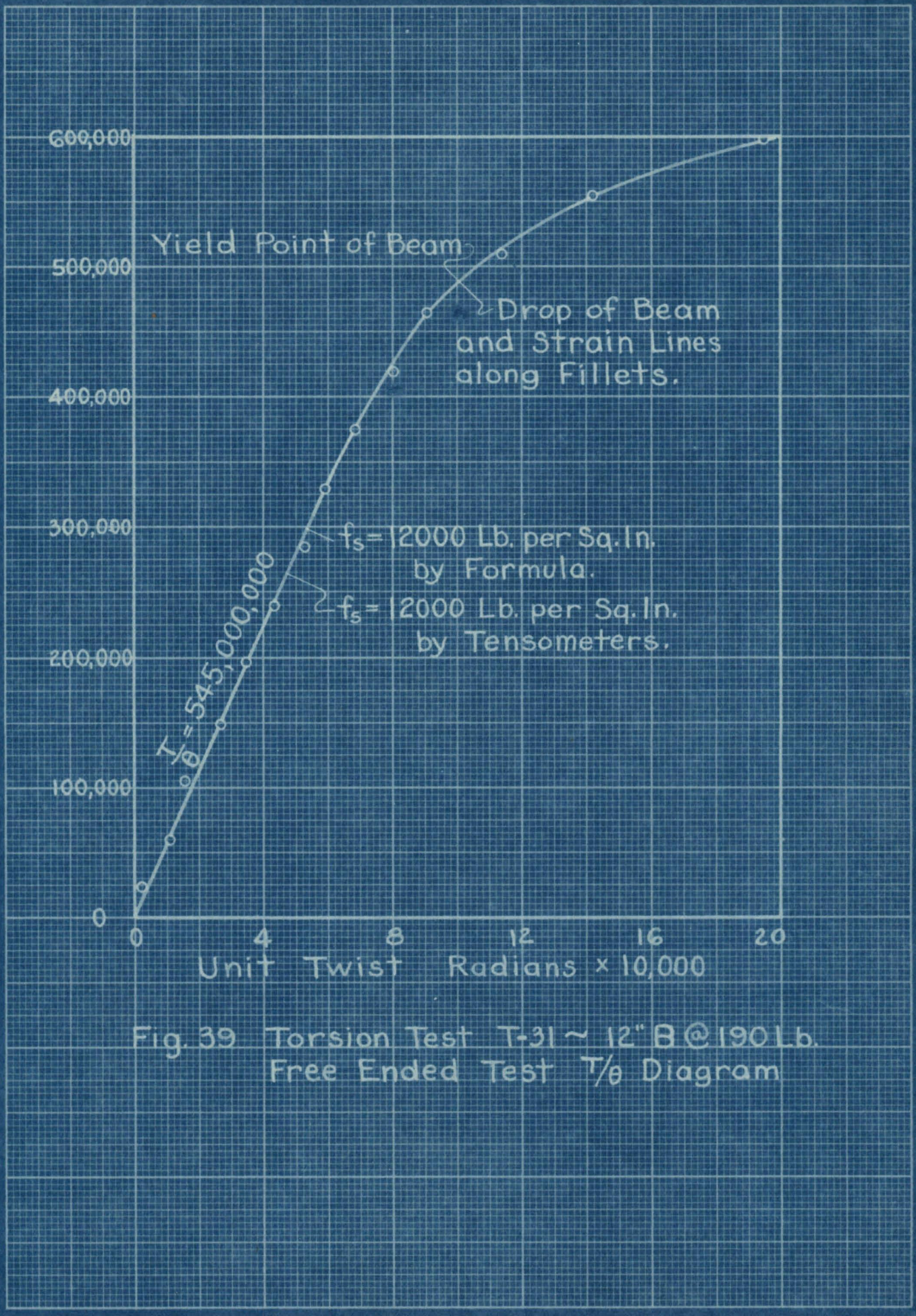

Fig. 39 Torsion Test T-31 ~ 12" B @ 190 Lb.
Free Ended Test T/θ Diagram

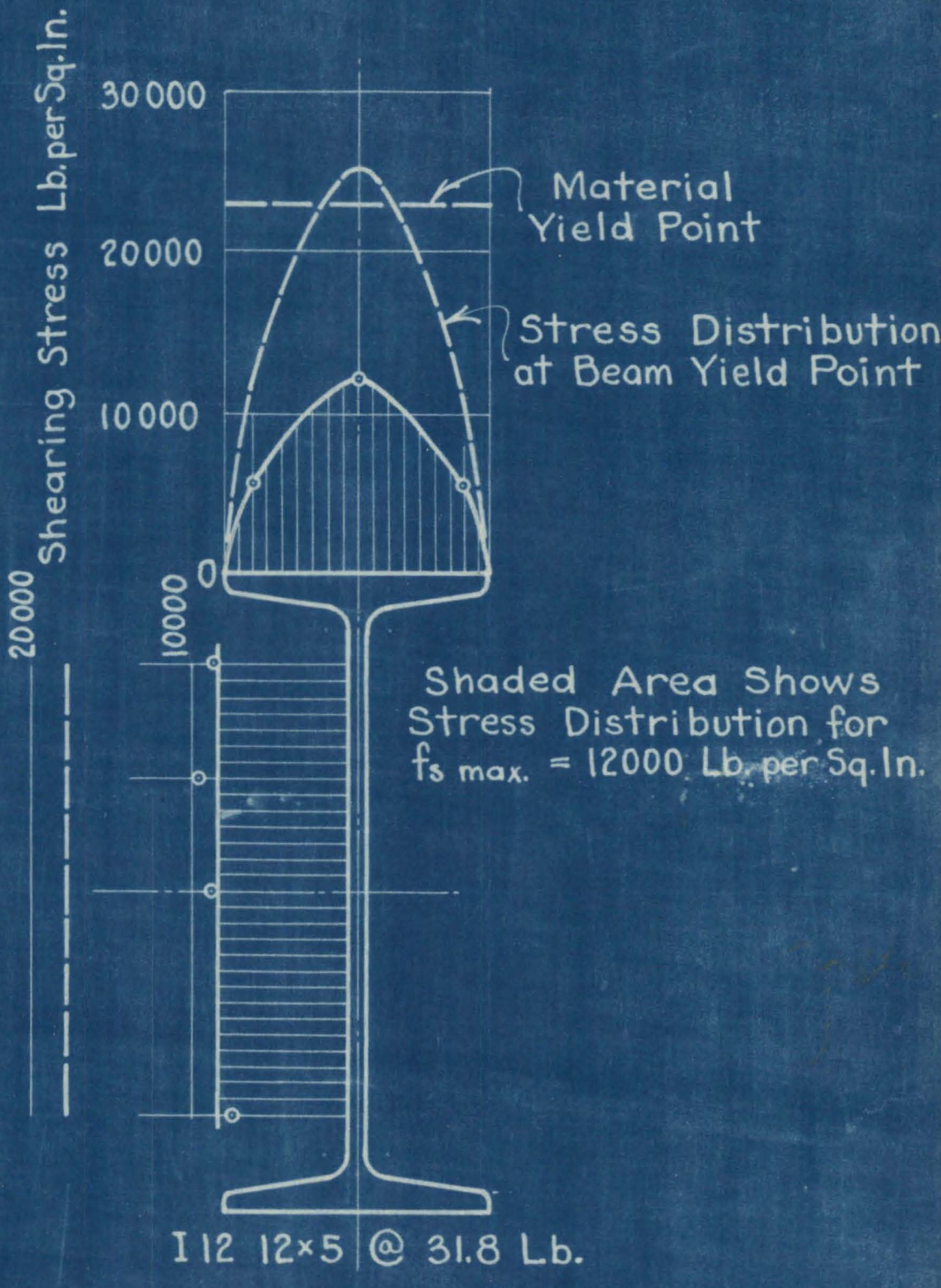

Fig. 40 Free Ended Torsion Test T-26
Shearing Stress Distribution
on Surface of Flange and Web.

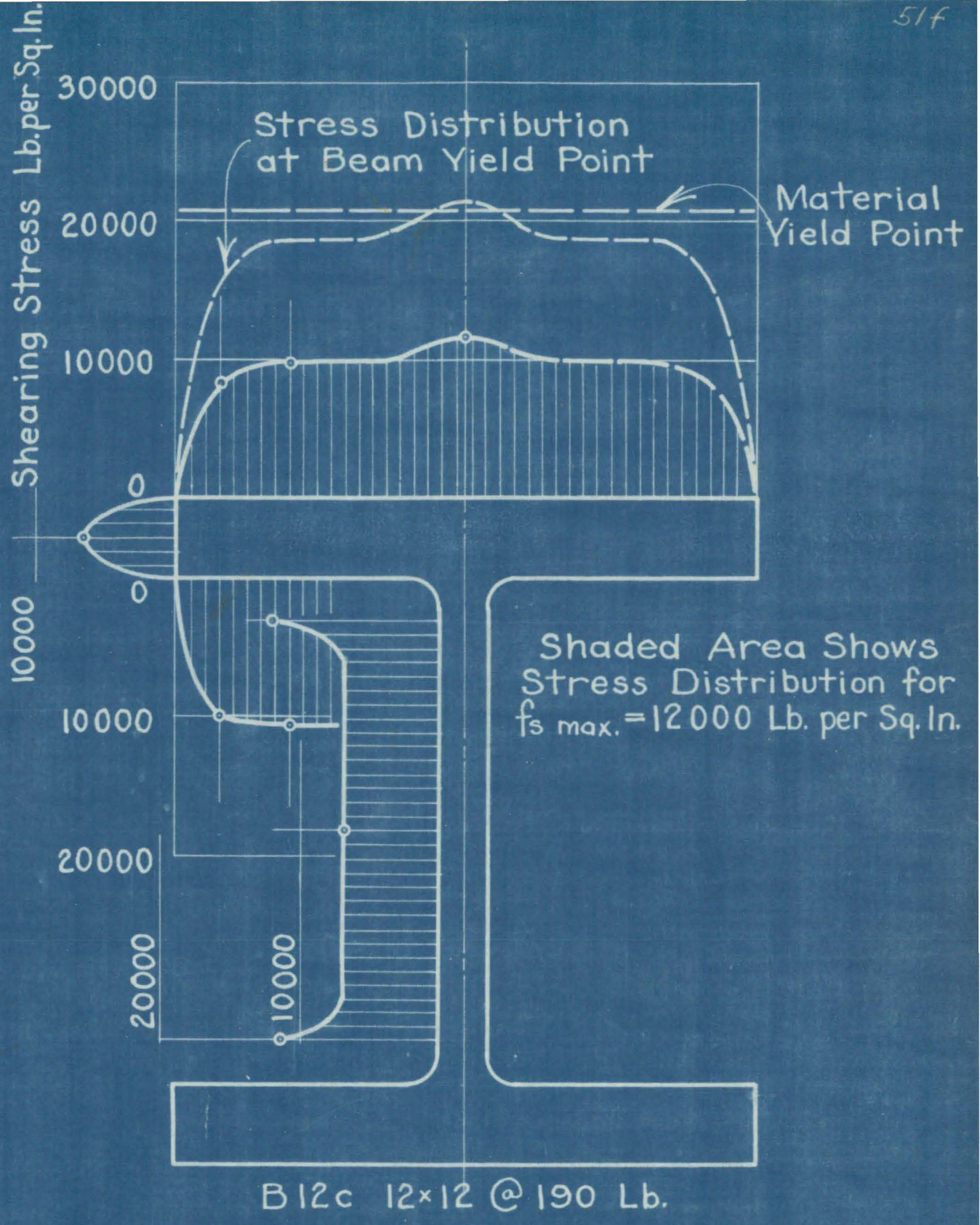

Fig. 41 Free Ended Torsion Test T-31
Shearing Stress Distribution
on Surface of Flange and Web.

readings taken in these same tests. The tensometers were placed on the flange and web surface about the center cross section of the beams and were set at an angle of 45° with the longitudinal axis of the beam in order to measure one of the principal strains which in the case of pure shear will be equal in both directions. Fig. 34 showed the tensometers in position for measuring shear on the flange surface of an eight-inch beam.

The data of actual stresses from tensometer readings were available at only a limited number of points. In drawing the curves of stress distribution the data have been supplemented by known facts, deducible from the general torsional theory, soap bubble tests and from the actual beam tests, i.e.,

(1) The shearing stress equals zero at outside corners.

(2) There is a "hump" in the stress curve at the outside center of the flange, particularly so if the fillets and web thickness are relatively large as compared with the flange thickness.

(3) The shearing stress on the surface of the flange and web is approximately proportional to the thickness of the material.

Table IV summarizes the results obtained in the free end tests.

TABLE IV.
FREE ENDED TESTS

(1) Test Number	(2) Nominal Size	(3) Nominal Weight lbs. per foot	(4) K from Measured Dimensions	(5) K by Test	(6) Per Cent Variation of K	(7) Yield Point of Beam in inch-lbs.	(8) Maximum Shearing Stress in Flange at Yield Point by Equation 27	(9) Maximum Shearing Stress in Flange at Yield Point by Tensometers	(10) Shearing Stress in Web at Yield Point by Equation 29	(11) Shearing Stress in Web at Yield Point by Tensometers.	(12) Shearing Yield Point Strength of Material
T-14	6x6	20	0.243	0.243	0.0	15,900	30,400	29,700	22,400	19,700	26,000
T-22	8x8	31	0.463	0.451	-2.6	25,610	29,800	31,400	22,600	22,200	23,900
T-25	10x12	62	2.101	1.960	-6.7	50,900	19,100	23,400	12,600	17,900	24,050
T-26	12"I	31.8	0.833	0.804	-3.5	25,000	23,800	25,400	14,900	17,700	23,000
T-30	12"I	55	3.318	3.380	+1.9	64,000	20,700	20,200	17,100	18,500	19,000
T-31	12x12	190	48.440	48.870	+0.9	480,000	19,300	21,400	12,400	12,600	20,750
T-32	8x8	67	4.928								
T-33	12x12	65	2.227	2.222	-0.2	76,400	26,600	29,300	—	—	—
Average					2.26		24,240	25,830	17,000	18,100	22,780

There is good agreement shown in the table between the torsion constant computed from the measured dimensions and that obtained from the test results. The test K was obtained from the slope of the torque-twist diagram and from equation (7).

$$T = KG\theta$$

$$\text{or} \quad K = \frac{T}{G\theta}$$

The maximum variation for K of test results was 6.7 per cent and the average of seven tests was 2.26 per cent. It is noted that K for the heaviest beam tested was about two hundred times greater than the lightest and that the corresponding test agreement for these tests was 0.9 per cent and 0.0 per cent variation.

The shearing stress computed by equation 27 gave average stresses seven per cent lower than those based on tensometer readings. The stresses in the web by equation 28, which should be theoretically correct, were much lower than as figured from tensometer readings and equation 29 was suggested on the basis of these tests, which are of course not complete enough to definitely substantiate its adoption. However, both equation 27 and equation 29 are believed to be usable for practical design purposes with ordinary values of allowable shearing unit stress.

The following special remarks apply to the individual free-end tests:

T-12: Strain lines appeared along fillets at 13,500 in-lb; along outside center line of flange at 15,200 in-lb. Yield point of beam as determined by slope of torque-twist diagram was 15,900 in-lb.

T-22: In this test the freedom of the ends from restraint was checked by means of tensometers placed longitudinally near the ends. The strains were negligible.

The first shear strain line along the center line of the flange appeared at 21,210 in-lb. At 25,610 in-lb. strain lines progressed rapidly along flange and in fillets and a definite drop of beam was noted.

T-25: Strain lines appeared along fillets at 50,900 in-lb. Henceforth the slope of the torque-twist diagram became very nearly 50 per cent greater than for lower loads, maintaining very nearly the same slope up to 100,000 in-lb. The yield point was taken as 50,900 in-lb. Strain lines appeared along the outside of the flange at 77,340 in-lb.

T-26: Slight checking in fillets noted at 23,000 in-lb. with drop of beam yield point at 25,000 in-lb. strain lines progressed along outside of flange at 26,500 in-lb.

T-30: Yield of beam by 1-1/2 slope of torque-twist diagram at 64,000 in-lb. First strain lines appeared over web at an indeterminate load due to presence of heavy scale on section.

T-31: Drop of beam with strain lines along fillets at 48,800 inb-lb. Yield point by 1-1/2 slope at 480,000 in-lb.

T-33: Strain lines along fillets at 65,600 in-lb. Yield point and strain lines along outside of flange at 76,400 in-lb.

Fixed-Ended Tests - Twenty-two fixed-ended tests were made on beams of different sizes. Tests T-4 to T-13 inclusive, were made with different lengths of a 3-in., 7.5-lb. I-beam. These specimens were welded to one-inch thick end plates with a continuous 3/8-inch fillet weld. The end plates were bolted to 1-1/4 inch thick plates which attached to the jaws of the standard 26,000 in-lb. torsion machine. The relative rotation of the end plates were measured by level bar readings taken at each end. The remainder of the beams were tested in the cable testing rig. These beams were all larger than the three-inch I beams and were welded to 1-1/4 inch thick end plates with additional end stiffeners, fitted and welded between the flanges as was illustrated in Fig. 19.

Relative rotation of the end plates was observed on all beams by means of level bar observations and the twist of the large beams having stiffener plates was also measured at points just inside the stiffener plates. Strain readings for longitudinal and shearing strains were observed wherever feasible. Fig. 42 shows a typical fixed ended torque-twist diagram, and Fig. 43 shows the computed stresses from strain readings at the yield point of the beam. These observations are typical of all the fixed-ended tests.

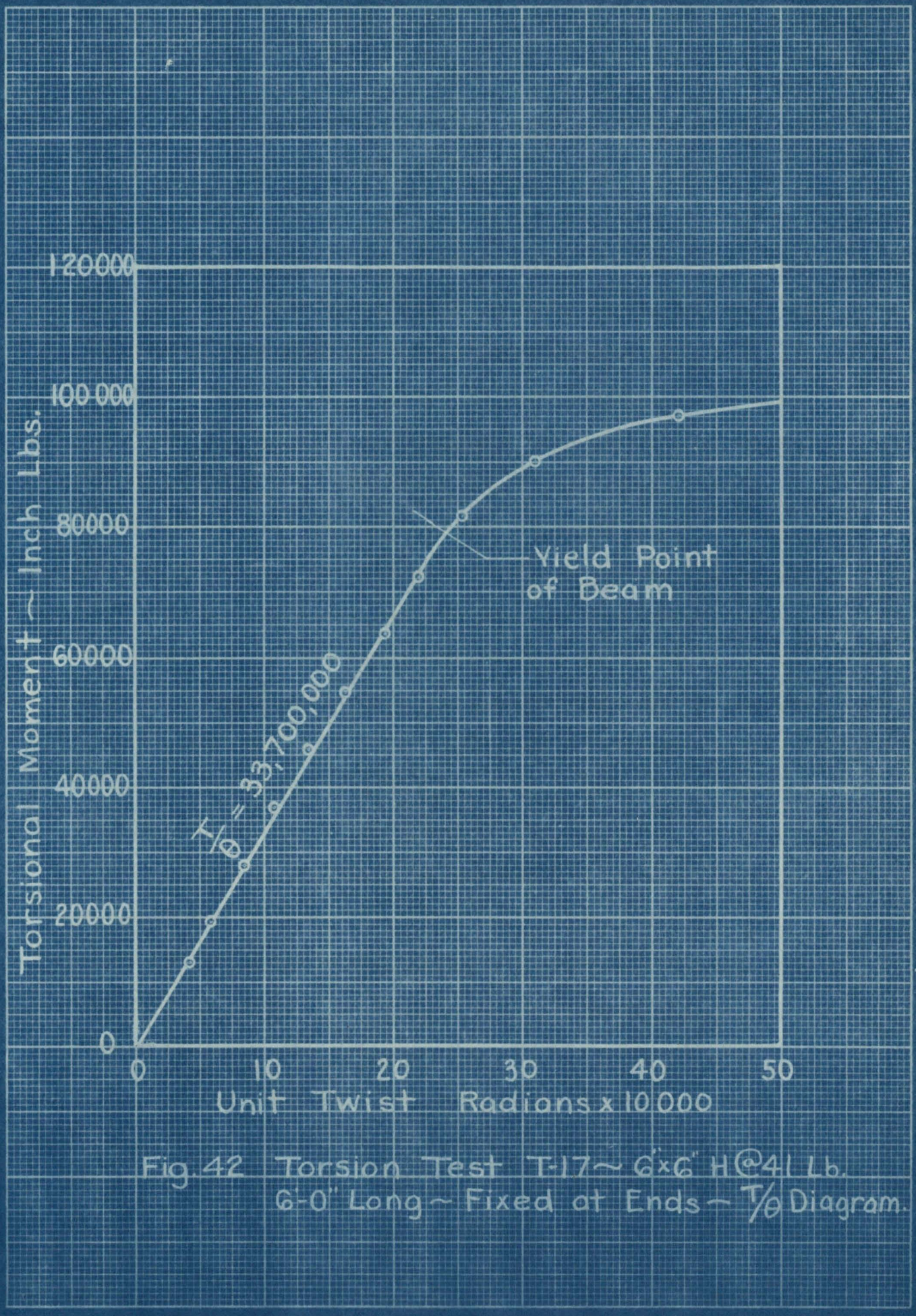

Fig. 42 Torsion Test T-17 ~ 6"x6" H @ 41 Lb. 6-0" Long ~ Fixed at Ends ~ T/θ Diagram.

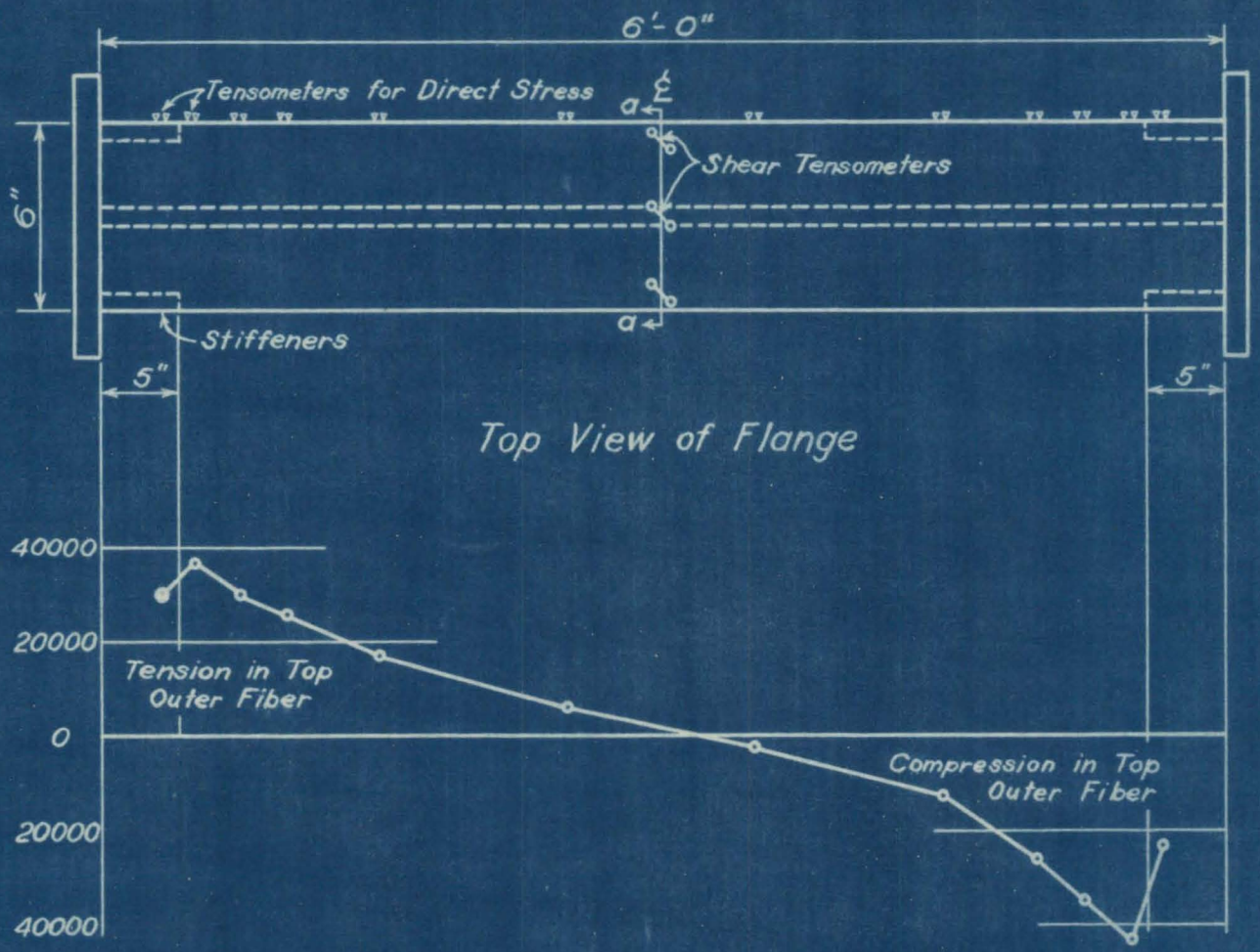

Direct Stress in Outer Fibers of Flange at Beam Yield Point

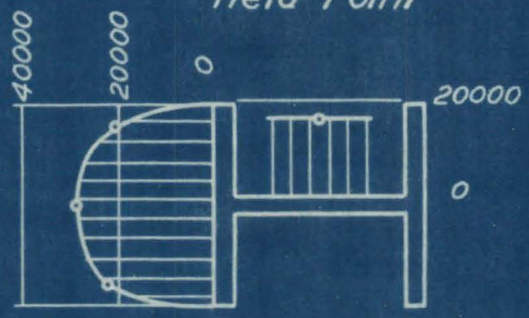

Shearing Stress at Center Section a-a at Beam Yield Point

Fig. 43 Stresses at Beam Yield Point in Fixed Ended Test T-17

TABLE V.
FIXED ENDED TESTS

(1) Test Number	(2) Nominal Size	(3) Nominal Weight lbs. per foot	(4) l = Length of Beam	(5) I_y from Measured Dimensions	(6) K from Measured Dimensions	(7) $a = 0.806h\sqrt{\frac{I_y}{K}}$	(8) $\frac{l}{2a}$	(9) C_c Computed by Equation 48	(10) C_A Computed	(11) C_A by Test	(12) Per Cent of End Fixity	(13) Yield Point of Beam by Test	(14) Maximum Direct Stress at End by Equation 42	(15) Direct Stress near end by Tensometers	(16) Maximum Shearing Stress in Flange at Yield Point by Equation 49	(17) Maximum Shearing Stress in Flange at Yield Point by Tensometers.	(18) Shearing Stress in Web at Yield Point by Equation 50	(19) Shearing Stress in Web at Yield Point by Tensometers
T-4	3"I	7.5	3.2	0.57	.0865	5.67	0.282	0.7998	0.943	0.787	83.5	26,000	58,700	—	30,500	—	—	—
T-5	"	"	6.0	"	"	"	0.529	0.4558	0.605	0.474	78.3	16,000	70,500	—	24,500	—	—	—
T-6	"	"	9.0	"	"	"	0.794	0.2823	0.394	0.330	83.8	10,000	60,300	—	20,360	—	—	—
T-7	"	"	12.1	"	"	"	1.067	0.1996	0.284	0.258	90.8	8,500	61,100	—	22,000	—	—	—
T-8	"	"	18.1	"	"	"	1.596	0.1341	0.190	0.174	91.6	6,500	54,600	—	22,800	—	—	—
T-9	"	"	23.9	"	"	"	2.108	0.1102	0.154	0.153	99.4	6,160	54,500	—	25,400	—	—	—
T-10	"	"	39.0	"	"	"	3.439	0.0913	0.120	0.116	96.8	5,500	50,100	—	26,400	—	—	—
T-11	"	"	53.9	"	"	"	4.753	0.0875	0.109	0.111	101.8	5,400	49,300	—	27,000	—	—	—
T-12	"	"	5.5	"	"	"	0.485	0.5004	0.654	0.534	84.2	8,000†	32,900†	—	11,600†	—	—	—
T-13	"	"	8.8	"	"	"	0.776	0.2904	0.404	0.377	93.4	6,000†	35,600†	—	12,000†	—	—	—
T-15	6x6	20	72.0	13.1	.2433	33.7	1.068	0.6186	0.905	0.777	85.8	33,980	72,600	66,100+	28,000	29,600	18,700	13,500
T-16	"	"	36.0*	13.8	.2810	32.4	0.556	1.896	2.761	1.106	40.1	35,000	44,100	61,500+	11,100	23,200	—	—
T-17	"	40.5	72.0	28.5	1.7375	19.7	1.872	2.431	3.445	3.333	96.8	79,000	54,000	40,000	27,800	29,000	19,700	16,400
T-18	6x10	40	72.0	72.5	.8018	44.1	0.816	2.917	4.264	3.944	92.5	69,000	48,700	30,300	17,000	16,700	—	—
T-19	8x8	31	18.0	34.8	.4631	53.5	0.168	20.927	27.55	27.90	101.0	151,600	40,700	49,000	13,000	25,800	—	—
T-20	"	"	36.0	"	"	"	0.336	7.496	10.75	7.43	69.1	115,000	60,000	56,700	14,900	19,100	—	—
T-21	"	"	72.0	"	"	"	0.673	2.346	3.45	3.30	95.7	65,000	61,600	56,300+	18,100	19,500	—	—
T-23	"	67	72.0	86.2	4.9122	27.4	1.314	9.479	13.67	12.00	87.8	194,000	53,300	37,400	24,000	24,800	15,000	14,500
T-24	10x12	62	72.0	162.7	2.101	67.0	0.537	15.104	22.03	10.02	45.5	223,000	57,000	48,100	16,200	21,600	7,800	13,450
T-27	12"I	55	18.0	18.9	3.318	21.8	0.413	32.059	44.30	34.50	77.9	310,000	71,000	29,400	17,700	30,000	8,600	5,920
T-28	"	"	36.0	"	"	"	0.826	11.636	16.89	11.23	66.6	162,000	64,300	68,500	17,900	24,400	12,400	13,800
T-29	"	"	72.0	"	"	"	1.651	5.1675	7.39	6.58	89.0	105,000	57,100	65,800	22,700	20,200	18,100	23,740

NOTES:- * 36" = One-half total length on account of additional stiffener in middle.
† Not Yield Point.

Table V gives the summary of the test results for fixed-ended beams. In computing C_C and C_A the question arose as to the correct length to be used in computation. If one hundred per cent end fixity were possible the correct length would be slightly less than the overall length and somewhat greater than the length between end stiffener plates. However, the overall length is the simplest approximation and it gives the best results by comparison with the tests, except in the case of the very short beams with end stiffeners. In these two tests (T-19 and T-27) the apparent percentage of end-fixity seems inconsistently high. Two tests have unusually low percentages of end fixity (T-16 and (T-24). The explanation for this is given under the special remarks. The average percentage of end-fixity with T-16 and T-24 omitted is 88.3 per cent and all of the six-foot long beams except T-24 have an end efficienty greater than 85 per cent.

The yield points of the beams were in most cases determined from the slope of the torque-twist diagrams and the theoretical direct stresses computed on the basis of this yield point torque is given in column 14. It is noted that in spite of incomplete end fixity, these stresses are in every case above the tensile yield-point strength of the material as given in Table III. Hence all of the beams would have been safely designed on the basis of working

direct fibre stresses. The average of column 14 is fifty per cent above the average yield-point strength of the material in the test beams.

The computed and measured shearing stresses in the flange agree well for all of the six-foot beams with the exception of T-16 and T-24 where the low end fixity affects directly the shearing stress agreement. On the short 18-inch beams with stiffener plates (T-19 and T-27) the discrepancy between computations and test results is high, as might be expected. The computed stresses in the web give a very approximate check on the stresses indicated by tensometers.

Special Remarks on Fixed Ended Tests are as follows:

T-4 to T-12. This group of tests of different lengths of the same three-inch I beams was well adapted to show the influence of end fixity on the strength and stiffness with the length of beam the only variable. The flange of each beam was whitewashed so that the appearance of first strain lines might be noted. Fig. 44 gives a picture of the strain line pattern on the flange of one of these beams after yield had taken place. Fig. 45 gives a graph of test results for this series showing the influence of length upon the rigidity and Fig. 46 illustrated the influence of length on the yield-point strength of the beams. Special sttention in this series of tests was given to tests T-8 and T-10. Stress measurements were taken along the extreme

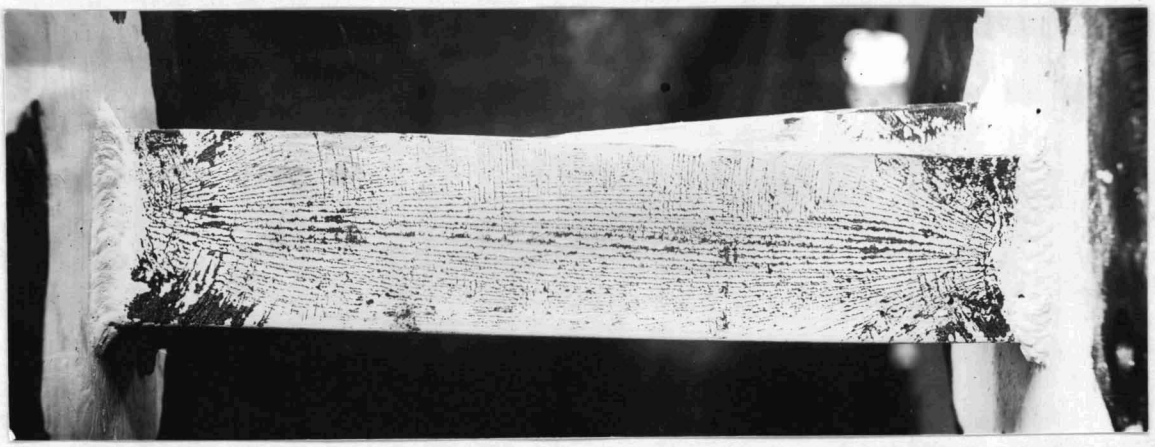

Fig. 44

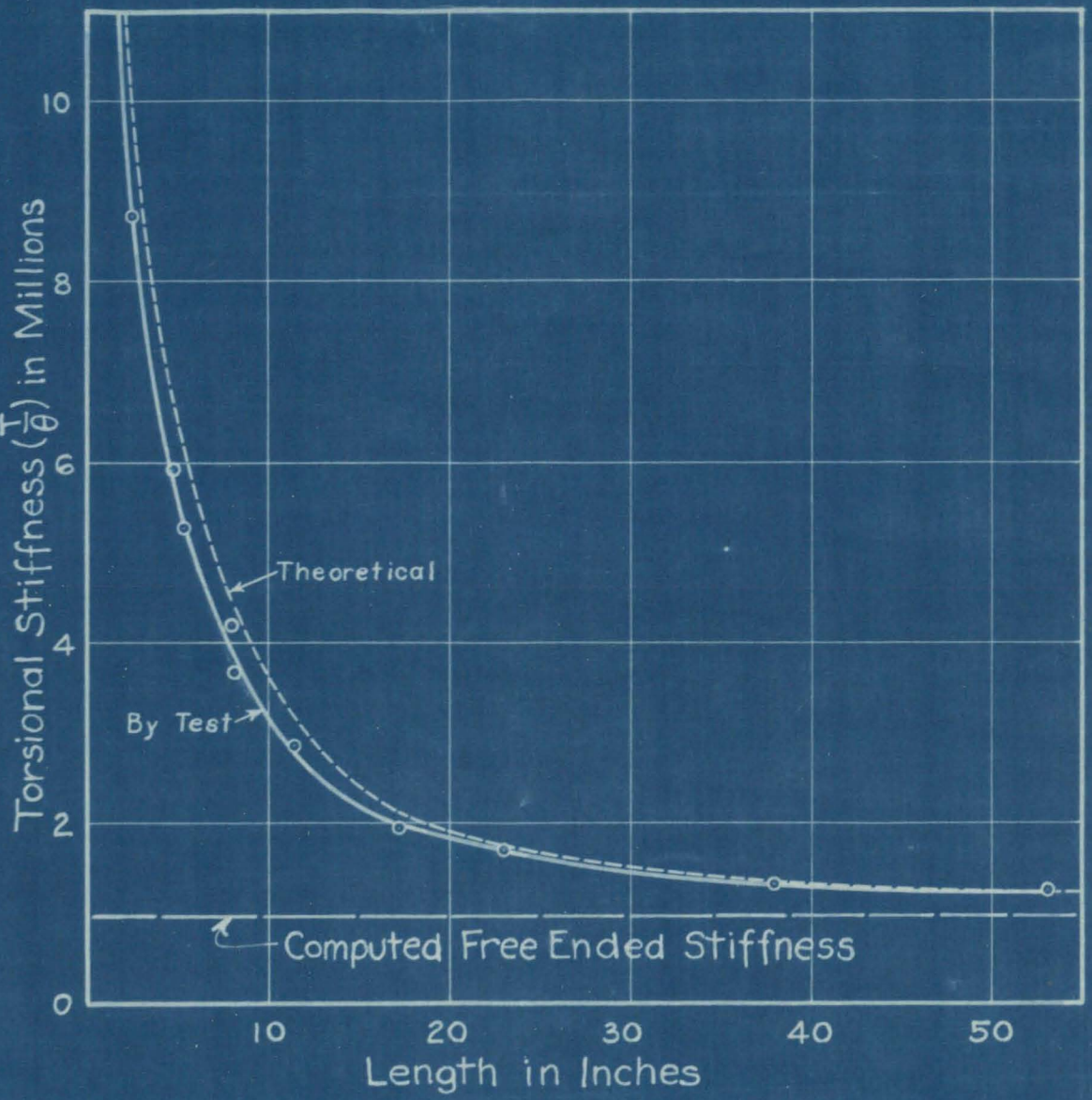

FIGURE 45 RELATION BETWEEN LENGTH AND STIFFNESS OF A 3"I BEAM @7.5#, FIXED AT BOTH ENDS.

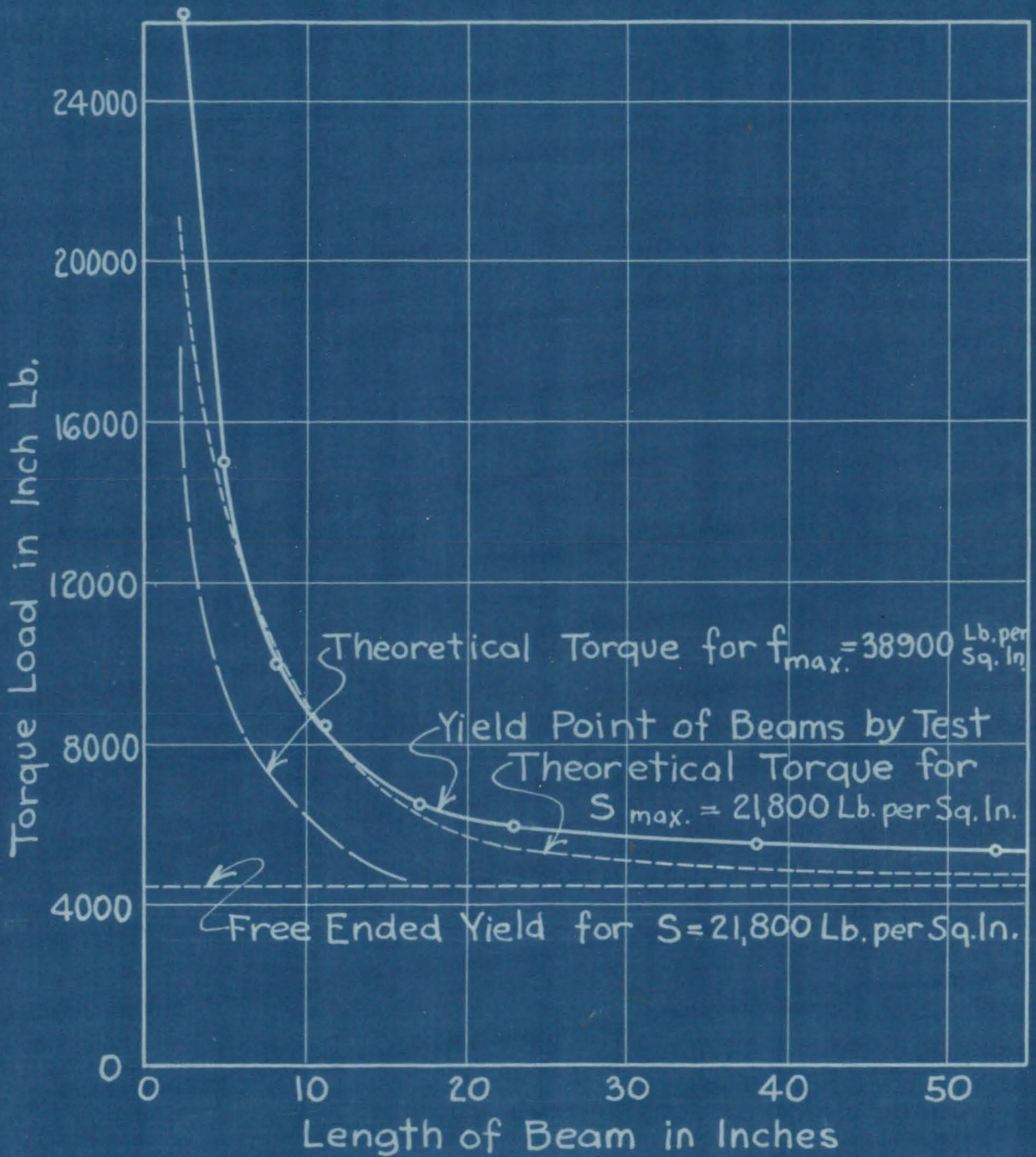

Fig. 46 Relation Between Length and Yield Point Strength of a 3" I@7.5 Lb. Fixed at Both Ends.

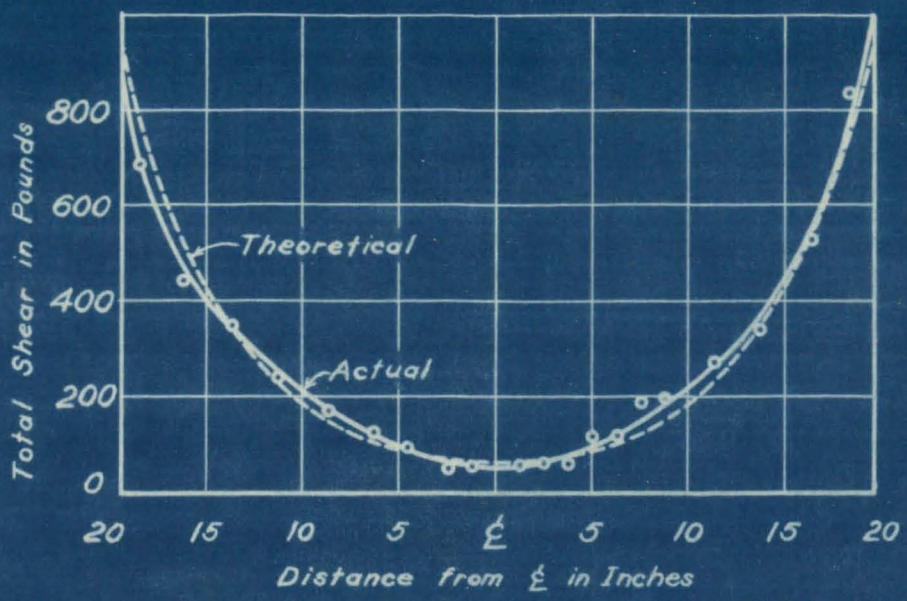

Test T-10 3" I Beam 38.96" long

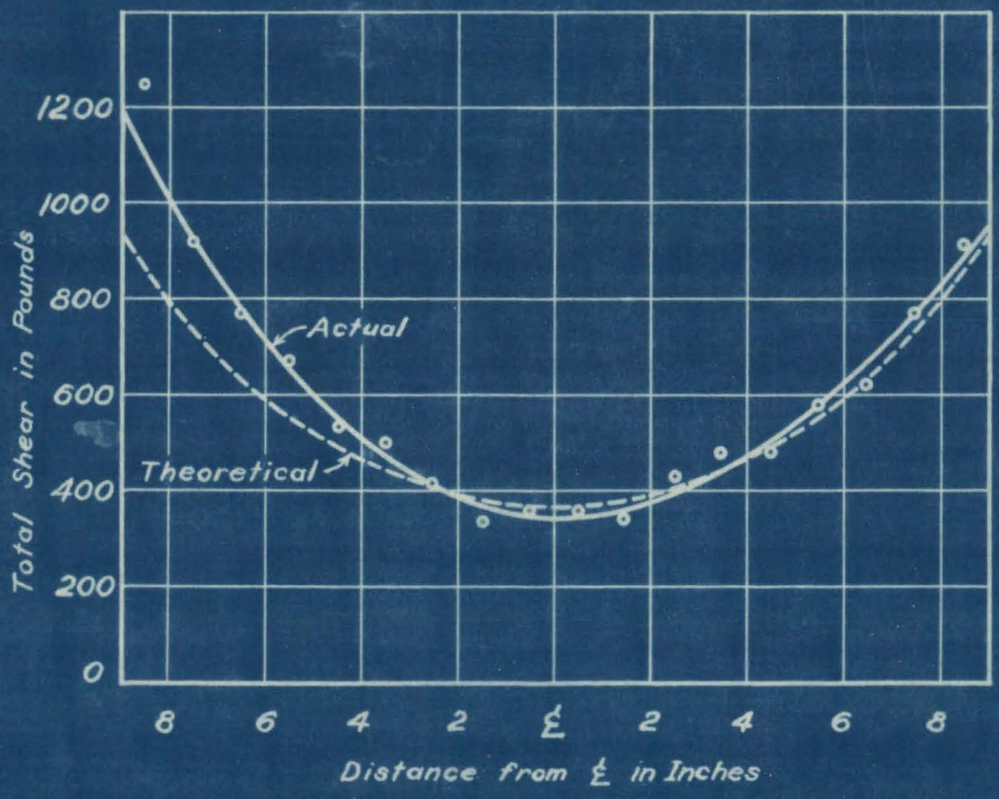

Test T-8 3" I Beam 18.10" long

Fig. 47 Shear Distribution in Flanges of Fixed Ended Beams for a Torque Load of 2500 in.-lb.

fibre of the flanges at small intervals of length and the lateral bending moment in the flanges for a definite torque load was computed from these readings. The bending moments along the beam were plotted and the curves were differentiated to give the lateral shear in the flanges. These results are compared in Fig. 47 with the theoretical variation in shear by equation 40.

T-15 and T-16. Tests T-15 and T-16 should be compared with free end test T-14 of the same section. T-16 was a special test with intermediate stiffeners placed midway along the section. These stiffeners were of the same type as the end stiffeners and were parallel in plane with the web. No outstanding stiffener was provided. This beam is illustrated in Fig. 48. While this additional stiffener gave the beam an average stiffness 42 per cent greater than test T-15, it provided only 40.1 per cent of the theoretical stiffness of a beam three feet in length, rigidly fixed at each end. The design of this beam would have been safe however, for strength if based on the three-foot length and designed for the proper longitudinal working stress.

T-17. This test, in contrast to T-15, was of the heaviest 6 by 6 H section rather than the lightest. It should be noted that an effective fixity of 96.8 per cent was attained in this test. The end stiffeners were 5/8-inch thick and 5 inches long. The torque-twist diagram and data on stress distribution are given in Fig. 42 and 43 as typical of the results for fixed-ended tests.

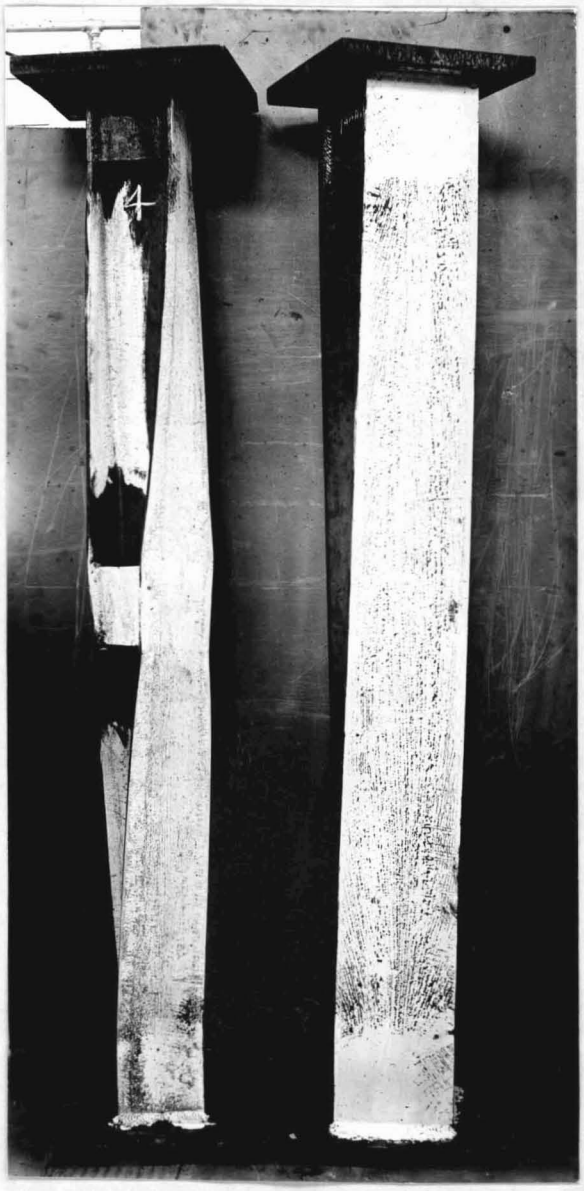

Fig. 48

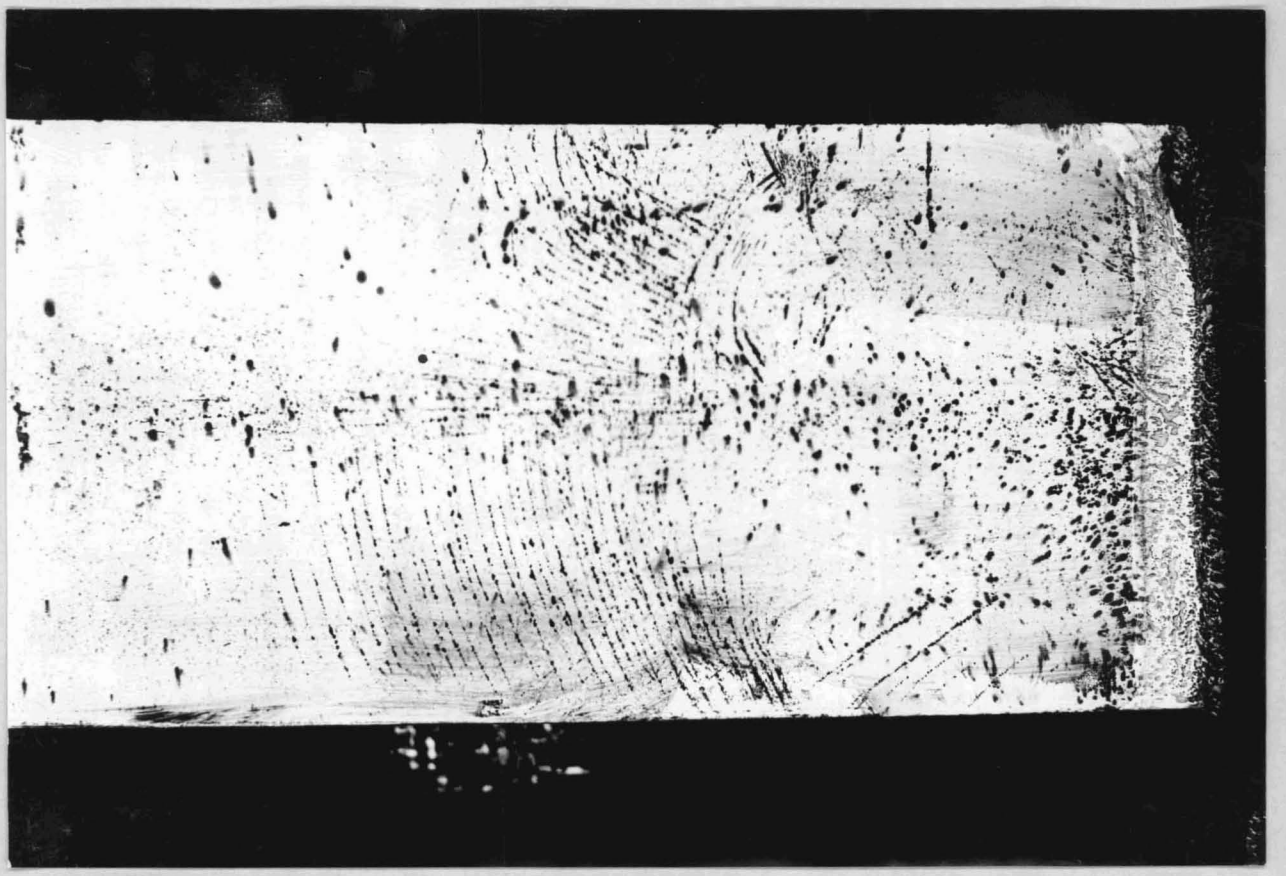

Fig. 49

T-18. Test T-18 of a subway column provided a test on a section of extreme proportions.

T-19 to T-21. These tests together with free end test T-22 on the same size section, provided a series of different lengths of 8 by 8 H section. It is noted that the shortest beam tested showed an end fixity efficiency of 101 per cent, whereas the general trend for shorter beams should be less end fixity because of the greater strains placed upon the end connection. This effect is explained by the fact that the overall length was used in the computations; while this is a very good approximation for the longer beams the stiffness changes rapidly in the short length range and the correct length is something less than that used. Fig. 49 shows the strain line distribution near the end of test beam 21 after yielding had occurred.

T-23. This test is of the heaviest section of the 8 by 8 H sections, while tests T-19 to T-22 were of the lightest weight section. Fig. 48 (on right) shows a photograph of this beam after yield.

T-24. This test is of interest because it had the lowest end fixity efficiency of the six-foot beam sections, with an end fixity of only 45.5 per cent. All the rest of the six-foot sections were over 85 per cent in end-fixity. The explanation is found in the fact that the end stiffeners were not in this case properly designed and the beam

not only pulled loose at the weld from the end plate, but the end plate was badly warped during test. The stiffeners were 9/16 inch thick and 6 inches long. Had they been 9 inches long and 1 inch thick as provided in the suggestions for design, specification (1) and (2), page 33, it is believed that much higher efficiency would have resulted.

T-27 to T-29. These tests are of three different lengths of 12-inch I beam. The remarks concerning tests T-19 to T-21 appear to apply here also.

VII. SUMMARY AND CONCLUSIONS

(a) Torsional Theory and the Torsion Constant - (1) The essential features of the general torsion problem are outlined.

(2) The theory and application of Prandtl's Membrane Analogy is presented.

(3) An accurate and detailed method of evaluating the torsion constant of structural H beams is presented. This method is based on a known theoretical evaluation combined with factors to be determined by experiment from the Membrane Analogy.

(4) Formulas are proposed for the shearing stress in the flange and web due to pure torsion.

(5) The effect of shearing stress concentration in the fillets due to both torsion and bending is discussed.

(6) The problem of torsion with either one or both ends of the beam restrained is studied in detail and formulas for maximum shearing and longitudinal fibre stresses are given.

(7) Specifications are suggested for the design of a welded end connection which will give a high degree of end fixity efficiency in torsion.

(8) Detailed design examples are presented to illustrate the application of the formulas to torsional design.

(b) Test Results - (1) The purpose of the soap film tests was to experimentally determine the additive factor in the K factor due to the added rigidity accruing from the juncture of the web and flange with the corresponding fillets.

(2) Soap film experiments were made on 57 differently proportioned sections both with parallel and sloping flanges.

(3) The application of the membrane analogy as developed by this investigation was restricted to volume measurement only. The method used was rapid, and it is believed, gave results having an error considerably less than ±1 per cent.

(4) In computing the K values of structural sections as listed in Appendix II, the experimentally determined part of K amounts in the most extreme case to ten per cent of the total K. Hence an experimental error of ±1 per cent would

give a possible error of only 0.1 per cent in the total K value.

(5) Free-end torsion tests were made on seven different beams ranging in size from a 6 by 6-inch H at 20 lb. per ft. to a 12 by 12-inch H at 190 lb. per ft. The heaviest beam had a torsion constant about two hundred times as great as the lightest.

(6) The method of applying the torque to the ends of the beam provided a very high degree of end freedom.

(7) By measuring the unit twist of the free-ended beams and obtaining the slope of the torque-twist diagram the free-end torsion tests provided through the following relation a definite check upon the torsion constant as computed by the proposed method:

$$\frac{T}{\theta} = KG$$

(8) Using G = 11,150,000 lb. per sq.in. which is theoretically correct for E = 29,000,000 lb. per sq.in. and μ= 0.30 the test results checked well with computed K values. The maximum variation was 6.7 per cent and the average for the seven tests was 2.26 per cent. Results are given in Table IV.

(9) The yield point of the beams in both free end and fixed end tests was determined by a study of the torque twist diagram and in some cases by a drop of the beam.

(10) In the free end tests the distribution of shearing stress across the flange was studied by measuring with tensometers the principal stress at an angle of 45° around the center section.

(11) The fixed end testsprovided a means of studying the additional rigidity and strength over free end tests due to fixing the ends of the beams. Twenty-two various lengths and sizes of beams were tested ranging in size from a 3-in. I beam at 7.5 lb. per ft. to a 10 by 12 in. beam at 62 lb. per ft. The heaviest beam had a K factor 57 times greater than the least and with ends fixed the most rigid fixed end beam had a rigidity 310 times as great as the least rigid with ends fixed.

(12) The distribution of longitudinal direct stresses in the extreme fibers of the flanges was studied by strain measurements taken along the outer edges of the flanges by means of tensometers. The total shearing stress distribution at the center section was studied by measurement of principal strains at an angle of 45°.

(13) The fixed ended tests furnished information on the proper design of welded end connections for high torsional rigidity.

(14) The tensometers in both the free ended and fixed ended tests were of value in studying the relative distribution of stress. Some of the results are erratic.

The warping of the section during twist made it difficult to obtain a steady setup for the tensometers but in most cases the test results checked fairly well with the formulas.

(15) In spite of variations in result and incomplete end fixity it is noted that every beam tested would have been amply strong if designed on a basis of working longitudinal stresses at the ends.

(16) The present investigation has it is believed, covered accurately the question of torsional rigidity and the evaluation of the torsion constant. The formulas for stresses which are proposed are not exact but will be satisfactory for practical design purposes. Further study and application of the Membrane Analogy should be given to the subject of torsional stresses and stress concentration in fillets. Additional tests might also be made to establish the K factors of angle and channel shapes accurately. A program of full-size tests on combined bending and torsion of structural beam sections would also be desirable at some future date.

VIII. LIST OF REFERENCES

1. Navier: RESUME DES LECONS--third edition with notes and appendices by Saint Venant. Article 5 on Torsion presents Saint Venant studies in complete form.

2. Prandtl, L: Zur Torsion von Prismatischen Staben. Physikalische Zeitschrift, IV, 1903, p.758. Brief presentation by Prandtl of the membrane analogy.

3. Griffith, A.A., and Taylor, G.I.: Technical Reports of the Advisory Committee for Aeronautics, No.333, June, 1917.
Report covering the experimental work with soap films by Griffith and Taylor.

4. Trayer, George W. and March, H.W.: The Torsion of Members Having Sections Common in Aircraft Construction. N.A.C.A.Report 334.
Reports on the application of soap film tests applied to torsional rigidity of wood airplane struts. Has an excellent bibliography on torsion and summarizes formulae for numerous shapes.

5. Timoshenko: THEORY OF ELASTICITY, 1st Edition, 1934, Chapter 9 presents a very complete study of all aspects pertaining to the problem of pure torsion.

6. Timoshenko: STRENGTH OF MATERIALS, Vol. 1.

7. R. Sonntag: ZEITSCHRIFT FUR ANGEWANDTE MATHEMATIK, 1929, Vol. 9, p. 369.

A theoretical study of torsion with end restraint at both ends.

8. Trefftz, E., Z. angew. Mathematik. und Mech. Vol. 2, p.263, 1922.

9. Foppl, Ing. Aug., and Foppl, Ludwig: DRANG UND ZWANG 1924, Vol. 2.

Complete study of all phases of torsion problem from German viewpoint.

10. Seely, Putnam, and Schwalbe: THE TORSIONAL EFFECT OF TRANSVERSE BENDING LOADS ON CHANNEL BEAMS, gives a theoretical discussion of the problem of channels as cantilever beams fixed at one end. University of Illinois Bulletin No.211.

11. Campbell: Torsion tests made at Northwestern University. Engineering News-Record, Vol.101, 1928, p.154.

12. Nadai, PLASTICITY. 1931

Chapters 19 and 20 present the problem of torsion after the material has yielded and during which plastic flow occurs.

13. Cushman, P. Allerton: Shearing Stresses in Torsion and Bending by Membrane Analogy. Presented before the A.S.M.E. in June, 1932.

APPENDIX I

SHEAR CONCENTRATION AT FILLETS

IN BENDING AND TWISTING OF ROLLED SHAPES

by

H. M. Westergaard

Professor of Theoretical and Applied Mechanics

University of Illinois

SUMMARY

The results obtained are stated in equations (6) and (13).

Notation

b = thickness of the web or flange at the beginning of the fillet.

r = radius of the fillet.

τ = shearing stress.

τ_1 = shearing stress at the fillet.

τ_0 = Shearing stress along the edge of the cross section near the fillet.

$\frac{\tau_1}{\tau_0}$ = concentration factor.

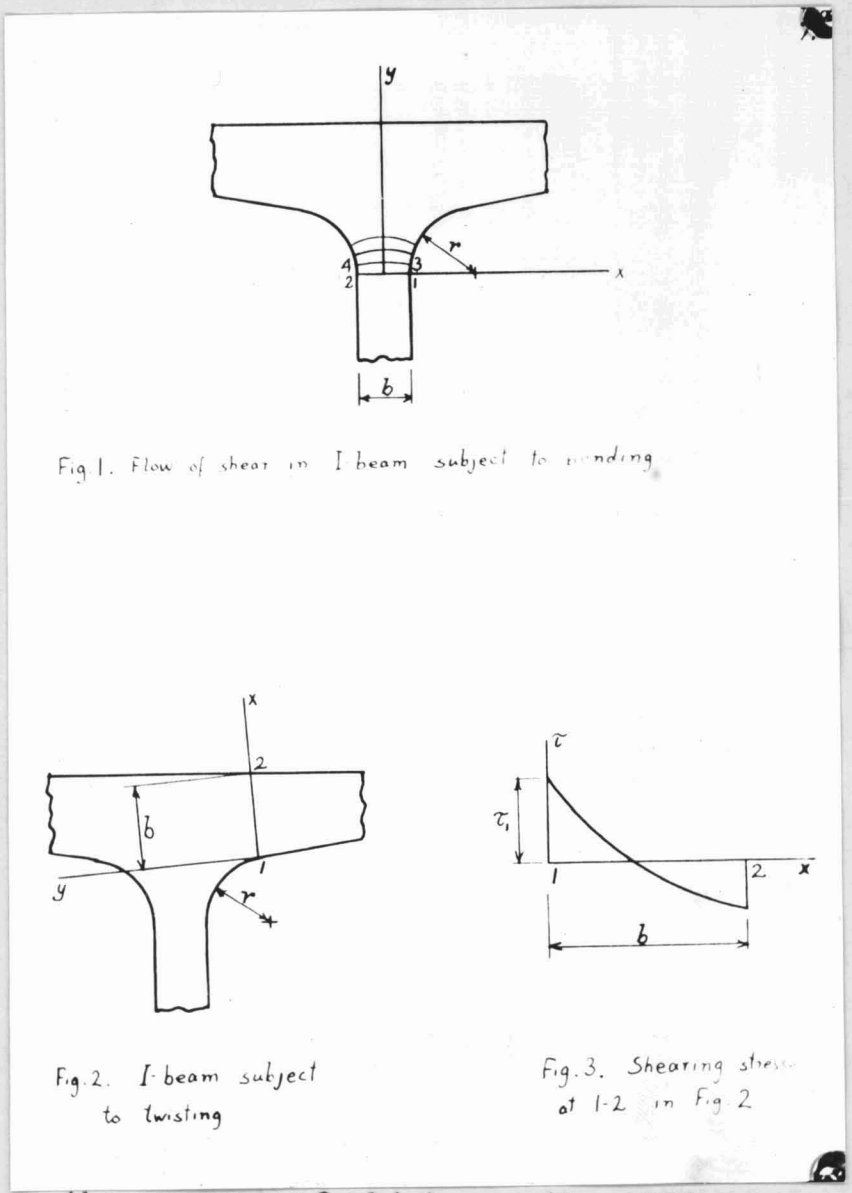

Fig. 1. Flow of shear in I beam subject to bending

Fig. 2. I-beam subject to twisting

Fig. 3. Shearing stress at 1-2 in Fig. 2

Bending

Fig. 1 shows a part of the cross section of an I-beam. The shearing stresses can be represented as velocities in a flow, the sources of which are the differences between the normal stresses on two adjacent cross sections. Except for a discrepancy which is unimportant here, and which is introduced

by Poisson's ratio, this flow can be defined by a surface, the velocity being in the direction of the fall of the surface and proportional to the fall.* Fig. 1 shows some contour lines of such a surface. The end tangents of the contour lines must be normal to the boundary. It is reasonable to assume that the contour line 3-4 is approximately a parabola. If its equation is written in the form,

$$y = c\left(1 + \frac{b}{4r} - \frac{x^2}{br}\right) \qquad (1)$$

one finds at point 3: $y = c$, $\frac{dy}{dx} = -\frac{c}{r}$, which shows that the requirement of the end tangent is satisfied. Accordingly the shearing stresses in the direction of y between 1-2 and 3-4 may be written as:

$$\tau = \frac{\tau_1}{1 + \frac{b}{4r} - \frac{x^2}{br}} \qquad (2)$$

τ_1 being the stress between points 1 and 3.

Point 1 is close to the place where the greatest concentration may be expected. Equation (2) is rewritten approximately as:

$$\tau = \tau_1\left(1 - \frac{b}{4r} + \frac{x^2}{br}\right) \qquad (3)$$

The average value of τ over the width of the web is the stress τ_0 that would exist over the whole width if the fillets were a little farther away. This average is found from equation (3) to be:

$$\tau_0 = \tau_1\left(1 - \frac{b}{6r}\right) \qquad (4)$$

---

* Compare A. and L. Föppl, Drang und Zwang, Vol. 2, second edition, 1928, p.128.

Equation (4) gives the desired concentration factor as:

$$\frac{\tau_1}{\tau_0} = \frac{1}{1 - \frac{b}{6r}} \qquad (5)$$

This equation, however, can be replaced without essential loss of accuracy by the still simpler formula,

$$\frac{\tau_1}{\tau_0} = 1 + \frac{b}{6r} \qquad (6)$$

which is recommended for practical use.

Twisting

Fig. 2 shows a part of the cross section of an I-beam which is subject to twisting. It is desired to determine the shearing stress τ_1 at point . The soap-film analogy introduced by Prandtl* in 1903 furnishes the key to the following simple solution. This solution is a modification of one given by A. and L. Foppl;** that a slightly greater concentration factor is obtained in the present analysis, is explained by the consideration given to the conditions at the straight edge opposite the fillet.

---

* L. Prandtl, Zur Torsion von prismatischen Staben, Physikalische Zeitschrift, Vol.4, 1903, p.758

** Loc. cit. p.73. See also S. Timoshenko, Theory of Elasticity, 1934, p.259.

The soap film is stretched out over an opening shaped like the cross section and is inflated a small amount by an excess air pressure on one side. The shearing stresses on the original cross section follow the contour lines on the film, the edge being one of the contour lines. Furthermore, the shearing stresses are proportional to the slopes on the film, or, proportional to the density of the contour lines.

The contour lines at section 1-2 in Fig. 2 must be approximately perpendicular to that section. Accordingly the shearing stresses τ at that section are approximately in the direction of y. Since the slope of the film is $c\tau$, c being a constant, the curvature of the film at 1-2 in the direction of x becomes $c\frac{d\tau}{dx}$. The curvature of the film in the direction of y at 1-2 is accounted for by the curving of the contour lines. If the radius of curvature of the contour line at a particular point is ρ, then the curvature of the film in the direction of y at the same point becomes $c\frac{\tau}{\rho}$. The curvature of the surface is the sum of the curvatures in the directions of x and y, that is, $c(\frac{d\tau}{dx} + \frac{\tau}{\rho})$.

The equilibrium of the film requires this combined curvature to be constant. Since $\rho = r$ at 1 and $\rho = \infty$ at 2, it follows that:

$$\left(\frac{d\tau}{dx}\right)_2 - \left(\frac{d\tau}{dx}\right)_1 = \frac{\tau_1}{r} \qquad (7)$$

Since points 1 and 2 are on the same contour line, it is also required that

$$\int_0^b \tau dx = 0 \tag{8}$$

It is concluded that the diagram of the shearing stresses at section 1-2 must be shaped about as shown in Fig. 3. The following formula has been constructed so that it satisfies this general requirement of shape as well as the specific requirements in equations (7) and (8), and it may therefore be assumed to represent the shearing stress approximately:

$$\tau = \tau_1 \left[1 - (2 + \frac{b}{3r}) \frac{x}{b} + \frac{x^2}{2br} \right] \tag{9}$$

The constant curvature of the film may be computed as:

$$c \left[\frac{d\tau}{dx} \right]_2 = - \frac{2c\tau_1}{b} (1 - \frac{b}{3r}) \tag{10}$$

If the fillet were some small distance away, this curvature would remain the same, τ_1 would re replaced by τ_0, and the term containing r would disappear.

Consequently,

$$\tau_0 = \tau_1 (1 - \frac{b}{3r}) \tag{11}$$

which gives the concentration factor,

$$\frac{\tau_1}{\tau_0} = \frac{1}{1 - \frac{b}{3r}} \tag{12}$$

The important indications of equation (12) are preserved when the following simpler formula is substituted:

$$\frac{\tau_1}{\tau_0} = 1 + \frac{b}{3r} \qquad (13)$$

S. Timoshenko* obtained a result of the same form as equation (13), only with 4r in the denominator of the last term instead of 3r. The formula derived by A. and L. Föppl gives nearly the same values as that stated by S. Timoshenko. Equation (13) shows a slightly greater concentration and is recommended for practical use.

---

* Loc. cit.

APPENDIX II

TABLES OF TORSIONAL FACTORS

These computations have been furnished through the courtesy of McClintic-Marshall Corporation and are based on Equations 22 and 23 of this report.

Torsional Properties
Parallel Flange Sections

Section Number and Nominal Size	Depth of Section	Weight per Foot	Torsion Constant K	D	Flange Thickness n
	18.69	426	338.601	3.591	3.033
	18.50	412	307.848	3.491	2.938
	18.31	398	278.709	3.388	2.843
	18.12	384	251.813	3.288	2.748
	17.94	370	226.986	3.186	2.658
	17.75	356	203.372	3.084	2.563
	17.56	342	181.482	2.982	2.468
	17.38	328	161.470	2.878	2.378
	17.19	314	142.603	2.774	2.283
	17.00	300	125.291	2.670	2.188
	16.81	287	109.963	2.571	2.093
	16.62	273	95.345	2.465	1.998
	16.50	264	86.857	2.399	1.938
B 14 e	16.37	255	78.474	2.330	1.873
14 x 16	16.25	246	70.928	2.262	1.813
	16.12	237	63.634	2.193	1.748
	16.00	228	57.103	2.124	1.688
	15.87	219	50.723	2.054	1.623
	15.75	211	45.487	1.993	1.563
	15.63	202	40.223	1.923	1.503
	15.50	193	35.211	1.852	1.438
	15.38	184	30.805	1.782	1.378
	15.25	176	26.873	1.719	1.313
	15.12	167	23.078	1.648	1.248
	15.00	158	19.785	1.578	1.188
	14.88	150	16.955	1.514	1.128
	14.75	142	14.390	1.453	1.063
B 14 f	16.81	320	134.075	2.818	2.093
	14.75	136	16.744	1.445	1.063
	14.62	127	13.907	1.371	.998
B 14 d	14.50	119	11.651	1.304	.938
14 x 14½	14.37	111	9.606	1.238	.873
	14.25	103	7.835	1.170	.813

Torsional Properties
Parallel Flange Sections

Section Number and Nominal Size	Depth of Section	Weight per Foot	Torsion Constant K	D	Flange Thickness n
B 14 d 14 x 14½	14.12	95	6.296	1.104	0.748
	14.00	87	4.986	1.036	.688
B 14 c 14 x 12	14.18	84	4.476	1.123	.778
	14.06	78	3.570	1.063	.718
B 14 b 14 x 10	14.19	74	3.924	1.126	.783
	14.06	68	3.057	1.059	.718
	13.91	61	2.223	.981	.643
B 14 a 14 x 8	14.06	58	2.545	1.054	.718
	13.94	53	1.968	.990	.658
	13.81	48	1.468	.923	.593
	13.68	43	1.063	.857	.528
B 12 c 12 x 12	14.38	190	49.956	2.171	1.736
	14.12	176	39.887	2.039	1.606
	13.88	161	31.200	1.898	1.486
	13.62	147	23.844	1.763	1.356
	13.38	133	17.949	1.628	1.236
	13.12	120	13.126	1.502	1.106
	12.88	106	9.233	1.365	.986
	12.75	99	7.540	1.294	.921
	12.62	92	6.093	1.226	.856
	12.50	85	4.866	1.156	.796
	12.38	79	3.901	1.096	.736
	12.25	72	2.976	1.026	.671
	12.12	65	2.212	.956	.606
B 12 b 12 x 10	12.31	64	2.810	1.040	.701
	12.19	58	2.139	.971	.641
	12.06	53	1.608	.912	.576

Torsional Properties
Parallel Flange Sections

Section Number and Nominal Size	Depth of Section	Weight per Foot	Torsion Constant K	D	Flange Thickness n
B 12 a 12 x 8	12.19	50	1.823	.976	.641
	12.06	45	1.343	.908	.576
	11.94	40	.971	.841	.516
	11.88	136	26.691	1.865	1.498
	11.62	124	20.374	1.727	1.368
	11.38	112	15.313	1.591	1.248
	11.12	100	11.050	1.453	1.118
	10.88	89	7.875	1.324	.998
B 10 b 10 x 10	10.62	77	5.187	1.183	.868
	10.50	72	4.227	1.123	.808
	10.38	66	3.318	1.052	.748
	10.25	60	2.529	.980	.683
	10.12	54	1.868	.907	.618
	10.00	49	1.395	.846	.558
	10.12	45	1.525	.899	.618
B 10 a 10 x 8	10.00	41	1.147	.841	.558
	9.88	37	.839	.783	.498
	9.75	33	.586	.724	.433
	9.00	67	5.145	1.206	.933
	8.75	58	3.371	1.075	.808
	8.50	48	1.991	.928	.683
B 8 b 8 x 8	8.25	40	1.133	.808	.558
	8.12	35	.778	.733	.493
	8.06	33	.650	.703	.463
	8.00	31	.540	.673	.433
B 8 a 8 x 6½	8.03	27	.489	.679	.448
	7.93	24	.348	.626	.398

Torsional Properties
Parallel Flange Sections

Section Number and Nominal Size	Depth of Section	Weight per Foot	Torsion Constant K	D	Flange Thickness n
	6.75	41	2.054	.972	.750
	6.38	30	.853	.759	.565
B 6	6.25	27	.611	.699	.500
6 x 6	6.12	23	.394	.620	.435
	6.00	20	.260	.560	.375
	7.23	88	8.889	1.388	.990
	7.06	80	6.754	1.281	.905
B 6a	6.85	70	4.636	1.150	.800
6 x 10	6.63	60	2.958	1.013	.690
	6.41	50	1.749	.875	.580
	6.18	40	.899	.731	.465

Torsional Properties Sloping Flange Sections (2 percent slope)

Section Number and Nominal Size	Depth of Section	Weight per Foot	Torsion Constant K	D	Flange Thickness	
					m	n
B 12L 12×4	12.31	22	.301	.615	.443	.405
	12.16	19	.189	.545	.368	.330
	12.00	16½	.114	.477	.288	.250
B 10L 10×4	10.25	19	.239	.586	.413	.375
	10.12	17	.160	.529	.348	.310
	10.00	15	.106	.477	.288	.250
B 8L 8×4	8.12	15	.140	.519	.333	.295
	8.00	13	.089	.466	.273	.235
B 6L 6×4	6.25	16	.230	.575	.423	.385
	6.00	12	.092	.461	.298	.260
BS6 6×6	6.09	18	.177	.512	.343	.285
	6.00	15½	.117	.466	.298	.240
BS4 4×4	4.16	13	.156	.536	.364	.326
	4.00	10	.073	.445	.284	.246
	3.87	7½	.033	.371	.219	.181
BJ 12	11.91	14	.072	.428	.243	.205
BJ 10	9.87	11½	.050	.403	.223	.185
BJ 8	7.90	10	.044	.398	.223	.185
BJ 6	5.83	8½	.034	.366	.213	.175

Torsional Properties Sloping Flange Sections (5 percent slope)

Section Number and Nominal Size	Depth of Section	Weight per Foot	Torsion Constant K	D	Flange Thickness	
					m	n
B 36a 36×16½	36.72	300	68.799	2.373	1.876	1.484
	36.50	280	56.427	2.256	1.766	1.374
	36.24	260	44.777	2.130	1.636	1.244
	36.12	250	39.679	2.067	1.516	1.184
	36.00	240	55.129	2.007	1.516	1.124
	35.88	230	30.943	1.946	1.456	1.064
B 36 36×12	36.48	194	23.693	1.815	1.402	1.118
	36.32	182	19.611	1.730	1.322	1.038
	36.16	170	16.034	1.644	1.242	.958
	36.00	160	13.228	1.567	1.162	.878
	35.84	150	10.775	1.489	1.082	.798
B 33a 33×15¾	33.50	240	39.294	2.061	1.588	1.212
	33.25	220	30.331	1.934	1.463	1.087
	33.12	210	26.313	1.869	1.398	1.022
	33.00	200	22.778	1.805	1.338	.962
B 33 33×11½	33.50	152	13.182	1.562	1.192	.918
	33.31	141	10.362	1.471	1.097	.823
	33.15	132	8.345	1.394	1.017	.743
	33.00	125	6.884	1.328	.942	.668
B30a 30×15	30.38	210	30.690	1.938	1.492	1.136
	30.25	200	26.528	1.870	1.429	1.071
	30.12	190	22.851	1.803	1.364	1.006
	30.00	180	19.582	1.737	1.304	.946
	29.88	172	17.012	1.680	1.244	.886
B30 30×10½	30.30	132	10.354	1.476	1.124	.876
	30.16	124	8.517	1.405	1.054	.806
	30.00	116	6.847	1.330	.974	.726
	29.82	108	5.346	1.249	.884	.636
B27a 27×14	27.31	171	21.567	1.781	1.357	1.023

Torsional Properties
Sloping Flange Sections (5 percent slope)

Section Number and Nominal Size	Depth of Section	Weight per Foot	Torsion Constant K	D	Flange Thickness	
					m	n
B27a 27×14	27.12	163	16.958	1.679	1.262	.928
	27.00	154	14.421	1.615	1.202	.868
	26.88	145	12.155	1.551	1.142	.808
	27.28	114	7.858	1.374	1.051	.813
B27 27×10	27.14	106	6.317	1.301	.981	.743
	27.00	98	4.998	1.229	.911	.673
	26.84	91	3.889	1.155	.831	.593
	24.72	160	17.817	1.665	1.303	.961
B24b 24×14	24.56	150	14.596	1.586	1.223	.887
	24.41	140	11.882	1.509	1.148	.812
	24.25	130	9.458	1.430	1.068	.732
B24a 24×12	24.31	120	8.845	1.410	1.074	.786
	24.16	110	6.919	1.329	.999	.711
	24.00	100	5.245	1.245	.919	.631
	24.29	94	5.581	1.248	.979	.765
B24 24×9	24.16	87	4.458	1.179	.914	.700
	24.00	80	3.404	1.102	.834	.620
	23.87	74	2.664	1.037	.769	.555
	21.46	142	15.274	1.600	1.251	.939
B21b 21×13	21.31	132	12.157	1.519	1.176	.864
	21.16	122	9.712	1.437	1.101	.789
	21.00	112	7.569	1.354	1.021	.709
	21.29	103	8.497	1.422	1.116	.904
B21a 21×9	21.14	96	6.862	1.346	1.041	.829
	21.00	89	5.491	1.272	.971	.759
	20.86	82	4.319	1.198	.901	.689
B21 21×8¼	21.24	73	3.232	1.105	.838	.642
	21.13	68	2.617	1.049	.783	.587

Torsional Properties Sloping Flange Sections (5 Per cent slope)

Section Number and Nominal Size	Depth of Section	Weight per Foot	Torsion Constant K	D	Flange Thickness	
					m	n
B 21 21 × 8¼	21.00	63	2.038	.987	.718	.522
	20.91	59	1.673	.942	.673	.477
	18.64	124	12.569	1.542	1.211	.931
B 18b 18 × 11¾	18.48	114	9.934	1.452	1.131	.850
	18.32	105	7.818	1.368	1.051	.771
	18.16	96	6.013	1.284	.971	.690
	18.32	85	5.823	1.283	1.015	.807
B 18a 18 × 8¾	18.16	77	4.417	1.195	.935	.727
	18.00	70	3.318	1.113	.855	.647
	17.87	64	2.558	1.044	.790	.582
B 18 18 × 7½	18.12	55	1.783	.936	.719	.541
	18.00	50	1.344	.873	.659	.481
	17.90	47	1.083	.828	.609	.431
	16.64	114	11.009	1.501	1.172	.897
B 16b 16 × 11½	16.48	105	8.712	1.415	1.092	.818
	16.32	96	6.746	1.328	1.012	.738
	16.16	88	5.193	1.248	.932	.658
	16.32	78	5.085	1.251	.976	.774
B 16a 16 × 8½	16.16	71	3.862	1.166	.896	.695
	16.00	64	2.850	1.082	.816	.614
	15.86	58	2.134	1.009	.746	.544
	16.25	50	1.621	.925	.712	.544
B 16 16 × 7	16.12	45	1.189	.857	.647	.479
	16.00	40	.853	.791	.587	.419
	15.85	36	.590	.726	.512	.344
B 14 14 × 6¾	14.24	42	1.163	.860	.654	.492
	14.12	38	.860	.800	.594	.432
	14.00	34	.614	.739	.534	.372

Torsional Properties
Sloping Flange Sections (5 per cent slope)

Section Number and Nominal Size	Depth of Section	Weight per Foot	Torsion Constant K	D	Flange Thickness	
					m	n
B14 14×6¾	13.86	30	.410	.674	.464	.302
	12.24	36	.896	.795	.618	.462
B12	12.12	32	.638	.732	.558	.402
12 × 6½	12.00	28	.435	.668	.498	.342
	11.87	25	.295	.614	.433	.277
	10.22	29	.625	.725	.569	.431
B10	10.12	26	.458	.671	.519	.381
10 × 5¾	10.00	23	.312	.613	.459	.321
	9.90	21	.229	.572	.409	.271
B8	8.19	21	.312	.624	.466	.340
8×5¼	8.09	19	.225	.579	.416	.290
	8.00	17	.160	.536	.371	.245

Torsional Properties Sloping Flange Sections (Standard I-Beams)

Section Number and Nominal Size	Depth of Section	Weight per Foot	Torsion Constant K	D	Flange Thickness	
					m	n
	24	120.0	13.146	1.710	1.404	.800
I 24a	24	115.0	12.145	1.686	1.404	.800
24 × 7 1/8	24	110.0	11.252	1.662	1.404	.800
	24	105.9	10.622	1.644	1.404	.800
	24	100.0	7.701	1.471	1.142	.600
I 24	24	95.0	6.870	1.445	1.142	.600
24 × 7	24	90.0	6.137	1.420	1.142	.600
	24	85.0	5.533	1.395	1.142	.600
	24	79.9	5.014	1.371	1.142	.600
	20	100.0	9.704	1.598	1.183	.650
I 20a	20	95.0	8.554	1.565	1.183	.650
20 × 7	20	90.0	7.571	1.532	1.183	.650
	20	85.0	6.757	1.502	1.183	.650
	20	81.4	6.240	1.480	1.183	.650
I 20	20	75.0	4.660	1.334	1.029	.550
20 × 6 1/4	20	70.0	4.032	1.303	1.029	.550
	20	65.4	3.574	1.275	1.029	.550
	18	70.0	4.188	1.265	.922	.460
I 18	18	65.0	3.459	1.227	.922	.460
18 × 6	18	60.0	2.884	1.191	.922	.460
	18	54.7	2.410	1.155	.922	.460
	15	75.0	6.616	1.481	1.041	.590
I 15a	15	70.0	5.515	1.435	1.041	.590
15 × 6	15	65.0	4.623	1.390	1.041	.590
	15	60.8	4.025	1.354	1.041	.560
	15	55.0	2.732	1.148	.834	.410
I 15	15	50.0	2.145	1.103	.834	.410
15 × 5 1/2	15	45.0	1.714	1.061	.834	.410
	15	42.9	1.571	1.044	.834	.410

Torsional Properties Sloping Flange Sections (Standard I Beams)

Section Number and Nominal Size	Depth of Section	Weight per Foot	Torsion Constant K	D	Flange Thickness	
					m	n
	12.0	55.0	3.756	1.265	.859	.460
I 12a	12.0	50.0	2.853	1.205	.859	.460
12 × 5 1/4	12.0	45.0	2.194	1.148	.859	.460
	12.0	40.8	1.784	1.103	.859	.460
I 12	12.0	35.0	1.098	.950	.738	.350
12 × 5	12.0	31.8	.921	.918	.738	.350
	10.0	40.0	1.987	1.036	.673	.310
I 10	10.0	35.0	1.306	.960	.673	.310
10 × 4 5/8	10.0	30.0	.861	.891	.673	.310
	10.0	25.4	.617	.833	.673	.310
	8.0	25.5	.747	.844	.581	.270
I 8	8.0	23.0	.557	.800	.581	.270
8 × 4	8.0	20.5	.422	.759	.581	.270
	8.0	18.4	.344	.726	.581	.270
I 7	7.0	20.0	.456	.761	.534	.250
7 × 3 5/8	7.0	17.5	.322	.712	.534	.250
	7.0	15.3	.246	.672	.534	250
I 6	6.0	17.25	.379	.726	.488	.230
6 × 3 3/8	6.0	14.75	.243	.667	.488	.230
	6.0	12.50	.171	.618	.488	.230
I 5	5.0	14.75	.327	.701	.443	.210
5 × 3	5.0	12.25	.185	.626	.443	.210
	5.0	10.00	.116	.565	.443	.210
	4.0	10.50	.166	.609	.396	.190
I 4	4.0	9.50	.122	.572	.396	.190
4 × 2 5/8	4.0	8.50	.092	.538	.396	.190
	4.0	7.70	.074	.511	.396	.190
I 3	3.0	7.50	.093	.542	.350	.170
3 × 2 3/8	3.0	6.50	.061	.493	.350	.170
	3.0	5.70	.045	.457	.350	.170